Water Vapour Climate Change Initiative (WV_cci) - Phase Two

ATBD Part 2 - IMS L2 Product

Ref: D2.2

Date: 21/11/2023

Issue: 2.0

For: ESA / ECSAT

Ref: CCIWV.REP.005

This Page is Intentionally Blank

Project : **Water Vapour Climate Change Initiative (WV_cci) - Phase Two**

Document Title: **ATBD Part 2 - IMS L2 Product**

Reference : **D2.2**

Issued : **21 November 2023**

Issue : **2.0**

Client: **ESA / ECSAT**

Author(s) : Richard Siddans

Document Change Log

Issue/ Revision	Date	Comment
1.0	29 March 2019	Initial issue covering IMS-v1 scheme.
2.0	21 Nov 2023	Update to describe v2 “IMS-extended” scheme now used in CCI+ phase 2. Includes modifications for CrIS/ATMS.

This Page is Intentionally Blank

TABLE OF CONTENTS

INDEX OF TABLES

INDEX OF FIGURES

This Page is Intentionally Blank

1. INTRODUCTION

1.1 Purpose

This document is the algorithm theoretical baseline document (ATBD) for the RAL Infra-red and Microwave Sounder (IMS) scheme, as used within the ESA CCI Water Vapour project and the UK EOCIS project.

The purpose of the ATBD is to provide detailed mathematical and physical descriptions of this algorithm, along with an overview of algorithm inputs and outputs, data products, algorithm validation and error analysis

1.2 Scope

This document describes version 2 of the IMS algorithm (also known as *IMS-extended*) which has been applied to generate the data used in the second phase of the project. The algorithm was developed prior to, and in parallel with, the CCI project via a Eumetsat study and funding from the UK National Centre for Earth Observation (NCEO).

While this document provides an overview of product quality from previous work, note that these topics will be covered in more depth by other CCI documents including the E3UB and PVIR.

2. ALGORITHM DEFINITION

2.1 Introduction

The Infrared Microwave Sounding (IMS) scheme employs the optimal estimation method (OEM) to jointly retrieve atmospheric and surface parameters from operational sounding instruments. The first version of the scheme (used in CCI+ phase 1) retrieved water vapour, temperature and ozone profiles and surface spectral emissivity and cloud parameters from the Metop sounding instruments IASI, MHS and AMSU (see section 2.4.1). The latest version (2) of the scheme, described in this ATBD and referred to as "IMS-extended", also includes retrieval of several additional minor trace gases and two types of aerosol (dust and volcanic sulphate).The scheme has also been extended to the sounders on the NOAA/NASA Joint Polar Satellite System (JPSS), see section 2.4.2.

2.2 Heritage

The IMS scheme was developed in the context of a Eumetsat study ([RD01]) which started with the specification of the Eumetsat operational optimal estimation scheme used for the version 6 operational product ([RD03]).

The Eumetsat version 6 product is generated using a series of algorithms, including a piece-wise linear regression (PWLR) scheme which uses measurements by IASI, AMSU and MHS together to predict water vapour, temperature and ozone profiles. This PWLR is based on regressing observed radiances from the three sounders against ECMWF analyses. In cloud free scenes, output from the PWLR is used as *a priori* information for an OEM retrieval from IASI only. PWLR results are directly reported in the L2 product, as well as results from the OEM (for the sub-set of cloud-free scenes). Separate schemes are used to perform cloud flagging and to retrieve trace-gases (e.g. carbon monoxide). It is specifically the temperature and water vapour OEM algorithm which was used as a basis for the RAL IMS development.

During the study three advances over the Eumetsat OEM were developed:

- Information from IASI, AMSU and MHS measurements are combined
- Spectral emissivity is jointly retrieved
- Cloud parameters are included in the retrieval, enabling the scheme to be applied to cloudy scenes.

Those three extensions were found to improve agreement with ECMWF analyses of lower tropospheric water vapour and to reduce the sensitivity to small amounts of cloud contamination; significantly improving the coverage of useful data.

The IMS scheme was subsequently developed through work within the UK National Centre for Earth Observation (NCEO). The scheme now uses a weak prior constraint, based on zonal mean climatology. It is in practice therefore independent of ECMWF analyses or re-analyses. The IMS scheme uses the RTTOV radiative transfer model to simulate brightness temperature observations of the IASI and microwave sounders.

Via NCEO, the IMS scheme was been applied to process the complete IASI Metop A mission from 2007 to 2016. This “Version-1” dataset ([RD09]) is made available in Year-1 to the CCI+ Water Vapour project. The data is now archived at CEDA (http://www.ceda.ac.uk/).

Since the generation of this dataset, the IMS scheme has developed further, building on new capabilities introduced in RTTOV 12 as follows:

- The quality of the height-resolved ozone retrieval has been much improved.
- Joint retrieval of additional trace gases carbon monoxide (CO), nitric acid (HNO_3), methanol (CH_3OH), ammonia (NH_3) and sulphur dioxide (SO_2). In the case of IASI/AMSU/MHS, formic acid (HCOOH) is also retrieved. In the case of CrIS/ATMS isoprene (C_5H_8) is also retrieved.
- Joint retrieval of dust and sulfuric acid aerosol optical depth.
- Cloud is now represented as a multiple scattering layer using spectral optical properties of ice / liquid cloud. Effective radius, altitude and optical depth of the cloud are now jointly retrieved.

This scheme is referred to as “IMS-extended”. Full mission processing of Metop-A and B with the with the improved scheme has now been completed. Processing of data from CrIS/ATMS is under way and is expected to be complete within the timeframe of the CCI+ Water Vapour Phase 2. Both datasets will be archived at CEDA.

2.3 Use of NWP data

IMS uses input from Numerical Weather Prediction (NWP) models is the following ways:

- To define the surface pressure.
- To define wind speed from which the ocean surface reflectance for solar radiation is initially estimated.
- To define the initial (first guess) temperature and water vapour profiles.

This ATBD refers generically to using “NWP” data for such purposes, as the actual source of the data can vary depending on the way IMS is run.

To date, NWP data from ECMWF has been used in all cases.

For near-real time processing ECMWF operational forecast data is used.

For retrospective processing, re-analysis data is used: ERA-interim [RD19] for IMS-v1 and ERA-5 [RD31] data for IMS-extended.

2.4 Instruments

2.4.1 Metop

The IMS scheme uses the three sounding instruments, IASI, AMSU and MHS, on-board the Metop platform of the Eumetsat Polar System (EPS). There are three Metop platforms, all of which are in a sun-synchronous orbit with 9:30 descending node crossing time: Metop-A, -B and –C were launched respectively on 19 October 2006, 17 September 2012 and 7 November 2018.

Data from the three IASI instruments is available as follows:

- Metop-A: 29 May 2007 to 15 October 2021.
- Metop-B: 20 February 2013 to present.
- Metop-C: 1 July 2019 to present.

Note that the “full” mission processing with IMS-extended applies to Metop-A data up to the end of 2018 and Metop-B data from the beginning of 2018. Only small sub-sets of data have been produced from Metop-C to data so far.

2.4.1.1 Infrared Atmospheric Sounding Interferometer (IASI)

Metop IASI ([RD04]) is a nadir viewing infra-red Fourier transform spectrometer which provides spectra at 0.5 cm^{-1} apodised resolution, sampled every 0.25 cm^{-1}, from 625 to 2760 cm^{-1}. Spectra are measured with 4 detectors, each with a circular field of view (FOV) on the ground (at nadir) of approximately 12 km diameter, arranged in a 2 x 2 grid within a 50 x 50 km^2 field-of-regard (FOR). IASI scans to provide 30 fields-of-regard (FOR) (i.e. 120 individual spectra) evenly distributed across a 2200 km wide swath.

IMS is currently applied to the reprocessed Metop-A data set ([RD29]) up to the end of 2017 and version 8.0 data from the on-line processing stream up to the end of 2018. The on-line processed versions of Metop-B data are used since the beginning of 2018 (i.e. versions 8.0, 8.2 and 8.4 depending on the date).

2.4.1.2 Advanced Microwave Sounding Unit (AMSU) and Microwave Humidity Sounder (MHS)

The ATOVS (Advanced TIROS (Television and Infrared Observational Satellite) Operational Vertical Sounder) is a sounding instrument package flown on operational polar orbiting platforms since NOAA-15 (launched May 1998). On Metop, it comprises

the Advanced Microwave Sounding Unit (AMSU), the Microwave Humidity Sounder (MHS) and the High Resolution InfraRed Sounder (HIRS/4; not used in the IMS scheme).

AMSU and MHS are across-track scanning microwave radiometers. AMSU measures in 15 spectral bands, including coverage of the 50GHz oxygen line, used for temperature sounding. MHS adds five channels around the 183 GHz water vapour line. The spectral coverage is summarised in Table 2-1 and illustrated in Figure 2-1.

Both the microwave sounders have a scan range of around ±48° from nadir, giving a swath width similar to that of IASI. While the instantaneous fields of view (IFOV) of the sounders differ, the scans are synchronised to give a systematic regular sampling pattern from the four instruments, as illustrated in Figure 2-2. The IFOV of AMSU (at nadir) is circular with a diameter of around 48km. 30 of these footprints are measured in each scan, closely matching the 30 FOR of IASI (i.e. there are 4 IASI measurements within each AMSU IFOV). MHS has a circular footprint of around 16km diameter at nadir. Three scans of MHS are made for each scan of IASI/AMSU (yielding 9 MHS measurements for each AMSU IFOV).

2.4.2 Suomi-NPP and JPSS

NASA/NOAA instruments with comparable functionality to IASI and AMSU/MHS are the Cross-track Infrared Sounder (CrIS) and the Advanced Technology Microwave Sounder (ATMS). These are carried by platforms in the Joint Polar Satellite System (JPSS), all of which have an ascending node equator crossing time of 13:30. I.e. providing complementary local time sampling compared to Metop. The first platform in the series was Suomi-NPP (launch 28 October 2011) followed by JPSS-1 (launched 18 November 2018, now renamed NOAA-20) and JPSS-2 (launched 10 October 2022, now renamed NOAA-21).

2.4.2.1 Cross-track Infrared Sounder (CrIS)

Similar to IASI, CrIS ([RD25]) is a nadir viewing scanning infra-red Fourier transform spectrometer. It provides spectra in 3 bands:

- LW: 650 – 1095 cm^{-1}
- MW: 1210 – 1750 cm^{-1}
- SW: 2155 – 2550 cm^{-1}

The scan pattern is similar to that of IASI except that CrIS has 9 detectors (arranged within each FOR in a 3x3 grid) compared to 4 (2x2) for IASI. Like IASI, there are 30

FOR in each cross-tack scan, spaced by approximately 50km. I.e. CrIS makes 270 soundings per scan compared to 120 for IASI (both covering a swath of ~2200km across x ~50km along-track). Each CrIS detector has a circular field-of-view with diameter 14km (cf 12km for IASI).

Initially Suomi-NPP CrIS was operated in a mode which provided measurements with 0.625, 1.25 and 2.5cm^{-1} unaopodised spectral resolution in the LW, MW and SW bands respectively. The operating mode was subsequently changed such that, since 2 November 2015, full spectral resolution data is provided (0.625cm^{-1} resolution in all bands). Data from NOAA-20 and NOAA-21 are all available at this full spectral resolution.

IMS has been applied to V3 full spectral resolution level 1B data ([RD26], [RD27], [RD28]) from Suomi-NPP and NOAA-20 only. Level 1B data is provided unapodised. We apodise the spectra with a Hamming function as discussed in [RD27], consistent with the assumption made by RTTOV. This gives an apodised spectral resolution of around 1.13cm^{-1} for CrIS, compared to 0.5cm^{-1} for IASI. Note however that CrIS offers generally better signal to noise (for single soundings) than IASI (in addition to better spatial sampling). The NESR (and spectral coverage) of the two instruments is illustrated in Figure 2-3.

Due to instrumental issues, MW band measurements are unavailable in Suomi-NPP CrIS data from March to June 2019 and from May 2021 onwards. To produce timeseries unaffected by these outages, IMS has been applied to Suomi-NPP CrIS data from November 2015 to February 2019 and NOAA-20 data from the beginning of operations in February 2018.

2.4.2.2 Advanced Technology Microwave Sounder (ATMS)

ATMS ([RD23]) was designed to provide the comparable data to AMSU-A and MHS, while improving on those previous instruments in terms of spatial sampling, stability and signal to noise. The channels are very similar (see Table 2-2 cf Table 2-1). Spatial resolution is also similar in all channels except 1 and 2. A key difference compared to AMSU/MHS is that the ATMS scans rapidly to spatially oversample its resolution. L1B processing exploits this oversampling to provide observations precisely co-located with CrIS. IMS uses version 3 Level 1B data ([RD24]).

Channel	Channel frequency / GHz	Nominal bandwidth / MHz	Noise Equivalent Brightness Temperature / K	Approximate field of view diameter (at nadir) / km
1	23.8	270	0.3	48
2	31.4	180	0.3	48
3	50.3	180	0.4	48
4	52.8	400	0.25	48
5	53.59±0.115	170	0.25	48
6	54.4	400	0.25	48
7	54.94	400	0.25	48
8	55.5	330	0.25	48
9	F_{LO}= 57.290344	330	0.25	48
10	F_{LO} ± 0 .217	78	0.4	48
11	F_{LO} ± 0 .3222 ± 0.048	36	0.4	48
12	F_{LO} ± 0 .3222 ± 0.22	16	0.6	48
13	F_{LO} ± 0 .3222 ± 0.01	8	0.8	48
14	F_{LO} ± 0 .3222 ± 0.0045	3	1.2	48
15	89	<6000	0.5	48
16 (MHS H1)	89	2800	1	16
17 (MHS H2)	157	2800	1	16
18 (MHS H3)	183.311±1.00	500	1	16
19 (MHS H4)	183.311±1.00	1000	1	16
20 (MHS H5)	190.311	2200	1	16

Table 2-1: AMSU (1-15) and MHS (16-20) channel characteristics. For the AMSU channels 9-14, F_{LO} indicates the local oscillator frequency about which the spectral response is indicated (from [RD05]).

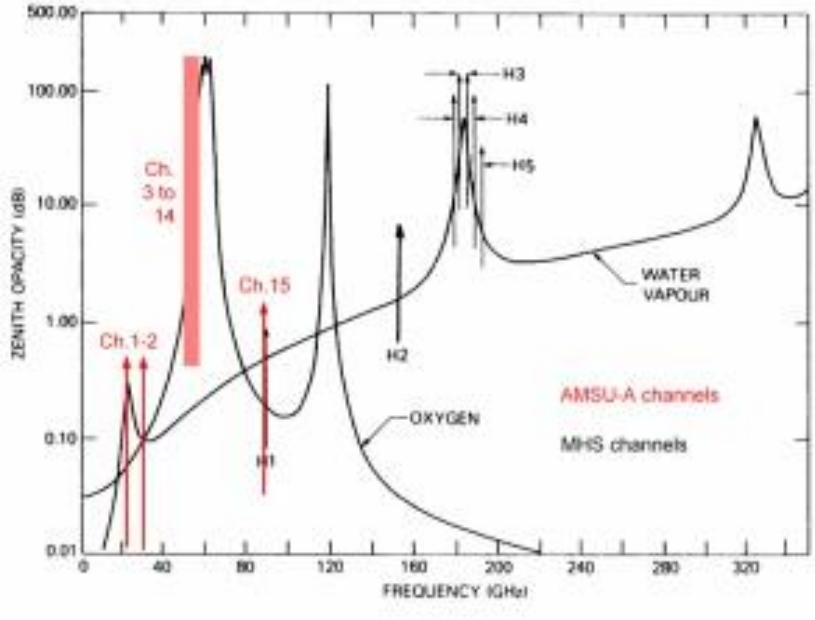

Figure 2-1: Illustration of the spectral coverage of AMSU and MHS channels (from Eumetsat web-site).

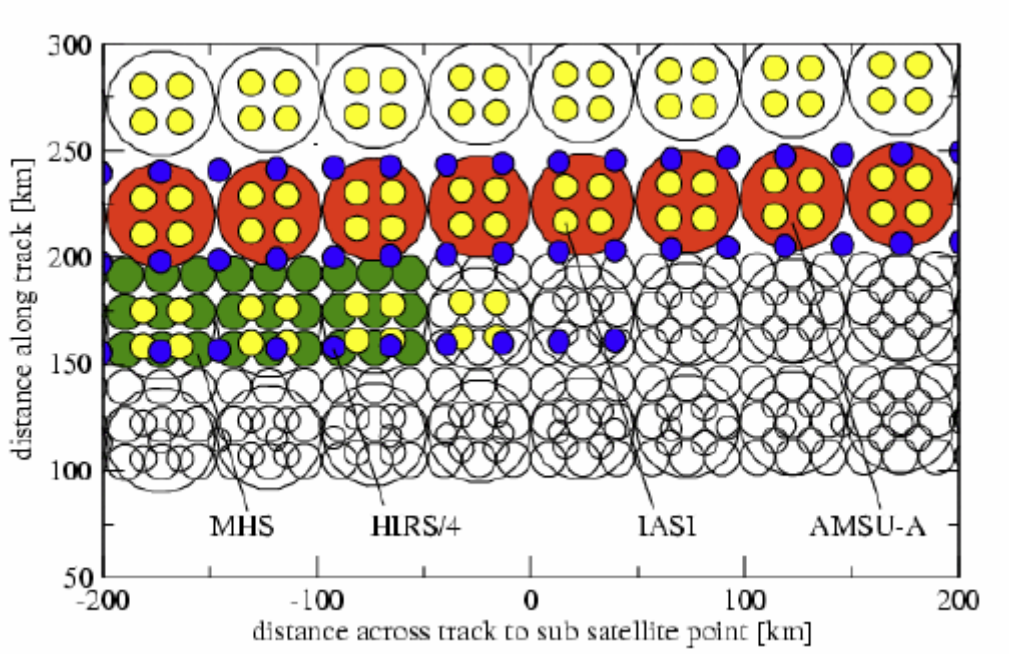

Figure 2-2: Illustration of the footprints of Metop AMSU (red), MHS (green), IASI (yellow) and HIRS/4 (blue) from [RD06].

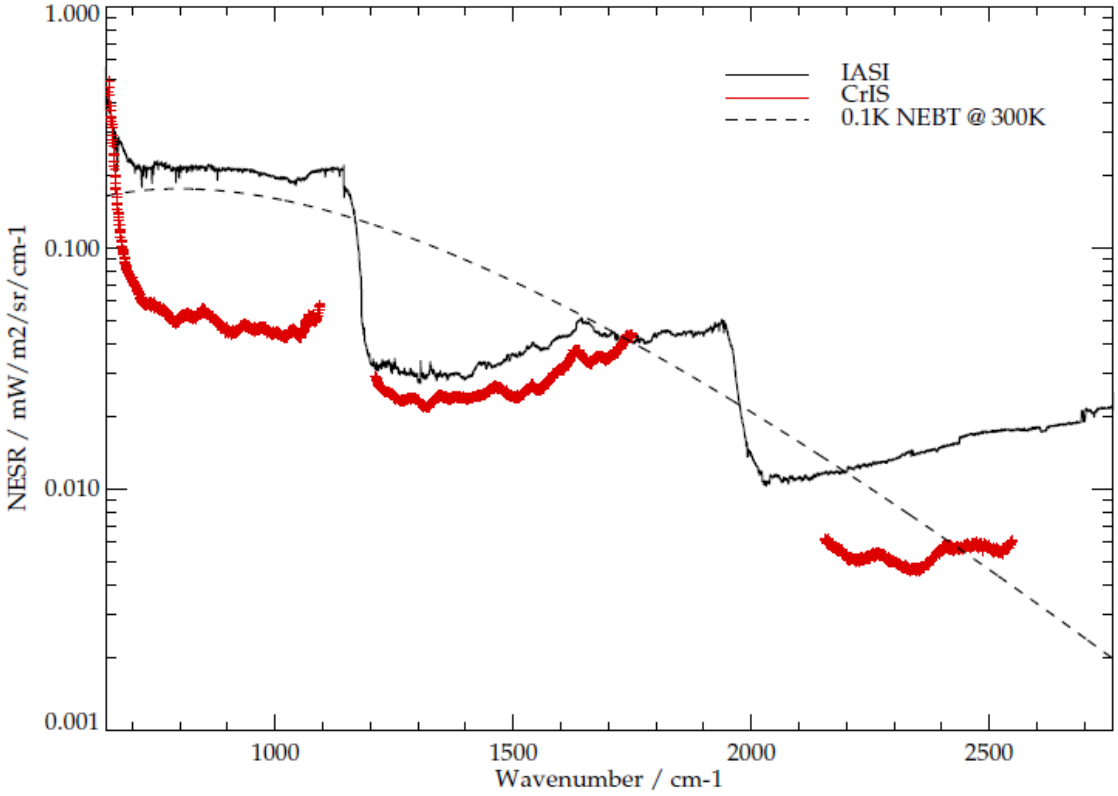

Figure 2-3: Comparison of spectral coverage and noise-equivalent spectral radiance (NESR) of IASI and CrIS. For comparison the dashed lines shows the NESR corresponding to 0.1 noise equivalent brightness temperature (NEBT) for a black body at 300K.

Channel	Channel frequency / GHz	Nominal bandwidth / MHz	Noise Equivalent Brightness Temperature / K	Approximate field of view diameter (at nadir) / km
1	23.8	270	0.25	141.8
2	31.4	180	0.31	141.8
3	50.3	180	0.37	60
4	51.76	400	0.28	60
5	52.8	400	0.28	60
6	53.596±0.115	170	0.29	60
7	54.4	400	0.27	60
8	54.94	400	0.27	60
9	55.5	330	0.29	60
10	F_{LO}=57.290344	330	0.43	60
11	F_{LO}±0.217	78	0.56	60
12	F_{LO}±0.3222±0.048	36	0.59	60
13	F_{LO}±0.3222±0.022	16	0.86	60
14	F_{LO}±0.3222±0.010	8	1.23	60
15	F_{LO}±0.3222±0.0045	3	1.95	60
16	88.2	2000	0.29	60
17	165.5	3000	0.46	30
18	183.31±7.0	2000	0.38	30
19	183.31±4.5	2000	0.46	30
20	183.31±3.0	1000	0.54	30
21	183.31±1.8	1000	0.59	30
22	183.31±1.0	500	0.73	30

Table 2-2: ATMS channel characteristics. For the channels 10-15, F_{LO} indicates the local oscillator frequency about which the spectral response is indicated (from [RD05]).

2.5 The Optimal Estimation Method

The scheme is based on the optimal estimation method (OEM, [RD07]), which solves an otherwise under-constrained inverse problem by introducing prior information. The method finds the optimal state vector $\boldsymbol{x}$ (which contains the parameters we wish to retrieve) by minimising the following cost function:

$$\chi^2 = \left(\boldsymbol{y} - F\left(\boldsymbol{x}\right)\right)^T \boldsymbol{S_y^{-1}}\left(\boldsymbol{y} - F\left(\boldsymbol{x}\right)\right) + \left(\boldsymbol{a} - \boldsymbol{x}\right)^T \boldsymbol{S_a^{-1}}\left(\boldsymbol{a} - \boldsymbol{x}\right)$$

Equation 1

where $\boldsymbol{y}$ is a vector containing each measurement used by the retrieval; $\boldsymbol{S_y}$ is a covariance matrix describing the errors on the measurements; $\boldsymbol{F}(\boldsymbol{x})$ is the *forward model* (FM), which predicts measurements given $\boldsymbol{x}$; $\boldsymbol{S_a}$ is the *a priori* covariance matrix, which describes the assumed errors in the *a priori* estimate of the state, $\boldsymbol{a}$. Minimising this cost function, corresponds to maximising the probability of the solution state being correct, given the uncertainties on the measurements and prior state as expressed by their respective covariances.

If the FM is linear then the solution is given by:

$$\hat{\boldsymbol{x}} = \boldsymbol{a} + \left(\boldsymbol{K^T S_y^{-1} K} + \boldsymbol{S_a^{-1}}\right)^{-1} \boldsymbol{K^T S_y^{-1}} \left(\boldsymbol{y} - F(\boldsymbol{a})\right)$$

Equation 2

where $\boldsymbol{K}$ is the weighting function matrix, the rows of which contain the derivatives of the FM with respect to each element, j, of the state vector:

$$\boldsymbol{K_j} = \frac{\partial\, F(\boldsymbol{x})}{\partial\, \boldsymbol{x_j}}$$

Equation 3

In practice, the FM is non-linear and the solution state needs to be found iteratively, starting from a first guess state, $\boldsymbol{x_0}$. We adopt the well known Levenburg-Marquardt method ([RD08]) to find the solution by iterating the following equation:

$$\boldsymbol{x_{i+1}} = \boldsymbol{x_i} + \left(\boldsymbol{K_i^T S_y^{-1} K} + \boldsymbol{S_a^{-1}} + \gamma \boldsymbol{I}\right)^{-1} [\, \boldsymbol{K_i^T S_y^{-1}} \left(\boldsymbol{y} - F(\boldsymbol{x_i})\right) - \boldsymbol{S_a^{-1}}(\boldsymbol{x_i} - \boldsymbol{x_a})]$$

Equation 4

Where γ is a parameter which controls the magnitude of the state vector update at each iteration, i. $\boldsymbol{K_i}$ is the weighting function evaluated for the current estimate of the state, $\boldsymbol{x_i}$. If γ is negligible and the FM is linear (within the relevant range), then the iteration will immediately find the cost function minimum. However, if the FM is non-linear the iteration will not necessarily lead to the minimum and may even result in a higher cost function value. If γ is large, the iteration will tend to follow the gradient of the cost function, and this should always lead to a reduction in cost. Convergence towards the minimum will however be relatively slow. By controlling the magnitude of γ during the iteration, efficient convergence can usually be assured. Here we adopt the following approach:

1. Initially, γ is (somewhat arbitrarily) set equal to 0.001

2. First guess, $\boldsymbol{x_i}$, (for i=0) is defined. The cost function for this state, χ_i^2, is evaluated.

3. $\boldsymbol{x_{i+1}}$ is estimated, using Equation 4 and the new cost function value is determined, χ_{i+1}^2. The iteration proceeds according to the following logic:

    - If the absolute difference between χ_{i+1}^2 and χ_i^2 is smaller than a given "convergence threshold" (usually 1) is then the scheme proceeds to step 4.
    - If χ_{i+1}^2 is larger than χ_i^2 (the updated state is worse than the previous estimate), then γ is increased by a factor of 10 and the retrieval returns to the beginning of step 3, starting again $\boldsymbol{x_i}$. I.e. iteration count i is not incremented.
    - If χ_{i+1}^2 is smaller than χ_i^2 (the updated state is better than the previous estimate), then γ is decreased by a factor of 10 and the retrieval returns to the beginning of step 3, starting from the updated (better) state, i.e at this point iteration count i is incremented.

4. At this point the last iteration will have resulted in a change of cost which is smaller than the convergence threshold. This could indicate the cost function minimum has been found but may also arise if γ has become very large. A further (potentially final) iteration of the retrieval is now carried out applying Equation 4 with γ=0, to give state $\boldsymbol{x_n}$ and cost χ_n^2. If again the cost function change is smaller than the convergence threshold then the retrieval finishes the final state $\boldsymbol{x_n}$ is reported as the solution. If the cost change is larger than the convergence threshold, then γ is reset to its initial value (0.001) and the retrieval "re-starts" from the state ($\boldsymbol{x_i}$ or $\boldsymbol{x_n}$) which gave the lowest cost.

   The number of allowed iterations and attempted "re-starts" from false minima are subject to pre-defined limits. If these are exceeded during the iteration approach above, then the retrieval is stopped. Results are still reported, with a flag indicating that

convergence has not been fully achieved. These results may still be useful (especially in the case that the solution cost function value is low), but must be used with caution.

Note iteration count $\boldsymbol{i}$ is only updated when a state vector update gives rise to an improvement in the cost. The final value of $\boldsymbol{i}$ is reported as the number of iterations, $\boldsymbol{N\_i}$. The total number of retrieval "steps" (i.e. any state vector update, good or bad), $\boldsymbol{N_s}$, is also usually recorded for information (e.g. to enable optimisation of computational cost by identifying scenes requiring a large number of evaluations of the FM).

The retrieval final cost function value at is always stored, so it can be used to quality-control retrievals later. For detailed analysis, the fit *residual spectum* ($\boldsymbol{y} - F\,(\boldsymbol{x})$ at solution) is also required.

2.6 IMS Measurement vector

2.6.1 IASI and CrIS

2.6.1.1 Channel selection

The version 1 of the IMS scheme was based closely on the operational Eumetsat OEM for IASI and implements the same approach to define the IASI measurement vector and associated covariance ($\boldsymbol{S_y}$). This defines (i) some pre-processing of IASI observations to reduce noise and filter instrument artefacts; (ii) a specific sub-set of 139 IASI channels to be used (determined via an information-content analysis); (iii) a scan angle dependent bias correction; (iv) a specific, fixed measurement error covariance matrix ($\boldsymbol{S_y}$) intended to reflect a combination of instrumental and forward model errors. Furthermore, IMS version 1 used IASI measured (L1C) spectra which have been compressed and re-constructed using the operational principal components ([RD16]). This has the effect of reducing noise on the sub-set of channels which are used in the scheme. A further filter was applied to remove some instrumental artefacts, described in [RD11].

For the version 2 IMS-extended scheme, 199 IASI channels are used, comprising 129 of the original 139 channels and 70 new channels. The additional channels were chosen to sample (with a few spectral points) particularly strong minor gas absorption features of HNO_3, HCHO, CH_3OH, NH_3, SO_2 and CO, avoiding strong water vapour or

CO_2 absorption features[1]. Channels were also added in the ozone spectral range between 950 and 1040cm^{-1}, using an information content analysis to prioritise channels with ozone sensitivity, avoiding water vapour sensitive channels or those which gave rise to unusually large fit residuals. Tests showed that including the upper part of the ozone band from 1050-1070cm^{-1} led to generally poor spectral fit residuals, so this range was completely excluded, including 10 of the original channels used in the version 1 scheme.

In IMS-extended, the operational principal components are still used to compress/filter the data, however the second filter of in [RD11], is no longer applied to measurements in the 875-1144cm^{-1} spectral range (as it was found to filter out useful information on tropospheric ozone).

For CrIS, 186 spectral channels were selected, mainly on a nearest-neighbour basis to match the IASI channel selection (limited by the gaps in the CrIS spectral coverage). The relatively high signal to noise of CrIS compared to IASI in the 890-910cm^{-1} spectral range (see Figure 2-3), enables useful retrieval of isoprene ([RD22], [RD30]), so 20 channels are added in this range to cover the isoprene spectral features. CrIS measurements are used without any principal component filtering applied to the operational full spectral sampling L1 data.

The new set of channels are illustrated Figure 2-4 to Figure 2-11, compared to selected trace gas and aerosol optical depths. Channels are also listed explicitly in Table 2-3. Both the plots and the table also illustrate the assumed measurement errors and bias correction patterns which are described in section 2.6.1.2.

2.6.1.2 Bias correction spectra

In the original Eumetsat scheme, a bias correction for IASI was determined by comparing simulated spectra based on PWLR retrievals (defining surface temperature and profiles of temperature, water vapour and ozone) to observed radiances for a representative subset of IASI scenes (3 complete days of cloud-screened observations from Metop-B data on 17 April 17 July and 17 October 2013). This gave a mean bias correction parameterised in terms of two vectors, $\boldsymbol{b_0}$ and $\boldsymbol{b_1}$, which define a fixed bias spectrum and a scan dependent term. The measurement used in the retrieval, $\boldsymbol{y}$, is then given by

$$\boldsymbol{y} = \boldsymbol{y''} - \boldsymbol{b_0} - \boldsymbol{b_1}\,(\sec(\theta) - \mu_0)$$

[1] *The original channel set included channels sensitive to SO_2 around 1360cm^{-1}.*

Equation 5

Where $\boldsymbol{y''}$ is the double-filtered measurement vector (see above); θ is the satellite zenith angle (at the ground) and μ_0 is a constant.

In the IMS scheme the same vectors $\boldsymbol{b_0}$ and $\boldsymbol{b_1}$ are still used, however the weights used in any given scene are retrieved parameters (see section 2.8 below) and the bias correction is instead applied to the simulated measurement:

$$F(\boldsymbol{x}) = R(\boldsymbol{x}) - x_{b0}\boldsymbol{b_0} - x_{b1}\boldsymbol{b_1}$$

Equation 6

Where x_{b0} and x_{b1} are the state vector elements for the two bias correction patterns and $R(\boldsymbol{x})$ denotes the result for RTTOV, which depends on all other elements of the state vector.

For IASI, IMS-extended uses the same approach, with the only changes being to repeat the measurement simulations (using RTTOV 12 as described in 2.7), for the extended set of spectral channels, using CAMS re-analysis ([RD31]) to define the assumed ozone profiles. The simulations by RTTOV includes HNO_3 assuming a fixed profile. The minor gases retrieved by IMS-extended are otherwise assumed not to be present in the atmosphere (for the purposes of deriving the bias correction patterns). Surface emissivity is defined from the RTTOV atlas. The analysis is only performed for channels below 2000cm^{-1} (no bias correction is performed upon channels above 2000cm^{-1}).

For CrIS, a similar approach is used, based on 3 days of cloud-free observations from JPSS-1/NOAA-20 (15 April, 15 July, 14 October 2018). However, PWLR profiles for the same locations as the CrIS observations are not available (these were produced by Eumetsat for IASI only). Instead, ERA-5 is used to define the temperature and water vapour profiles. Surface temperature is defined from a simple retrieval of surface temperature only from a window channel (956.875cm^{-1}), assuming assumptions for the atmospheric state and surface emissivity to be correct.

The derived bias correction patterns as illustrated in Figure 2-12.

Note that the same IASI bias correction patterns are used for Metop-A and B; the same CrIS bias correction patterns are used for SNPP and JPSS-1/NOAA-20.

2.6.1.3 Measurement covariance

For the v1 IASI scheme, the measurement covariance, $\boldsymbol{S_y}$, was determined by Eumetsat using the same set of 3 days of measurements and RTTOV simulations (based on PWLR), as was used for the derivation of the mean and scan dependent bias correction. The bias correction was applied to the measurements (Equation 5) and the statistics of the difference between bias-corrected measurement and simulation were used to populate the covariance. Since PWLR is "trained" using the same version of NWP data, this leads to a covariance matrix in representing errors in the simulations from atmospheric effects not included in PWLR (minor gas variability, surface spectral emissivity, residual cloud, aerosol etc) as well as random error in the measurements themselves. Errors are generally significantly larger than the IASI NESR, with significant cross-channel correlations.

It is not straightforward to extend this approach to the retrieval of minor gases, not represented by the PWLR, or to CrIS, for which PWLR retrievals are not available.[2] For the Metop IMS-extended scheme the following approach is adopted, with a view to adding the minor gas and ozone information without greatly changing the information content for temperature and humidity:

- The same covariance as used in the v1 scheme is adopted for the channels common to the original scheme and IMS-extended. This is intended to preserve similar information from the water vapour and temperature sensitive channels.
- Measurements above 2000cm^{-1} (none of which are used in the v1 scheme) are assumed to have random uncorrelated errors of 0.02mW/cm-1/m2/sr standard deviation, slightly larger than the IASI NESR in this region (Figure 2-1).
- New measurements in the ozone spectral range from 970-1080cm-1 are assumed to have random uncorrelated errors of 0.2 mW/cm-1/m2/sr standard deviation, comparable to the IASI NESR in this region (Figure 2-1).
- The specific channels added for NH_3, SO_2 and HCOOH are assumed to have error covariance defined by the sum of two terms:
    - Errors covariance which is fully correlated with a selected nearby "reference" window channel from the v1 scheme, i.e. this first term has

[2] The approach of using ERA-5 data instead of PWLR to derive bias correction patterns for CrIS, is not suitable for also deriving the measurement covariance matrix, because there are large additional quasi-random model differences between ERA-5 and the "true" atmospheric state relevant to the CrIS observation time/location, which would lead to grossly increased estimated measurement errors. ERA-5 can be used to derive the bias patterns because these quasi-random errors cancel out in the averaging performed to obtain the mean and scan dependent bias spectra.

the same standard deviation as the v1 covariance in the window channel, and the error is assumed fully correlated spectrally.

- A (smaller) random uncorrelated error with 0.2 mW/cm^{-1}/m^2/sr standard deviation.

This approach is intended to force the retrieval to fit spectral differences between the channels sampling the minor gas relatively closely, while allowing spectrally correlated differences consistent with the window channel error covariance. Channels where this two-term error covariance is used are indicated by the name of the relevant target gas in the second column of Table 2-3. Channels also used in the v1 scheme by the symbol “y” in this column, so the window channel used as reference for each gas is identified by “y” along with the name of the trace gas.

For CrIS the following approach is adopted.

- The instrument expected noise covariance is constructed using a typical NESR spectrum[3] (as illustrated in Figure 2-1). Correlations consistent with the Hamming apodisation function are included.
- Uncorrelated errors corresponding to a noise equivalent brightness temperature (NEBT) of 0.1K are added, as a crude estimate of limiting forward model errors. As shown in Figure 2-1, this assumed error is significantly larger than the CrIS NESR in most channels.
- In the isoprene spectral range from 890-908cm^{-1}, the two terms above are assumed to be fully spectrally correlated across that range and an additional uncorrelated random error of 0.021 mW/cm^{-1}/m^2/sr standard deviation is added. This effectively means that within this spectral range, spectral differences are fitted to a precision of mW/cm^{-1}/m^2/sr (similar to the CrIS NESR) but correlated differences of up to ~0.16 mW/cm^{-1}/m^2/sr (0.1K NEBT) are allowed, the intention being to focus the fit on the isoprene spectral features, rather than continuum-like residual errors e.g. related to aerosol, cloud or surface properties.

[3] NESR for the first detector pixel recorded in a specific L1 file is used for this purpos: SNDR.SNPP.CRIS.20180815T2342.m06.g238.L1B.std.v02_05.G.180816084413.nc

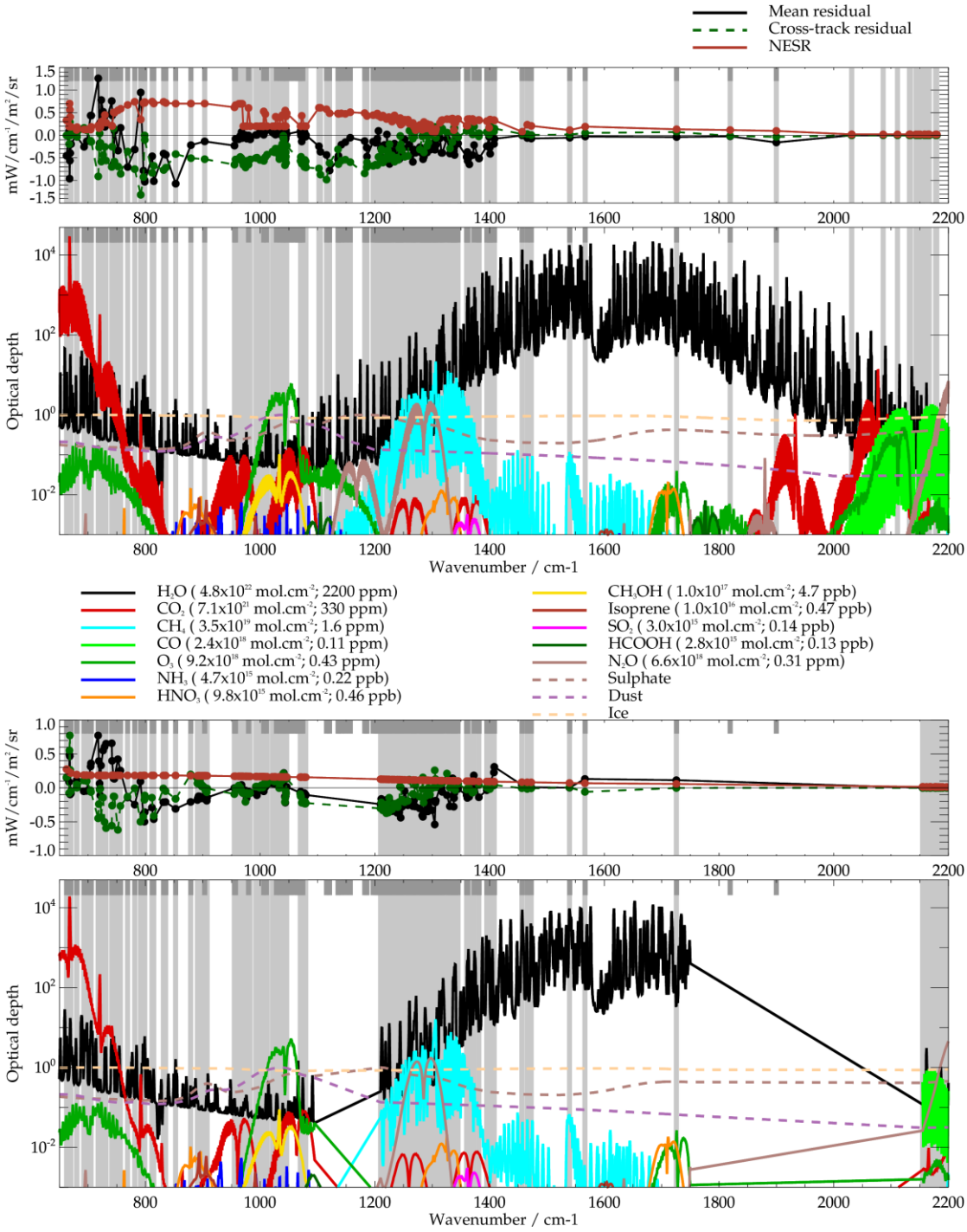

Figure 2-4 : Illustration of IMS spectral coverage, systematic residual spectral and assumed NESR, compared to trace gas and aerosol absorption spectra. Complete spectral range from 650 - 2200 cm-1. Upper pair of panels are for IASI; lower pair of panels are for CrIS. Light grey vertical bars indicate the spectral channels used by IMS-extended. Channels used by the previous IMS-v1 scheme are indicated by the smaller dark bars towards the top of each sub-panel.

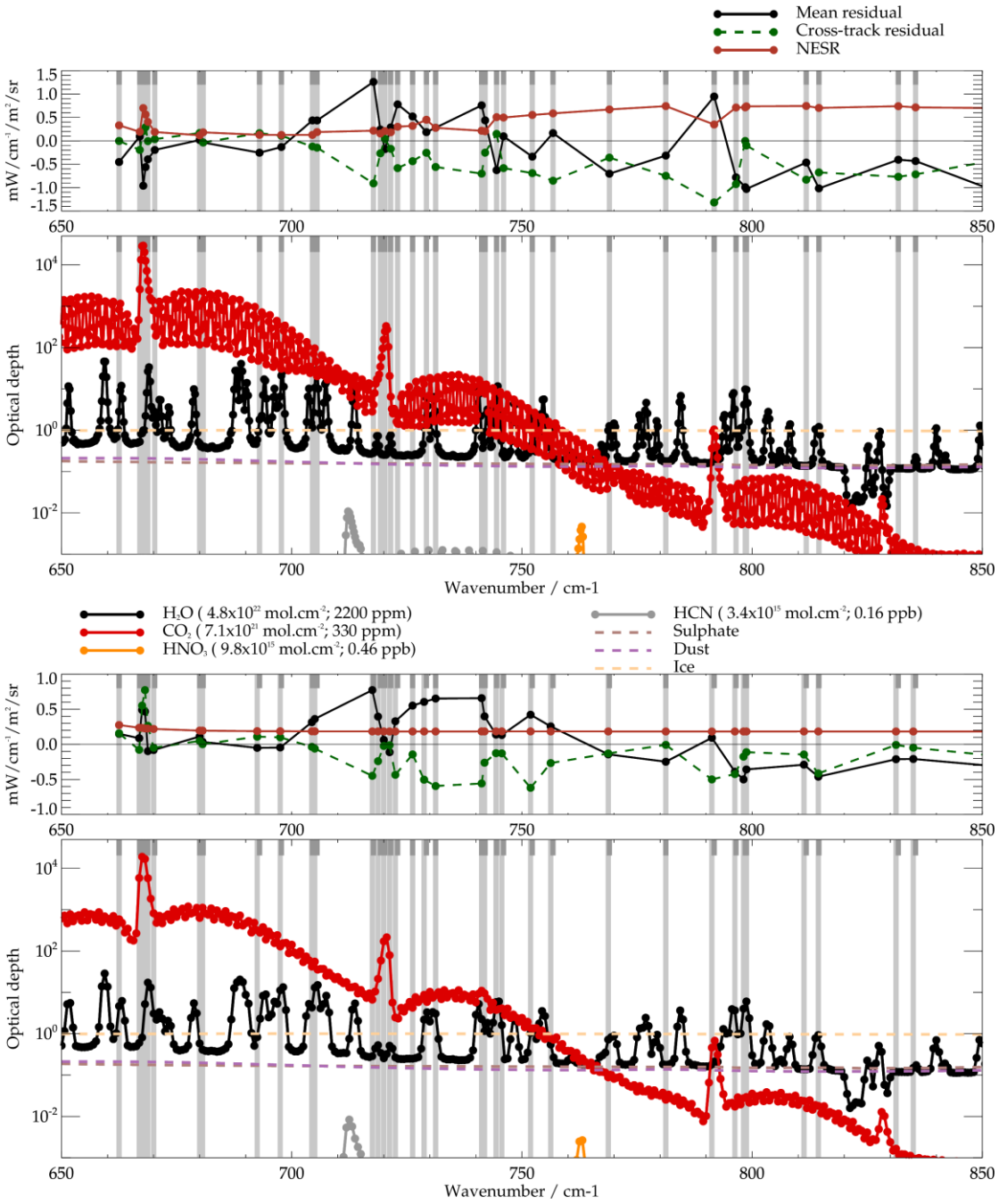

Figure 2-5 : Illustration of IMS spectral coverage, systematic residual spectral and assumed NESR, compared to trace gas and aerosol absorption spectra. Carbon dioxide / temperature sounding spectral range from 650 - 850 cm-1. Upper pair of panels are for IASI; lower pair of panels are for CrIS. Light grey vertical bars indicate the spectral channels used by IMS-extended. Channels used by the previous IMS-v1 scheme are indicated by the smaller dark bars towards the top of each sub-panel.

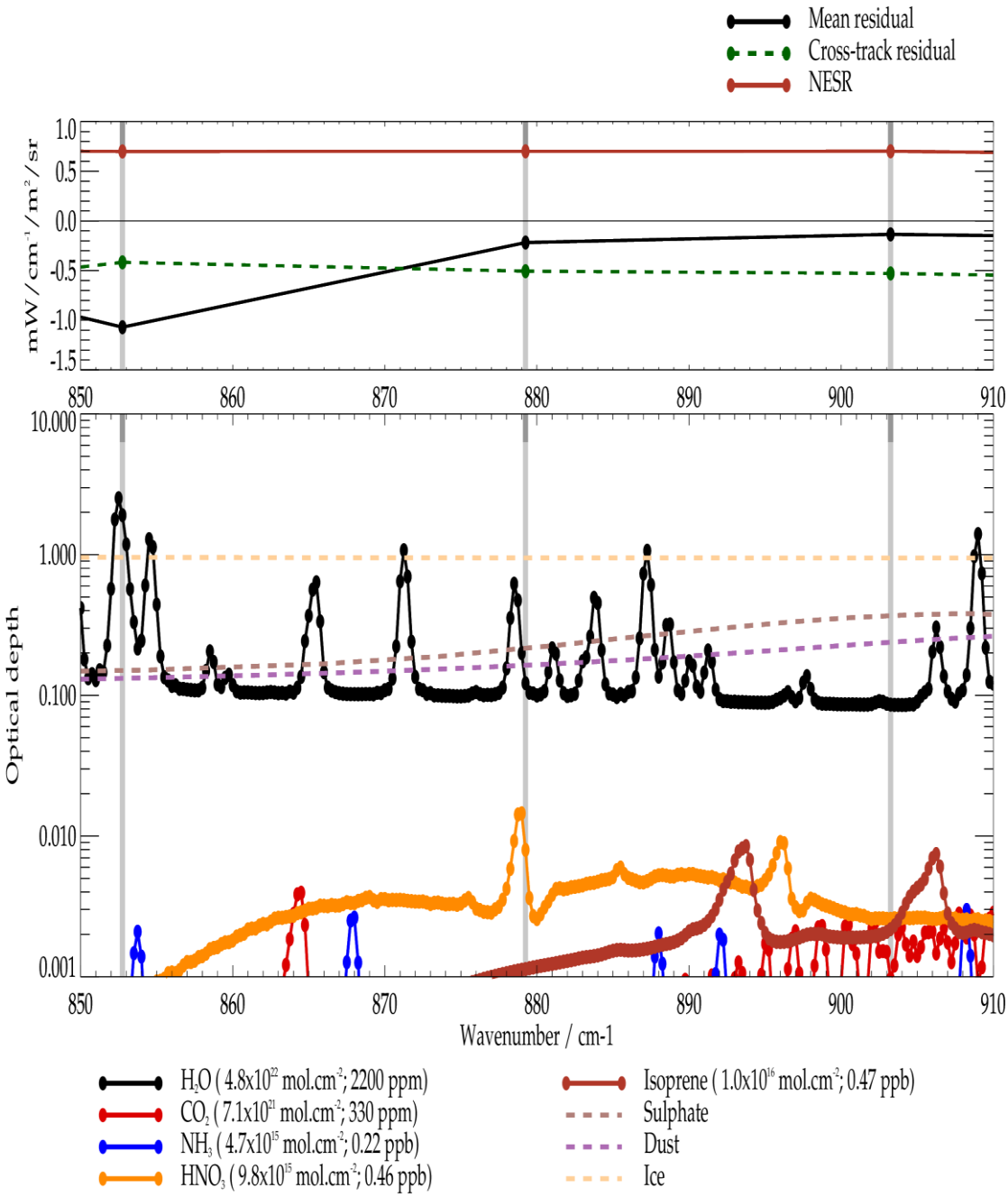

Figure 2-6 : Illustration of IMS spectral coverage, systematic residual spectral and assumed NESR, compared to trace gas and aerosol absorption spectra. Isoprene and nitric acide spectral range from 850 - 910 cm-1. Upper pair of panels are for IASI; lower pair of panels are for CrIS. Light grey vertical bars indicate the spectral channels used by IMS-extended. Channels used by the previous IMS-v1 scheme are indicated by the smaller dark bars towards the top of each sub-panel.

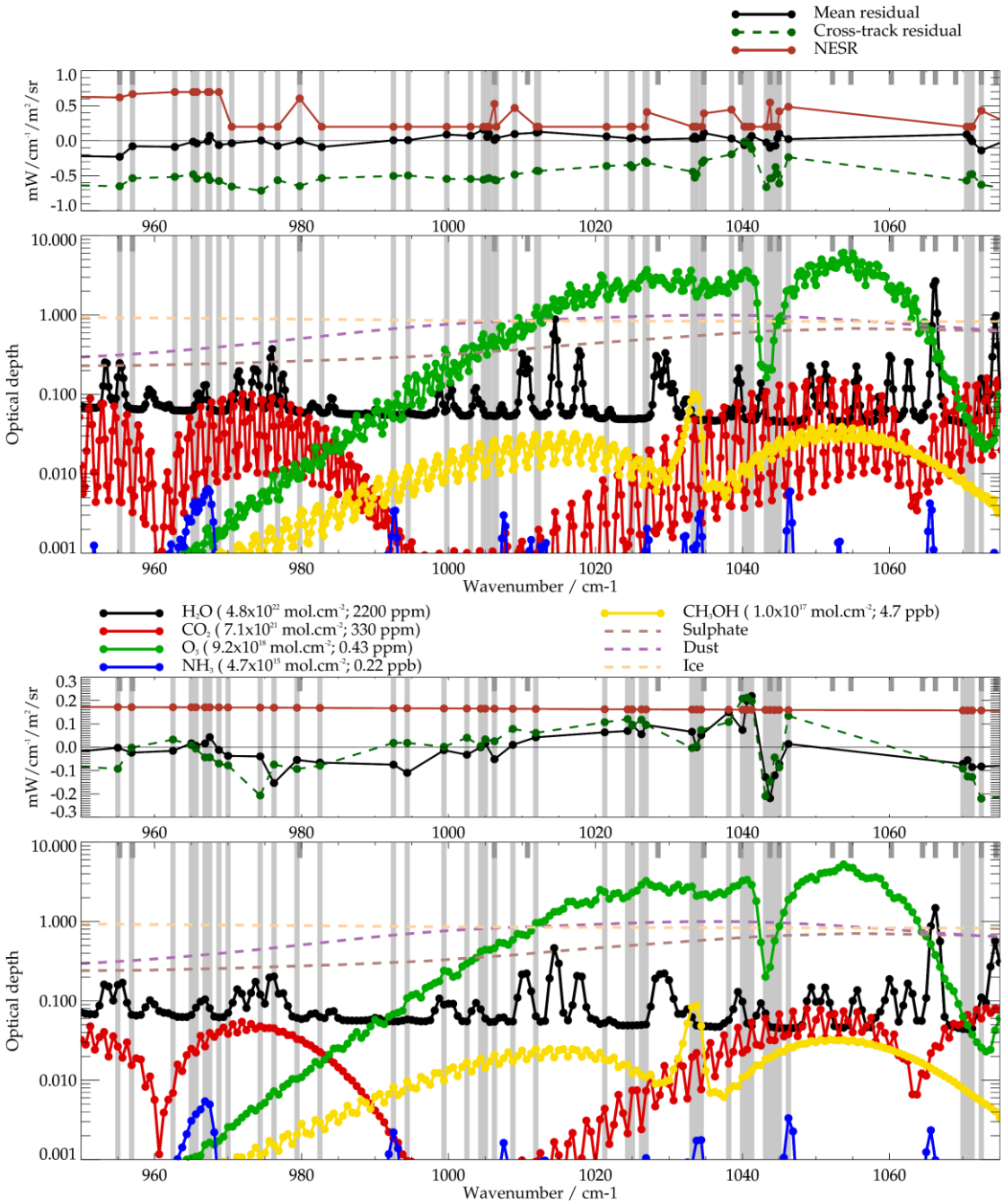

Figure 2-7 : Illustration of IMS spectral coverage, systematic residual spectral and assumed NESR, compared to trace gas and aerosol absorption spectra. Ozone and ammonia spectral range from 950 - 1075 cm-1. Upper pair of panels are for IASI; lower pair of panels are for CrIS. Light grey vertical bars indicate the spectral channels used by IMS-extended. Channels used by the previous IMS-v1 scheme are indicated by the smaller dark bars towards the top of each sub-panel.

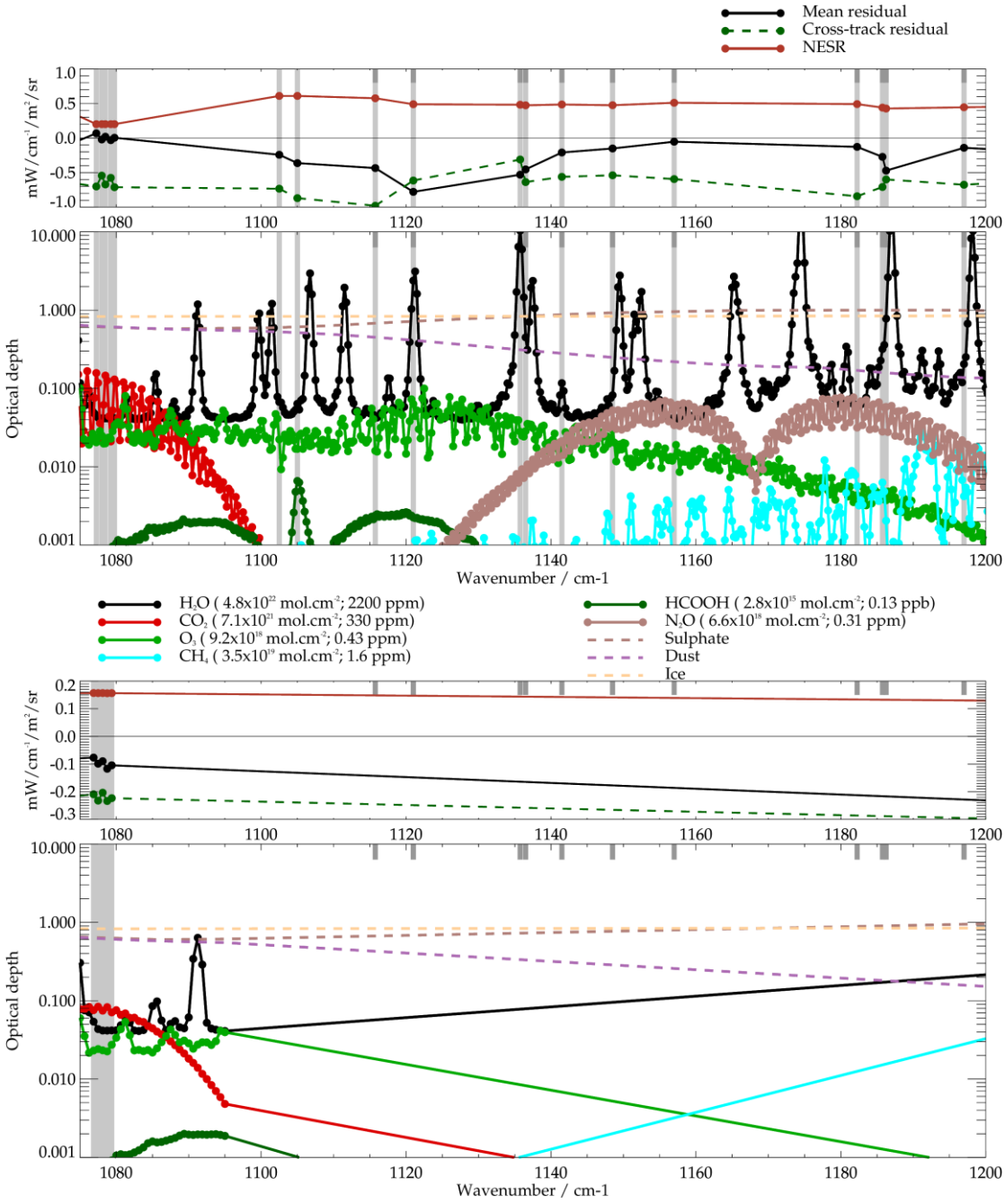

Figure 2-8 : Illustration of IMS spectral coverage, systematic residual spectral and assumed NESR, compared to trace gas and aerosol absorption spectra. Formic acid and water vapour spectral range from 1075 - 1200 cm-1. Upper pair of panels are for IASI; lower pair of panels are for CrIS. Light grey vertical bars indicate the spectral channels used by IMS-extended. Channels used by the previous IMS-v1 scheme are indicated by the smaller dark bars towards the top of each sub-panel.

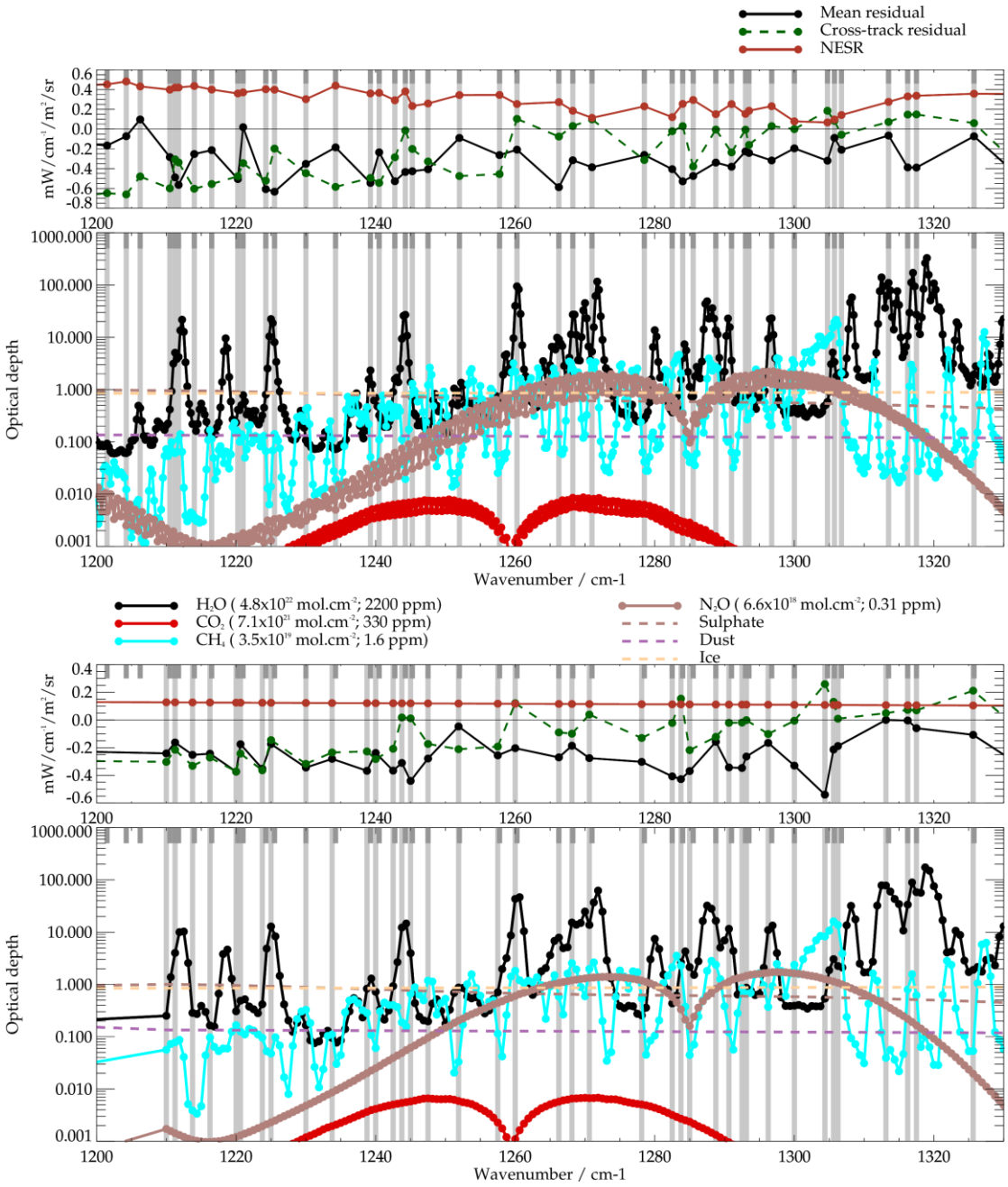

Figure 2-9 : Illustration of IMS spectral coverage, systematic residual spectral and assumed NESR, compared to trace gas and aerosol absorption spectra. Water vapour, methane and nitrous oxide spectral range from 1200 - 1330 cm-1. Upper pair of panels are for IASI; lower pair of panels are for CrIS. Light grey vertical bars indicate the spectral channels used by IMS-extended. Channels used by the previous IMS-v1 scheme are indicated by the smaller dark bars towards the top of each sub-panel.

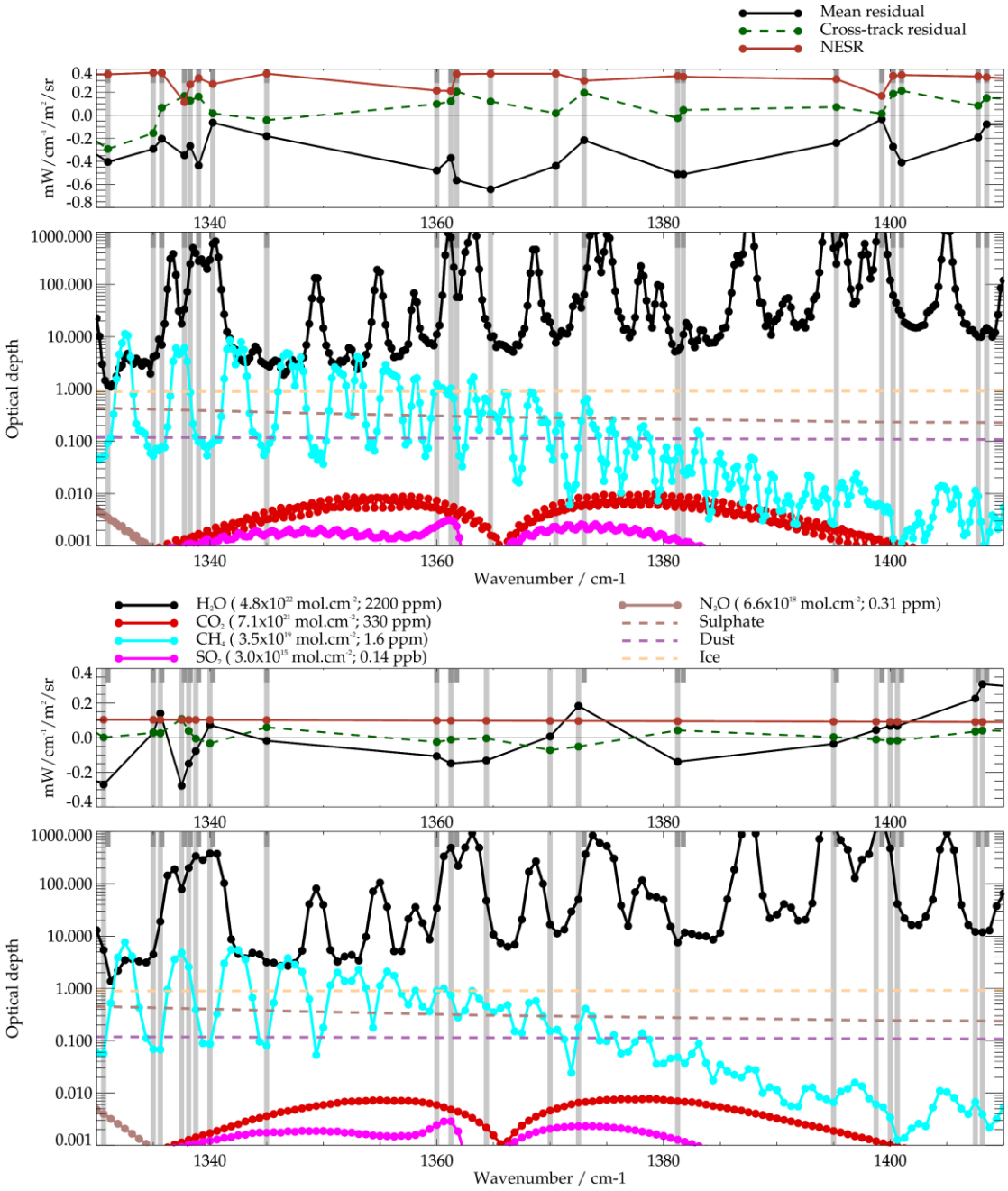

Figure 2-10 : Illustration of IMS spectral coverage, systematic residual spectral and assumed NESR, compared to trace gas and aerosol absorption spectra. Sulphur dioxide and water vapour spectral range from 1330 - 1410 cm-1. Upper pair of panels are for IASI; lower pair of panels are for CrIS. Light grey vertical bars indicate the spectral channels used by IMS-extended. Channels used by the previous IMS-v1 scheme are indicated by the smaller dark bars towards the top of each sub-panel.

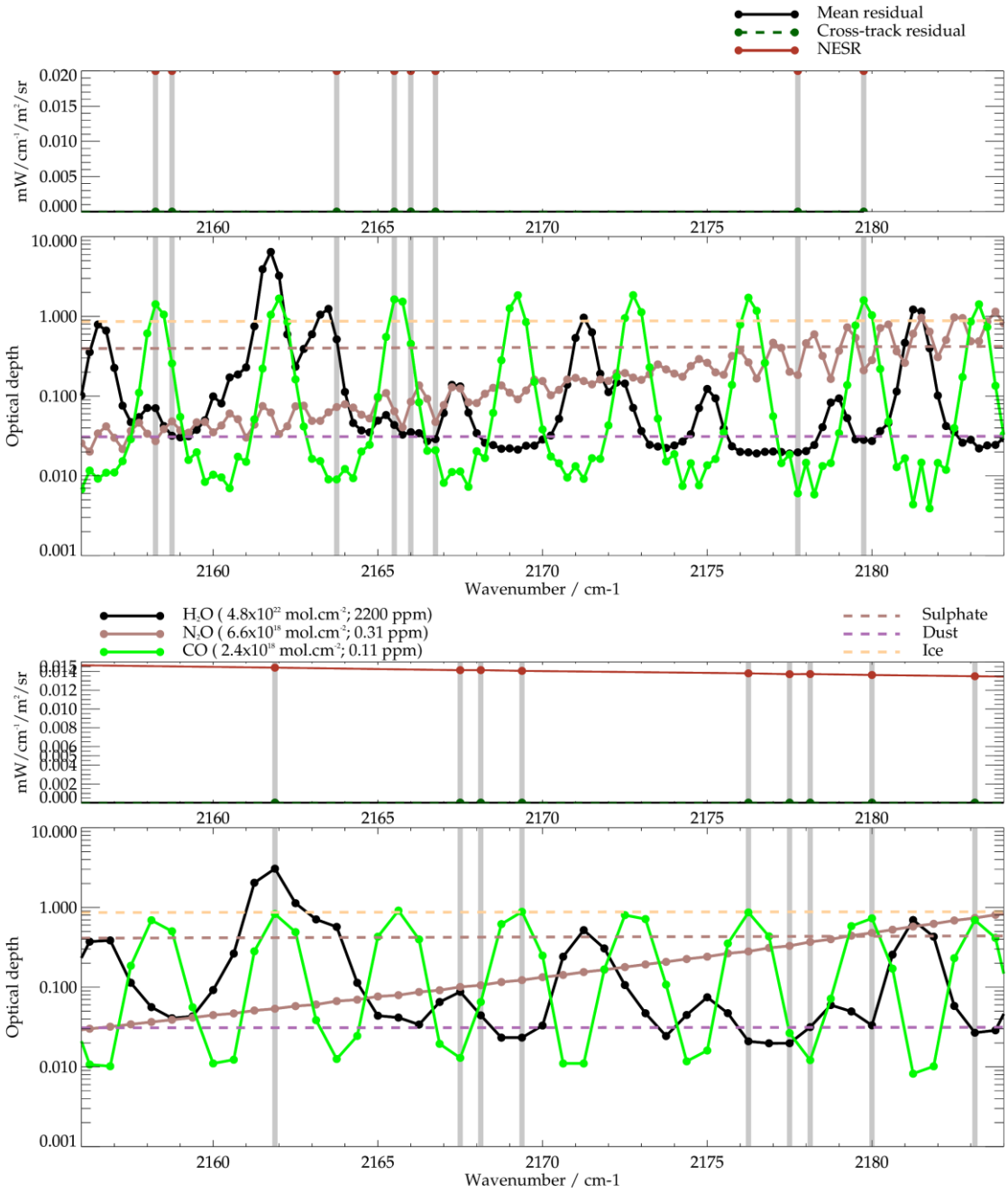

Figure 2-11 : Illustration of IMS spectral coverage, systematic residual spectral and assumed NESR, compared to trace gas and aerosol absorption spectra. Carbon monoxide spectral range from 2156 - 2184 cm-1. Upper pair of panels are for IASI; lower pair of panels are for CrIS. Light grey vertical bars indicate the spectral channels used by IMS-extended. Channels used by the previous IMS-v1 scheme are indicated by the smaller dark bars towards the top of each sub-panel.

IASI					CrIS			
Wave-number	V1?	Mean residual	Cross-track residual	NESR	Wave-number	Mean residual	Cross-track residual	NESR
cm^{-1}		$mW/cm^{-1}/m^2/sr$			cm^{-1}	$mW/cm^{-1}/m^2/sr$		
662.5	y	-0.45254	-0.00286	0.331096	662.5	0.149179	0.156156	0.275135
667	y	0.09308	-0.19434	0.192147	666.875	0.086977	-0.07801	0.235787
667.75	y	-0.95933	0.206869	0.699997	667.5	0.489463	0.551701	0.233565
668.25	y	-0.56131	0.291452	0.562344	668.125	0.467518	0.772194	0.226715
668.75	y	-0.39468	-0.00646	0.405571	668.75	-0.09723	0.264734	0.224887
670.25	y	-0.1952	0.035948	0.188097	670	-0.08135	-0.04896	0.218983
680	y	0.017899	0.167498	0.117238	680	0.111218	0.048709	0.195145
680.75	y	-0.03551	-0.03404	0.1809	680.625	0.035067	0.001918	0.194523
693	y	-0.25451	0.163769	0.127995	692.5	-0.0507	0.108862	0.187372
697.75	y	-0.13225	0.109027	0.125319	697.5	-0.04559	0.100085	0.186432
704.5	y	0.435983	-0.12141	0.12638	704.375	0.314887	-0.03652	0.18538
705.5	y	0.435442	-0.14609	0.187051	705	0.361301	-0.06126	0.185055
717.75	y	1.25909	-0.90919	0.217094	717.5	0.772403	-0.44893	0.183502
719.25	y	0.240908	-0.26805	0.156602	718.75	0.39463	-0.23987	0.183339
720.25	y	-0.17721	0.039748	0.207568	720	0.0635	-0.0234	0.183348
721.5	y	0.287368	-0.17047	0.1825	721.25	-0.11208	-0.01232	0.18273
723	y	0.778996	-0.58268	0.301309	722.5	0.32863	-0.43422	0.182925
726.25	y	0.520773	-0.43534	0.319925	726.25	0.551214	-0.14417	0.182696
729.25	y	0.185689	-0.25586	0.45005	728.75	0.604331	-0.50382	0.183133
731.25	y	0.27954	-0.55828	0.277633	731.25	0.651924	-0.59392	0.182963
741.25	y	0.758016	-0.70064	0.215086	741.25	0.657654	-0.5575	0.183717
742	y	0.437315	-0.25211	0.20404	741.875	0.398454	-0.26148	0.183657
744.5	y	-0.62676	0.148625	0.506223	744.375	0.138286	-0.12598	0.183623
746	y	0.096263	-0.58239	0.497805	745.625	0.133055	-0.12858	0.184068
752.25	y	-0.33796	-0.69017	0.552769	751.875	0.421428	-0.61973	0.183703
756.75	y	0.16554	-0.85263	0.586216	756.25	0.255609	-0.26683	0.183431
769	y	-0.70277	-0.35882	0.670277	768.75	-0.14297	-0.12989	0.183442
781.25	y	-0.31514	-0.74815	0.741602	781.25	-0.24762	-0.00747	0.182632
791.75	y	0.946238	-1.31669	0.34877	791.25	0.093276	-0.49977	0.182266
796.5	y	-0.78126	-0.92423	0.711819	796.25	-0.39012	-0.42444	0.182615
798.5	y	-0.99087	-0.00312	0.714891	798.125	-0.49962	-0.17595	0.182633
798.75	y	-1.02858	-0.09994	0.736431	798.75	-0.35784	-0.11178	0.182924
811.75	y	-0.46414	-0.83092	0.744797	811.25	-0.29007	-0.14532	0.183428
814.5	y	-1.01601	-0.67506	0.702507	814.375	-0.46121	-0.41488	0.183202
831.75	y	-0.40348	-0.76835	0.740048	831.25	-0.21188	-0.00853	0.18272
835.5	y	-0.432	-0.71627	0.714443	835	-0.20851	-0.04798	0.182667
852.75	y	-1.07033	-0.41671	0.69974	852.5	-0.30941	-0.16171	0.182878
879.25	y	-0.2177	-0.50623	0.701204	878.75	-0.20752	0.197823	0.179568
					890.625	-0.17924	0.065945	0.178248
					891.25	-0.1567	0.063898	0.178248
					891.875	-0.14826	0.093677	0.178248
					892.5	-0.12421	0.115592	0.178248
					893.125	-0.13543	0.088584	0.178248
					893.75	-0.12847	0.085625	0.178248
					894.375	-0.12819	0.088646	0.178248
					895	-0.12692	0.11317	0.178248
					896.875	-0.15555	0.056061	0.178248
					898.125	-0.153	0.020864	0.178248
					898.75	-0.13635	0.037389	0.178248
					900	-0.13448	0.027467	0.178248
					900.625	-0.14032	0.015106	0.178248
					901.875	-0.14709	0.005363	0.178248
					902.5	-0.13334	0.010137	0.178248
903.25	y	-0.13536	-0.5285	0.701589	903.125	-0.15369	-0.00328	0.178248
					903.75	-0.14634	-0.0137	0.178248
					904.375	-0.16919	-0.03655	0.178248
					905	-0.15669	-0.02814	0.178248
					906.875	-0.18998	-0.06472	0.178248
					907.5	-0.14262	-0.00917	0.178248
955.25	y	-0.22863	-0.64961	0.61843	955	-0.00231	-0.09248	0.171882
957	Y,NH3	-0.07825	-0.53533	0.666651	956.875	-0.02333	-0.00187	0.171511
962.75	NH3	-0.0874	-0.51545	0.696005	962.5	-0.01551	0.03272	0.171054
965.25	NH3	-0.01348	-0.47917	0.696005	965	0.016772	0.008931	0.170975
965.75	NH3	-0.03887	-0.54265	0.696005	965.625	0.006727	-0.00638	0.170972

IASI					CrIS			
Wave-number	**V1?**	**Mean residual**	**Cross-track residual**	**NESR**	**Wave-number**	**Mean residual**	**Cross-track residual**	**NESR**
cm^{-1}		**$mW/cm^{-1}/m^2/sr$**			**cm^{-1}**	**$mW/cm^{-1}/m^2/sr$**		
967.25	NH3	-0.00461	-0.50449	0.696005	966.875	0.016354	-0.04358	0.170724
967.5	NH3	0.07125	-0.56023	0.696005	967.5	0.04302	-0.04352	0.170685
968.75	NH3	-0.06253	-0.57389	0.696005	968.75	-0.01174	-0.06989	0.170746
970.5		-0.03511	-0.65392	0.2	970	-0.03717	-0.07809	0.170397
974.5		0.004211	-0.7129	0.2	974.375	-0.03934	-0.20682	0.170008
976.75		-0.07404	-0.56394	0.2	976.25	-0.15324	-0.0742	0.169398
979.75	y	-0.00305	-0.64801	0.603922	979.375	-0.0544	-0.09334	0.169147
982.75		-0.08934	-0.53402	0.2	982.5	-0.0659	-0.07903	0.168338
992.5		0.007146	-0.50254	0.2	992.5	-0.07465	0.018774	0.166996
994.5		0.008147	-0.49523	0.2	994.375	-0.10969	0.018725	0.166687
999.75		0.08909	-0.54482	0.2	999.375	-0.0128	0.001998	0.166087
1003		0.071307	-0.54553	0.2	1002.5	-0.03224	0.040543	0.165795
1004.75		0.159623	-0.55622	0.2	1004.375	2.60E-05	0.005	0.165264
1005.25		0.055043	-0.5418	0.2	1005	0.016328	0.033936	0.165253
1005.5		0.100761	-0.53301	0.2				
1006.25	y	0.010935	-0.55743	0.527366	1006.25	-0.05154	0.025475	0.165155
1006.5		0.038815	-0.56637	0.2				
1009		0.096086	-0.48269	0.468633	1008.75	0.010231	0.078499	0.164527
1012		0.115818	-0.42895	0.2	1011.875	0.042403	0.06132	0.163994
1012.25		0.12833	-0.43169	0.2				
1021.5		0.061984	-0.36	0.2	1021.25	0.063848	0.107035	0.16262
1024.75		0.033841	-0.34761	0.2	1024.375	0.069826	0.120499	0.162245
1025		0.041527	-0.37712	0.2	1025	0.09536	0.092398	0.162205
1026.75		0.013302	-0.29564	0.2	1026.25	0.055612	0.117955	0.162144
1027		0.018626	-0.31457	0.409908	1026.875	0.095418	0.096496	0.161982
1033.25		0.032783	-0.44184	0.2	1033.125	0.066093	-0.00353	0.161572
1033.5		0.059754	-0.52711	0.2				
1033.75		0.029454	-0.47718	0.2	1033.75	-3.54E-05	0.005435	0.161624
1034.5		0.050573	-0.31262	0.2	1034.375	0.0518	0.073552	0.161438
1034.75	y	0.11066	-0.28164	0.390313				
1038.5		0.031854	-0.19303	0.444121	1038.125	0.150203	0.108036	0.160965
1040.25		-0.06296	-0.01474	0.2	1040	0.073876	0.20843	0.160564
1040.5		-0.0453	-0.01087	0.2	1040.625	0.199169	0.21219	0.160557
1041		0.030866	-0.05932	0.2				
1041.25		0.068456	-0.11714	0.2	1041.25	0.219315	0.197627	0.16052
1043.25		-0.02521	-0.66168	0.2	1043.125	-0.1284	-0.20958	0.160028
1043.75	y	-0.10015	-0.53787	0.546601	1043.75	-0.21826	-0.14809	0.159692
1044		-0.07917	-0.53372	0.2				
1044.5		-0.06887	-0.37602	0.2	1044.375	-0.12085	-0.04376	0.159415
1044.75		0.037065	-0.4725	0.2				
1045	y	0.104169	-0.61017	0.41908	1045	-0.0713	-0.08651	0.15961
1046.25		0.023945	-0.23472	0.485005	1046.25	0.014003	0.134201	0.159464
1070.5		0.091462	-0.56786	0.2	1070	-0.07121	-0.09187	0.157748
1071		0.033519	-0.48216	0.2	1070.625	-0.05552	-0.12562	0.157692
1071.25		-0.00819	-0.47615	0.2	1071.25	-0.08537	-0.1278	0.157729
1072.5	y	-0.13826	-0.62816	0.430716	1072.5	-0.08262	-0.22015	0.157482
1077.25		0.067787	-0.70117	0.2	1076.875	-0.07661	-0.20949	0.156804
					1077.5	-0.09865	-0.23222	0.156504
1078		-0.02176	-0.54426	0.2	1078.125	-0.08958	-0.20349	0.156705
1078.5		0.018525	-0.6719	0.2	1078.75	-0.11704	-0.23369	0.155981
1079.25		-0.03124	-0.57649	0.2	1079.375	-0.10452	-0.22329	0.156454
1079.75		0.003491	-0.71173	0.2				
1102.5	HCOOH	-0.24264	-0.73367	0.608581				
1105	HCOOH	-0.36339	-0.86968	0.608581				
1115.75	Y,HCOOH	-0.43489	-0.9803	0.574779				
1121	y	-0.77888	-0.61523	0.488301				
1135.75	y	-0.53084	-0.31152	0.481196				
1136.5	y	-0.45449	-0.6376	0.472592				
1141.5	y	-0.20967	-0.56192	0.484701				
1148.5	y	-0.15162	-0.53937	0.474372				
1157	y	-0.054	-0.59438	0.509403				

IASI					CrIS			
Wave-number	**V1?**	**Mean residual**	**Cross-track residual**	**NESR**	**Wave-number**	**Mean residual**	**Cross-track residual**	**NESR**
cm^{-1}		**$mW/cm^{-1}/m^2/sr$**			**cm^{-1}**	**$mW/cm^{-1}/m^2/sr$**		
1182.25	y	-0.12828	-0.84236	0.490481				
1185.75	y	-0.27299	-0.70877	0.439522				
1186.25	y	-0.47173	-0.59994	0.425969				
1197	y	-0.14154	-0.67631	0.444191				
1201.5	y	-0.16643	-0.6487	0.451736				
1204.25	y	-0.0724	-0.66141	0.481482				
1206.25	y	0.096966	-0.47991	0.43123				
1210.5	y	-0.28362	-0.59986	0.398477	1210	-0.24165	-0.30304	0.127309
1211.25	y	-0.48896	-0.30628	0.420061	1211.25	-0.1629	-0.21579	0.127083
1211.75	y	-0.56508	-0.33763	0.420581				
1214	y	-0.25257	-0.60381	0.435702	1213.75	-0.25224	-0.33185	0.126471
1216.5	y	-0.2134	-0.55583	0.399554	1216.25	-0.24382	-0.27175	0.125847
1220.25	y	-0.50584	-0.47731	0.359923	1220	-0.37344	-0.37238	0.124993
1221	y	0.0189	-0.34463	0.370869	1220.625	-0.17525	-0.24294	0.124809
1224.25	y	-0.60806	-0.52239	0.402977	1223.75	-0.35238	-0.36375	0.124158
1225.5	y	-0.63346	-0.1979	0.398413	1225	-0.17393	-0.14562	0.123824
1230	y	-0.35201	-0.44629	0.302261	1230	-0.34424	-0.31737	0.122799
1234.25	y	-0.18553	-0.58502	0.439296	1233.75	-0.2814	-0.23504	0.122103
1239.25	y	-0.54487	-0.49429	0.360238	1238.75	-0.36742	-0.22763	0.121178
1240.5	y	-0.23532	-0.54483	0.3663	1240	-0.23862	-0.28291	0.120954
1242.75	y	-0.52746	-0.28555	0.291248	1242.5	-0.3661	-0.20825	0.120401
1244.25	y	-0.43389	-0.01417	0.380638	1243.75	-0.31059	0.017866	0.120196
1245.25	y	-0.42656	-0.20134	0.233192	1245	-0.4405	0.011349	0.119916
1247.5	y	-0.40691	-0.328	0.258425	1247.5	-0.27892	-0.1734	0.119375
1252	y	-0.08975	-0.47528	0.343826	1251.875	-0.04707	-0.21159	0.11847
1257.75	y	-0.2629	-0.45537	0.345146	1257.5	-0.25592	-0.19231	0.117376
1260.25	y	-0.20865	0.103146	0.253299	1260	-0.20411	0.121021	0.116915
1266.25	y	-0.58833	-0.07579	0.27273	1266.25	-0.27048	-0.08995	0.11568
1268.25	y	-0.31573	0.031109	0.185137	1268.125	-0.18647	-0.09911	0.115339
1271	y	-0.38652	0.098102	0.113414	1270.625	-0.27568	0.039237	0.114905
1278.5	y	-0.26192	-0.31328	0.22983	1278.125	-0.30275	-0.13038	0.113632
1282.5	y	-0.40586	-0.02186	0.120761	1282.5	-0.40767	-0.02177	0.112799
1284	y	-0.52862	0.029566	0.254436	1283.75	-0.42775	0.153801	0.11259
1285.5	y	-0.47472	-0.37872	0.294128	1285	-0.36928	-0.21815	0.112316
1288.75	y	-0.33918	-0.00535	0.150627	1288.75	-0.15792	-0.12247	0.111665
1291	y	-0.38113	-0.23606	0.25239	1290.625	-0.34307	-0.02088	0.111308
1293	y	-0.22615	-0.0066	0.153286	1292.5	-0.3472	-0.01916	0.110985
1293.5	y	-0.24167	-0.16048	0.185171	1293.125	-0.26456	-0.00145	0.110922
1296.75	y	-0.31782	0.029998	0.231371	1296.25	-0.16571	-0.10144	0.110251
1300	y	-0.19532	-0.00071	0.07802	1300	-0.3302	-0.00565	0.109515
1304.75	y	-0.31991	0.184988	0.066993	1304.375	-0.54003	0.258555	0.10862
1305.75	y	-0.08937	0.082471	0.096703	1305.625	-0.2139	0.130702	0.108354
1306.75	y	-0.2098	-0.05712	0.142154	1306.25	-0.18849	0.008992	0.108211
1313.5	y	-0.06538	0.071773	0.274801	1313.125	-8.14E-05	0.049261	0.106875
1316.25	y	-0.38808	0.146461	0.330228	1316.25	-0.00407	0.072867	0.106247
1317.5	y	-0.38973	0.148066	0.337084	1317.5	-0.05967	0.069462	0.106062
1325.75	y	-0.07306	0.060203	0.35738	1325.625	-0.10764	0.211325	0.104593
1331	y	-0.40458	-0.29277	0.354959	1330.625	-0.2714	0.001676	0.103885
1335	y	-0.29246	-0.15489	0.368577	1335	0.029497	0.028385	0.103279
1335.75	y	-0.20457	0.065496	0.366812	1335.625	0.140355	0.025903	0.103187
1337.75	y	-0.34703	0.166321	0.113408	1337.5	-0.27787	0.108507	0.102898
1338.25	y	-0.26703	0.125412	0.266699	1338.125	-0.15057	0.039342	0.102806
1339	y	-0.43618	0.161164	0.321598	1338.75	-0.07707	-0.00496	0.10267
1340.25	y	-0.06398	0.016375	0.270612	1340	0.072534	-0.03296	0.102487
1345	y	-0.1809	-0.0425	0.360807	1345	-0.01722	0.059689	0.101701
1360	y	-0.47945	0.096966	0.213166	1360	-0.10681	-0.02487	0.098956
1361.25	y	-0.37067	0.120539	0.210666	1361.25	-0.14891	-0.01073	0.098708
1361.75	y	-0.56455	0.20543	0.357054				
1364.75	SO2	-0.64186	0.119215	0.359777	1364.375	-0.13202	-0.00352	0.09816
1370.5	SO2	-0.43866	0.017526	0.359777	1370	0.007395	-0.07173	0.097241
1373	Y,SO2	-0.21626	0.195005	0.299064	1372.5	0.183864	-0.05127	0.096746
1381.25	y	-0.51163	-0.02515	0.339702	1381.25	-0.13912	0.042416	0.095294
1381.75	y	-0.51206	0.045238	0.33307				
1395.25	y	-0.24013	0.070762	0.312733	1395	-0.03559	0.003898	0.093001

IASI					CrIS			
Wave-number	**V1?**	**Mean residual**	**Cross-track residual**	**NESR**	**Wave-number**	**Mean residual**	**Cross-track residual**	**NESR**
cm^{-1}		**$mW/cm^{-1}/m^2/sr$**			**cm^{-1}**	**$mW/cm^{-1}/m^2/sr$**		
1399.25	y	-0.03425	0.013673	0.167363	1398.75	0.044504	-0.00998	0.092277
1400.25	y	-0.27289	0.185406	0.341412	1400	0.067838	-0.01793	0.092086
1401	y	-0.40978	0.212603	0.348605	1400.625	0.067374	-0.01644	0.092041
1407.75	y	-0.19153	0.082756	0.336909	1407.5	0.226425	0.035567	0.090811
1408.5	y	-0.07839	0.149255	0.329479	1408.125	0.309707	0.041519	0.090738
1456.75	y	-0.00281	0.026821	0.07835	1456.25	0.042777	-0.00529	0.08374
1465.75	y	-0.06018	0.026501	0.233574	1465.625	0.068284	-0.01618	0.082272
1472.75	y	-0.07154	0.005482	0.207917	1472.5	0.00807	-0.00679	0.081192
1539.75	y	-0.0547	0.01548	0.114161	1539.375	0.002092	0.005892	0.071752
1566.75	y	-0.02794	0.050313	0.19162	1566.25	0.131268	-0.05959	0.068124
1726	y	-0.03976	0.072946	0.133115	1725.625	0.112996	-0.00191	0.057682
1819.5	y	-0.02373	-0.01398	0.115777				
1900	y	-0.15952	-0.03641	0.096751				
2031.25		0	0	0.02				
2031.5		0	0	0.02				
2086.25		0	0	0.02				
2111.25		0	0	0.02				
2132		0	0	0.02				
2132.75		0	0	0.02				
2133.5		0	0	0.02				
2143.25		0	0	0.02				
2147		0	0	0.02				
2150.75		0	0	0.02				
					2155	0	0	0.014706
					2155.625	0	0	0.014672
2158.25		0	0	0.02				
2158.75		0	0	0.02				
					2161.875	0	0	0.014398
2163.75		0	0	0.02				
2165.5		0	0	0.02				
2166		0	0	0.02				
2166.75		0	0	0.02	2167.5	0	0	0.014131
					2168.125	0	0	0.014137
					2169.375	0	0	0.014054
					2176.25	0	0	0.013794
2177.75		0	0	0.02	2177.5	0	0	0.013703
					2178.125	0	0	0.013719
2179.75		0	0	0.02	2180	0	0	0.013619
					2183.125	0	0	0.013486
					2186.875	0	0	0.013338
					2190	0	0	0.01326
					2196.875	0	0	0.012914

Table 2-3: Definition of Channels used for IASI (right) and CrIS (left), together with the assumed mean and cross-track bias correction patterns and NESR. In the second column, IASI channels used in the version 1 IMS scheme are indicated by "y". Channels which are used for a specific minor gas signature are indicate by "NH3", "HCOOH", "SO2" in the same column. Rows in the table are organised such that IASI and CrIS with similar centre wavenumber are shown side-by-side.

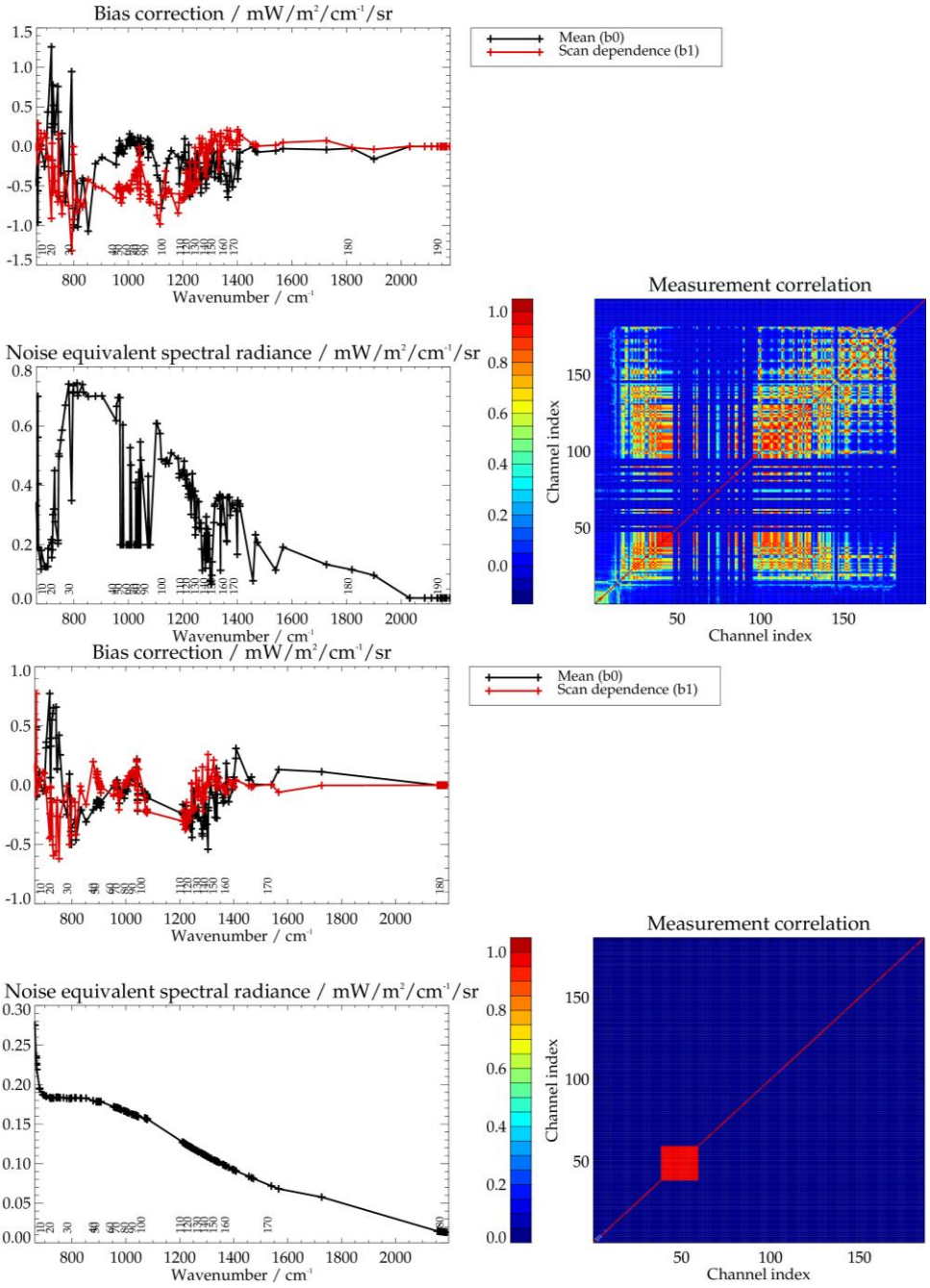

Figure 2-12 : Illustration of the IASI (upper panels) and CrIS (lower) bias correction and measurement error covariance. In each set of panels, the top left-hand panel shows the bias correction parameters. Numbers above the x-axis give the channel index from the subset used for the particular instrument. The bottom left panel in each set shows the estimated noise-equivalent spectral radiance, i.e. the square-root diagonal elements of the measurement covariance matrix. Bottom right shows the assumed measurement correlation matrix.

2.6.2 Microwave sounders

2.6.2.1 Channel selection

All channels of the microwave sounders would be used, however due to issues with specific channels on the Metop sounders the following channels are excluded, in order that a consistent set of channels can be used for each platform throughout the period processed:

- Metop-A: Channel 7 and 8 are excluded.
- Metop-B: Channel 15 is excluded. Channel 7 is excluded in data since November 2022.

The impact of excluding these channels was checked in the Eumetsat study ([RD01]) and found to be very small.

For SNPP/JPSS, all channels of AMSR are used.

2.6.2.2 Biasi correction and measurement covariance

An across track-bias dependent bias correction is applied to the AMSU and MHS measurements. The approach is the same for v1 IMS and IMS-extended. This was derived based on methods developed during the Eumetsat study ([RD01]) as follows:

- IMS is run without using the microwave channels to process 2-3 days of data (depending on the sensor):
  - Metop A: 23 March 2010, 17 October 2013
  - Metop B: 17 April, 17 July, 17 October 2013.
  - Suomi-NPP and JPSS-1: 15 April, 15 July, 14 October 2018.
- The resulting profiles are then used to simulate radiances in the microwave sounder channels over strictly cloud-free sea, between 60S and 60N (to avoid ice covered sea). The sea surface emissivity is modelled using the model internal to RTTOV.
- Differences between simulations and observations are averaged into six regularly spaced cross-track bins.
- The resulting mean differences are interpolated in cross-track index to obtain the bias correction applicable to a given scene.

The observation covariance assumed in the retrievals ($\boldsymbol{S}_y$) was also derived by computing the covariance of differences between simulations and the bias corrected

measurements, using the same set of cloud-free scenes over sea. A 3-sigma test was applied to exclude outliers.

The bias correction and measurement covariance are illustrated for the Metop sensors in Figure 2-13 and for S-NPP and JPSS1 in Figure 2-14.

Note that:

- Computed in this way, the bias correction and the measurement error covariance reflect a combination of errors in the measurements themselves and in the assumed forward model.
- Although he bias correction and measurement errors are computed from scenes over cloud-free sea only, but they are used for observations over both land and sea and in cloudy conditions. I.e. it is implicitly assumed that instrument and forward model errors are similar over both land and sea and in cloudy scenes.
- IASI measurement errors are assumed to be uncorrelated with those of AMSU and MHS.

2.6.3 Selection of scenes

In the version 1 processing, a simple brightness temperature difference test was applied to detect optically thick and/or high altitude cloud: This selection is based on the difference in brightness temperature between the IASI observation at 950 cm-1 and that simulated on the basis of the first guess state, which (as described below) is based on NWP analysis. If this difference (observation – simulation) is outside the range of -5 to 15K, the scene was not processed.

In the IMS-extended processing all scenes are now processed (including cloud). The brightness temperature difference test is still performed and the result reported as a flag in L2 output files.

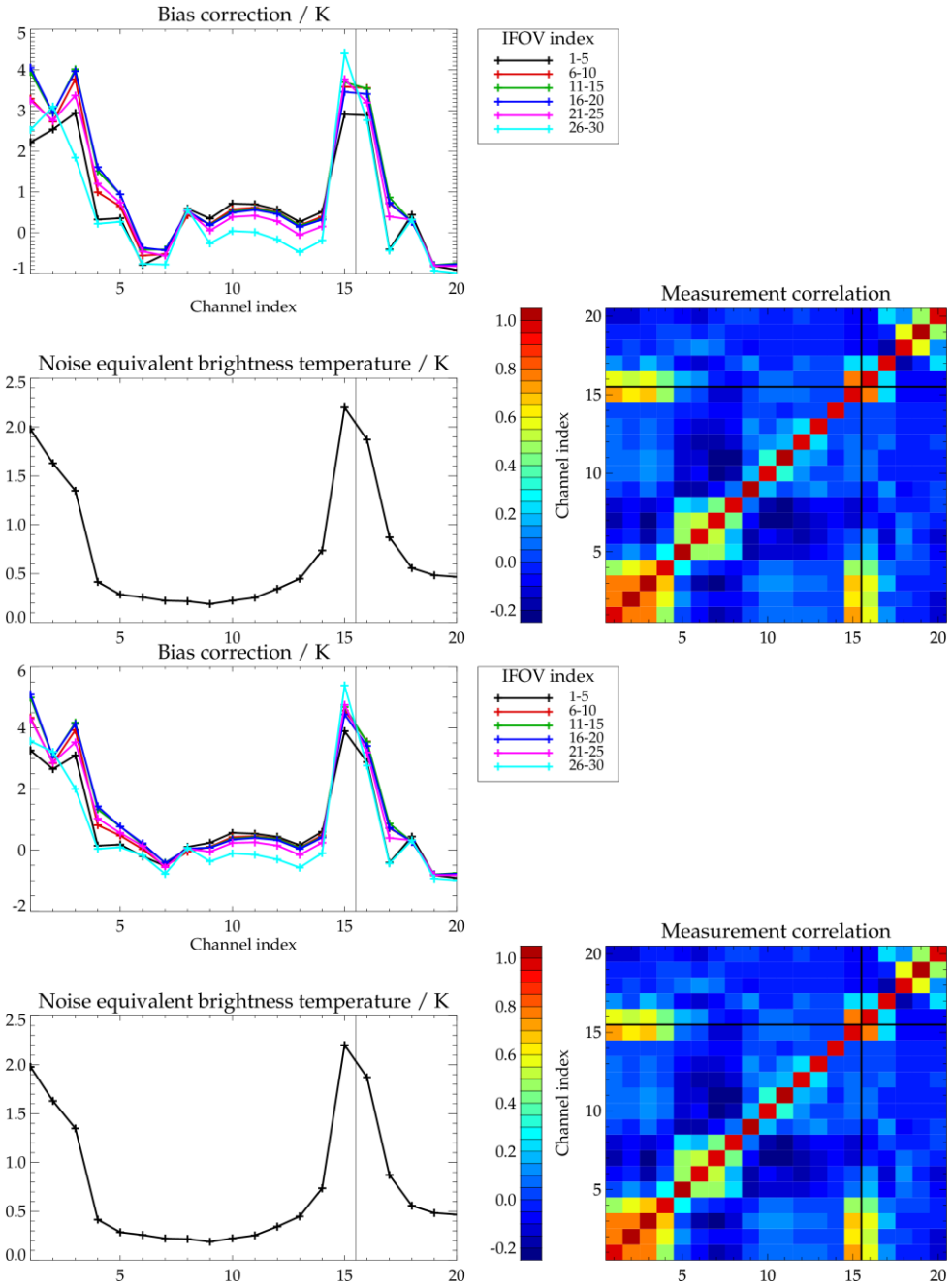

Figure 2-13 : Illustration of the Metop AMSU (channel index 1-15) and MHS (16-20) bias correction and measurement error covariance. Top left-hand panel shows the derived bias correction (top left) as a function of across-track IFOV index. Bottom left shows the estimated noise-equivalent brightness temperature (in K), i.e. the square-root diagonal elements of the measurement covariance matrix. Bottom right shows the measurement correlation matrix. Upper panels show Metop-A; lower panels show Metop-B.

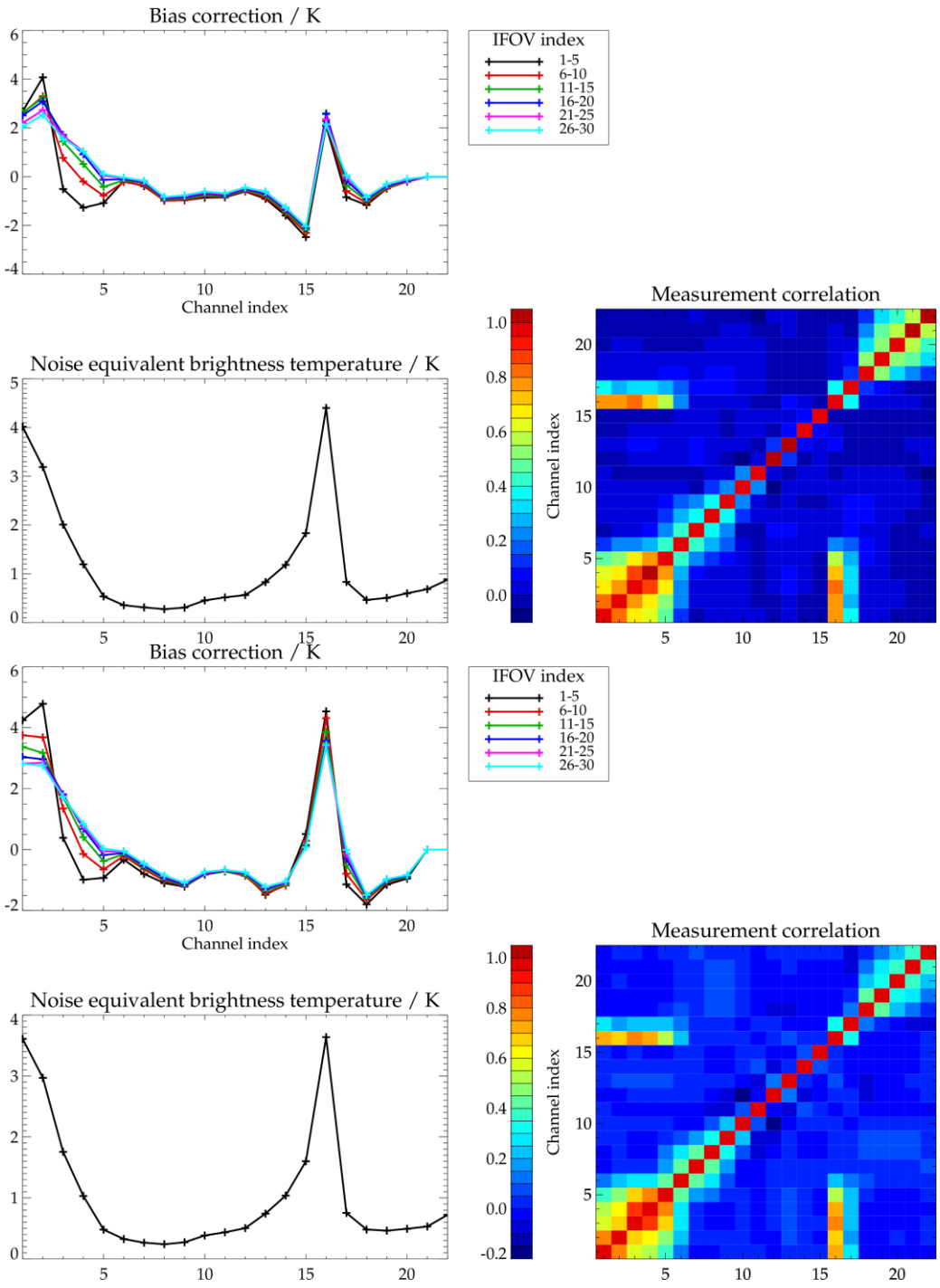

Figure 2-14 : Illustration of the ATMS bias correction and measurement error covariance. Top left-hand panel shows the derived bias correction (top left) as a function of across-track IFOV index. Bottom left shows the estimated noise-equivalent brightness temperature (in K), i.e. the square-root diagonal elements of the measurement covariance matrix. Bottom right shows the measurement correlation matrix. Upper panels show Suomi-NPP; lower panels show JPSS-1.

2.7 Forward model

2.7.1 RTTOV version

IMS uses RTTOV as the core radiative transfer model. RTTOV estimates radiances convolved with the IASI spectral response function by calculating spectrally-averaged layer transmittances, based on a fixed set of coefficients which weight atmospheric-state-dependent predictors. The model is sufficiently fast to enable global processing of the with available computational resources.

In the v1 scheme RTTOV version 10.2 ([RD13]) was used.

In IMS-extended version 12.2 ([RD14]) is now used.

2.7.2 RTTOV coefficients

The version 1 scheme used the following RTTOV coefficient files (obtained from the NWP SAF website):

- AMSU and MHS: Version 7 coefficients on 54 levels created on 16 May 2013. (Filenames rtcoef_metop_1_amsua.dat and rtcoef_metop_1_mhs.dat.)
- IASI: Version 9 coefficients on 101 levels created on 28 March 2013. (Filename rtcoef_metop_2_iasi.dat.)

With version 7 coefficients, RTTOV can simulate variations in water vapour and ozone (sufficient for modelling the MW channels). Most other trace-gases with significant absorption are included in the modelled transmissions assuming a fixed profile.

Version 9 coefficients enables RTTOV to also simulate variations in carbon dioxide (CO_2), methane (CH_4), nitrous oxide (N_2O) and carbon monoxide (CO).

The IMS-extended scheme uses the same version of AMSU and MHS coefficients. The IASI coefficients are updated to the NWP SAF version with creation date 5 December 2016 (rtcoef_metop_2_iasi.H5). In IMS-extended cloud and aerosol are simulated for IASI using cloud and aerosol properties contained in the further files (obtained from the NWP SAF website):

- Aerosol properties are simulated based on the file scaercoef_metop_2_iasi_cams.H5, with creation date 17 February 2018. This file is modified as described in section 2.7.6, below.
- Cloud properties are simulated using sccldcoef_metop_2_iasi.H5, with creation date: 22 July 2016.

For CrIS the following files are used :

- RTTOV9 coefficients on 101 levels created on 3 November 2016. (Filename rtcoef_jpss_0_cris-fsr.H5.)
- Aerosol properties are based on the NWP SAF provided file scaercoef_jpss_0_cris-fsr_cams.H5 with creation date 27 September 2018. The file is modifed as described in section 2.7.6, below.
- Cloud properties are modelled using the NWP SAF provided sccldcoef_jpss_0_cris-fsr.H5 with creation date 27 September 2018.

For ATMS, version 7 coefficients on 54 levels created on 29 January 2018 are used. (Filename rtcoef_jpss_0_atms.dat.)

2.7.3 Clear-sky atmospheric state

Profiles of water vapour, ozone, carbon monoxide and temperature are defined by the retrieval state vector (see below). The IMS scheme models the variations of the greenhouse gases (CO_2, CH_4 and N_2O) using a monthly latitude dependent climatology derived from MACC flux inversions. These profiles are defined on the 101 pressure levels on which the RTTOV 9 coefficients are given (for IASI). Profiles are interpolated from this grid to the coarse 54 level grid used for the MW coefficients. Surface temperature and surface emissivity are also defined by the state vector. 2m temperature and 2m water vapour (also input parameters to RTTOV) are defined by interpolating the profiles defined by the state vector.

Surface pressure is defined from NWP, adjusted to the mean altitude within the IASI footprint assuming the logarithm of the surface pressure varies linearly with the difference between the IASI altitude and that of the NWP model.

2.7.4 Surface spectral emissivity and reflectance

IMS retrieves the surface spectral emissivity as described in section 2.8.3.

Over land, IMS-extended uses the Lambertian surface reflectance model in RTTOV12 for IASI and CrIS. Over sea the previous specular reflection model is used. The specular reflection model is used over both and sea for the MW sensors.

The reflected component of terrestrial thermally emitted radiation is modelled internally within RTTOV (see [RD15]) and depends on the user defined spectral emissivity.

For the *solar* reflected contribution, which is modelled in channels above 2000cm^{-1}, a separate surface reflectance is defined. Over land, this is assumed to be

$$\boldsymbol{R} = \frac{1 - \boldsymbol{e}}{\pi}$$

Equation 7

Where $\boldsymbol{e}$ is the retrieved surface emissivity spectrum.

Over water surfaces, the retrieval fits a wavelength independent scale factor g_f which multiplies the default RTTOV water reflectance spectrum, $\boldsymbol{R_g}$, for the given view/solar geometry and wind speed (assuming wind speed for the scene from NWP analysis). This includes the effect of sun-glint. I.e. over water, for the solar contribution only, the retrieval assumes reflectance given by

$$\boldsymbol{R} = g_f \boldsymbol{R_g}$$

Equation 8

2.7.5 Cloud and aerosol modelling

RTTOV is capable of simulating cloud and aerosol either as scattering and absorbing profiles (defined in terms of profiles of cloud cover, liquid and ice water content). Alternatively, cloud can be modelled as a simple opaque black body at defined altitude, occupying a defined area fraction of the scene.

The simple black body model was adopted in the version 1 scheme. IMS-extended uses the more realistic cloud and aerosol models prescribed by the aerosol and cloud scattering coefficient files identified above. Note that cloud and aerosol are only explicitly modelled for the infra-red sounder (IASI/CrIS). IMS assumes the impact of cloud (and precipitation) on the microwave sounder observations is either negligible or can be accommodated by the co-retrieved microwave surface emissivity parameters. This assumption works well for most scenes, though high fit residuals are encountered in a subset of very cloudy scenes. Such cases can be identified via the reported solution cost function value and results should be considered unreliable.

IMS-extended uses the following RTTOV options to approximate multiple scattering when modelling cloud and aerosol:

- For channels below 2000cm^{-1}, the “Chou-scaling” approach is used (see [RD13]).
- For channels above 2000cm-1, the discrete ordinate method (DOM) is used with 2 computational streams (see [RD14]).

Cloud and aerosol are based on the pre-defined optical properties in the scattering coefficient files defined above. For liquid cloud the properties which are tabulated as a function of effective diameter are used. For ice cloud the SSEC/Baum parameters are used, specified in terms of effective diameter use the McFarquar parameterisation (see [RD15]). The user of RTTOV defines profiles of mass mixing ratio of each of the pre-defined cloud/aerosol types, together with the effective diameter profiles in the case of cloud. IMS defines these profiles based on the state vector parameters described in sections 2.8.5. Together with modelled radiances RTTOV (v12 onwards) returns the derivatives of the modelled radiance with respect to the assumed mass mixing ratio profiles, enabling the weighting functions needed for the OEM to be efficiently computed.

2.7.6 Aerosol optical properties

The aerosol scattering property files are modified explicitly for IMS to represent only the following aerosol types, needed to represent parameters retrieved by IMS:

- For sulphate aerosol (SA), based on the OPAC sulphate droplet ("SUSO") aerosol type, at zero relative humidity. The scattering parameters are taken directly from the NWP SAF provided aerosol scattering coefficient file.
- Coarse mode desert dust, assumed to have same size distribution parameters as the CAMS dust coarse mode provided in the NWP-SAF file[4], however using refractive indices for wind filtered Saharan sand collected from Mauritania by Peters (2009), acquired from the University of Oxford Aria Database[5]. The Oxford Mie scattering tools[6] were used to compute the single scattering parameters (single extinction coefficient scattering albedo, phase function).
- An artificial aerosol type which is purely absorbing (single scattering albedo=0) with no spectral dependence. This “aerosol” type is always modelled to have negligible optical depth in forward calculations but is included to obtain the corresponding radiance derivatives, subsequently used to model absorption by minor trace gases (see below).

---

[4] Log normal distribution with mode radius 0.29 microns, geometric standard deviation 2, and bin limits from 0.9 to 20 microns.

[5]http://eodg.atm.ox.ac.uk/ARIA/data?Sand_and_Dust/Sand/Saharan_sand/Mauritania_-_50%25_humidity_(Peters)/sand_50RH_peters_2009.ri

[6] http://eodg.atm.ox.ac.uk/MIE/index_nocol.html

The extinction coefficients of all the aerosol components in the modified file are normalise by their peak extinction in the IASI spectral range up to 2000cm^{-1}.

Extinction and absorption coefficients of the modelled aerosol and cloud are illustrated in figure Figure 2-15. Absorption coefficients are also illustrated in Figure 2-4 to Figure 2-9.

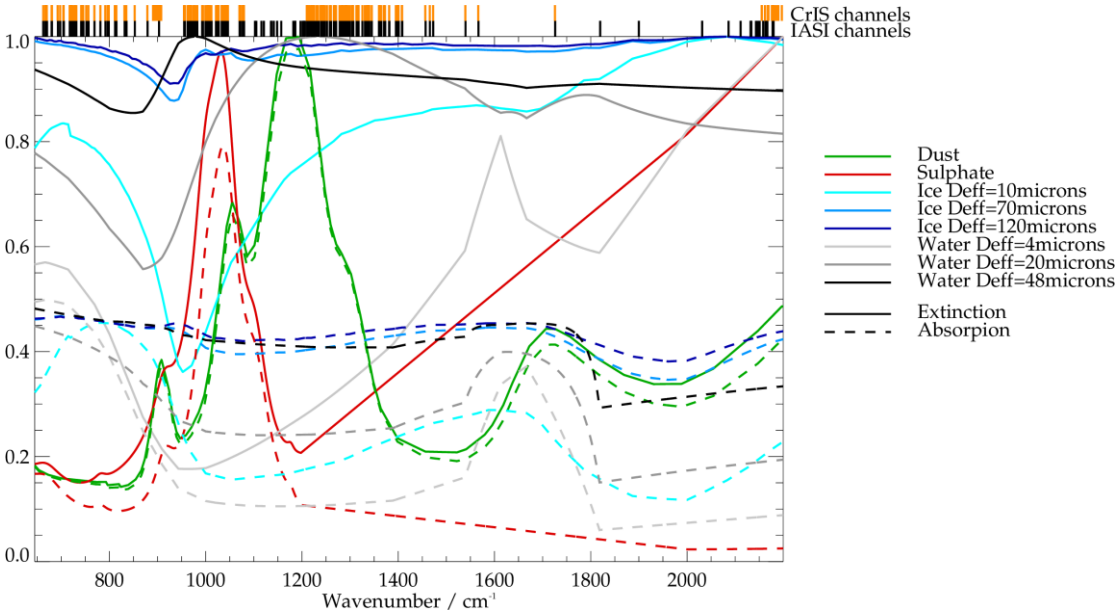

Figure 2-15 : Assumed aerosol and cloud extinction and absorption coefficients. Values are normalised by the peak extinction coefficient in the spectral range shown. Bars along the top of the panel indicated the selected spectral channels of IASI and CrIS.

2.7.7 Minor gas absorption

As described above, using standard v9 coefficients, RTTOV can simulate variable absorption by CO_2, CH_4, N_2O, H_2O, O_3 and CO. It assumes fixed profiles for some other minor trace gases, including HNO_3, NH_3 and SO_2. In IMS-extended, radiances which include variable minor trace gases, $R'(\boldsymbol{x})$, are simulated via a linear approximation. This is accomplished using weighting functions returned by RTTOV for the artificial pure-absorbing aerosol type (described above) as follows:

$$R'(\boldsymbol{x}) = R(\boldsymbol{x}) + \sum_j X_j C_j \sum_i \frac{dR(\boldsymbol{x})}{dk_i} n_{ij}$$

Equation 9

Where

- $R(\boldsymbol{x})$ is the RTTOV model simulation for a particular spectral channel, dependent on state vector, $\boldsymbol{x}$.
- X_j is the channel averaged absorption cross section (dimensions [m^2.$mole^{-1}$]) of the jth minor gas. In the current scheme these are assumed to be altitude independent. Minor gases simulated in this way (in IMS-extended) are HNO_3, NH_3, CH_3OH, HCOOH, SO_2 and isoprene. The cross section for isoprene is taken from Hitran(2018), convolved to match the IASI or CrIS spectral sampling. Cross sections for the other species are obtained from RFM ([RD32]) line-by-line calculations of the total nadir optical depth[7], which assume realistic profiles for each gas (illustrated in Figure 2-17). The total optical depth is convolved with the IASI/CrIS spectra response and then normalised by the column number density to obtain "column averaged" cross sections for each gas.
- n_{ij} define the assumed number density profile (dimensions [$mole.m^{-3}$]) of the jth minor gas in the ith RTTOV model layer (100 model fixed pressure layers use). In the case of gases included in RTTOV coefficients as fixed gases (HNO_3, NH_3), these profiles represent offsets from the RTTOV profile. In the current version of IMS-extended n_{ij} for all gases are correspond to a fixed, height independent volume mixing ratio of 1ppbv.
- C_j is a dimensionless, retrieved, height independent scaling factor for the assumed profile of the jth minor gas. In the current version of IMS-extended, since the profile which is scaled is height independent volume mixing ratio, retrieved scale factors are equivalent to the column averaged volume mixing ratio of the minor gas (i.e. the total number density of the minor gas divided by the total air number density). Again, this should be considered as an offset to the column-amount implicitly assumed in RTTOV for HNO_3 and NH_3.
- $\frac{dR(\boldsymbol{x})}{dk_i}$ is the derivative of the RTTOV calculation with respect to spectrally independent perturbation in absorption coefficient in ith layer (dimensions [radiance units]/[m^{-1}]).

This approach assumes the minor gas absorption is optically thin and spectrally uncorrelated with that of any optically thick absorber in the channel bandwidth (channels used for the minor gases are selected to avoid strong absorption by the water vapour and carbon dioxide). The approach does account for modulation and

[7] These calculations were performed by A.Dudhia (Univ.Oxford), and are also used in the zenith sky optical thickness browse tool here: http://eodg.atm.ox.ac.uk/ATLAS/zenith-absorption

obscuration of trace-gas absorption by cloud and aerosol as well as the main gases modelled explicitly by RTTOV. It is also important to note that it is possible to use the absorption coefficient derivatives to compute height-resolved "averaging kernels" for the retrieved scale factor, which give its derivative with respect to perturbations in the "true" trace gas profile, n_{ij}:

$$A_{ij} = \frac{d\widehat{C_j}}{dn_{ij}} = \sum_k G_{jk} X_{jk} \frac{dR_k(\boldsymbol{x})}{dk_{ik}}$$

Equation 10

Where $G_{jk} = \frac{d\widehat{C_j}}{dR_k(\boldsymbol{x})}$ are elements of the retrieval gain matrix for the state vector element corresponding to then scale factor for minor gas j and measurement vector element k (see section 2.9). These kernels can then be used to estimate what would be retrieved given an independent estimate of the profile shape (without re-running the retrieval), enabling e.g. the consistency between retrievals and models to be assessed without influence from the simple fixed mixing ratio profile assumed in the retrieval (see section 2.11.1).

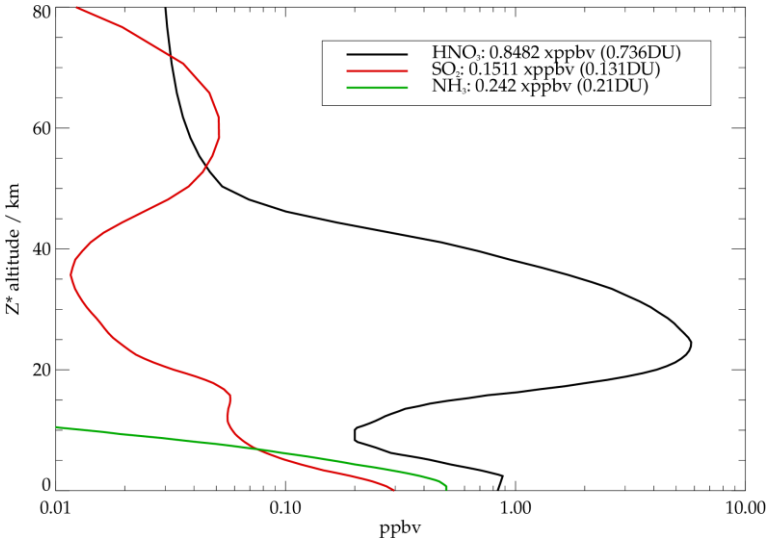

Figure 2-16 : Fixed minor gas profiles assumed in RTTOV. Figures in the legend give the corresponding column averaged mixing ratio and column amount in Dobson units (DU).

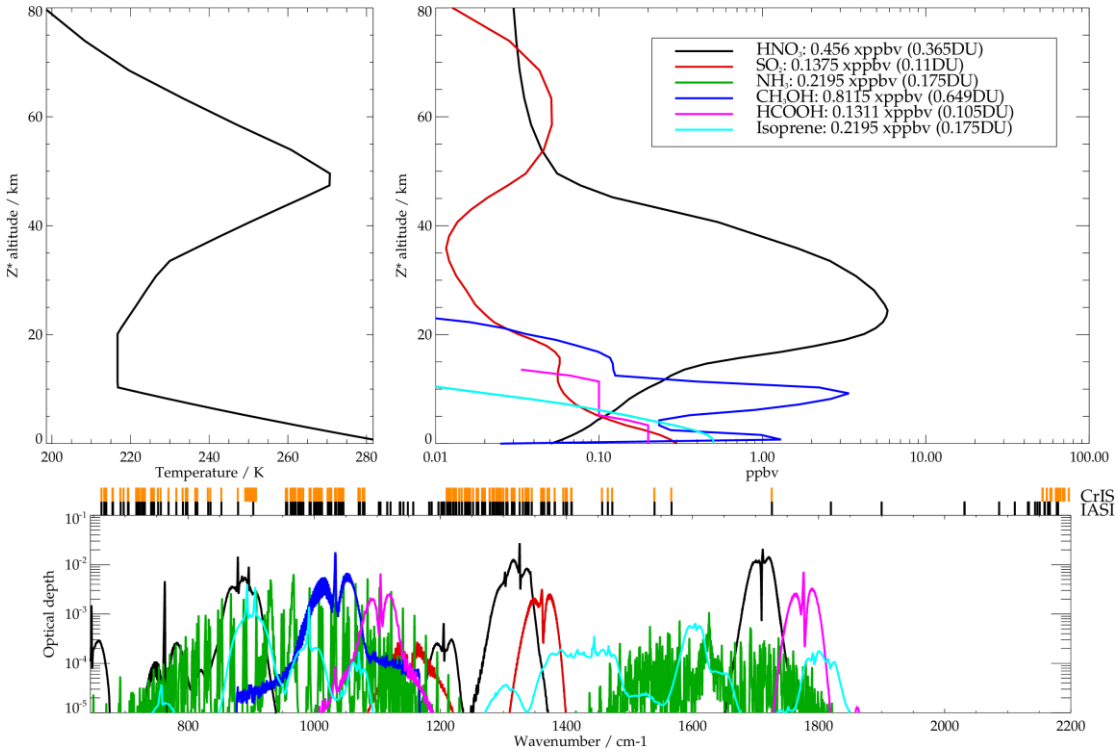

Figure 2-17 : Minor gas profiles assumed in RFM optical depth simulations used to define column-averaged minor gas cross-sections (upper right-hand panel). These are from the FASCODE U.S. Standard Atmosphere model with minor constituents (19 Dec. 1999). Upper left-hand panel shows the assumed temperature profile. Bottom panel shows the derived optical depths. Note that the same profile is assumed for ammonia (NH_3) and isoprene (the line for ammonia is hidden by that of isoprene in the upper left-hand panel).

2.8 IMS State vector

IMS jointly retrieves a number of products, which are represented in the state vector $\boldsymbol{x}$. Each of the products are defined individually below. Products are defined such that the *a priori* covariance is diagonal i.e. no correlations are assumed either between the elements corresponding to an individual product or between the different products.

2.8.1 Temperature, water vapour, ozone and carbon monoxide profiles

In IMS, H_2O, temperature, O_3 and CO profiles are internally represented using basis functions which are the Eigenvectors of an assumed covariance matrix which represents the prior variability of the profile on the 101 RTTOV pressure levels. In the original Eumetsat scheme the *a priori* state was defined from the PWLR and covariances were derived from differences between PWLR and ECMWF analysis. In IMS a weaker, "climatological" prior constraint, intended to capture the full variability of the state is used:

- For H_2O and temperature, the covariance matrices are computed using ECMWF analysis fields for the 3 test days of the Eumetsat study (17 April, 17 July, 17 October 2013). The zonal mean over all 3 days is computed. The covariance is then calculated using the differences between all the individual ECMWF profiles and the zonal mean state (linearly interpolated to each latitude). I.e. the covariance of departures from the 3 day zonal mean is computed: The assumed mean state varies with latitude but a single covariance applicable globally is derived. For temperature the mean state and covariances are computed in K. For water vapour they are computed using the logarithm of the volume mixing ratio in ppmv.
- For O_3, the state and covariance are defined in a similar way to that used in the nadir uv ozone profile scheme of CCI Ozone ([RD34]): The ozone profile is considered to be represented by piece-wise linear interpolation in pressure of a profile defined on 11 pressure levels corresponding to z* values of 0, 6, 12, 16, 20, 24, 28, 32, 40, 50 and 60 km (with extrapolation at fixed volume mixing ratio above), where z* is a simple conversion of pressure, p, to approximate altitude in km:

$$\boldsymbol{z^* = 16\,(3 - \log_{10} p)}$$

Equation 11

On these levels, the climatology of [RD35], which varies by month and latitude, is used to define the *a priori* profile. For a specific retrieval, profiles for the relevant month are used, without interpolation in time; profiles are linearly interpolated in latitude. The diagonal elements of the *a priori* error covariance matrix (on these levels) are set to the larger of the climatological percentage standard deviation and the following level specific values: 0–12 km (100 %), 16 km (30 %), 20–50 km (10 %), 60 km (50 %). In practice, it is these fixed percentage values that apply in the troposphere, except at very high latitudes where the climatological standard deviation is greater. A Gaussian correlation length of 6km is imposed to specify the off-diagonal elements of the covariance. Having defined the profiles on the chosen set of 11 levels, $\boldsymbol{S_{a:L}}$, the covariance on the 101 RTTOV levels, $\boldsymbol{S_a}$, is calculated via

$$\boldsymbol{S_a} = \boldsymbol{B_L^T S_{a:L} B_L}$$

Equation 12

Where $\boldsymbol{B_L}$ is a (11x101) matrix containing weights to perform linear interpolation in pressure from the 11 chosen levels to the 101 RTTOV levels.

- For CO, the covariance matrices are computed using MACC reanalysis [RD39] CO fields for August 2008, sampled daily at 00 and 12 UT. Individual MACC profiles are smoothed in the vertical with a Gaussian of width 6km (in z*). *A priori* profiles are defined by linearly interpolating in latitude the zonal mean of this data aggregated in 5 degree bins. The *a priori* covariance is a single matrix representing departures from this zonal mean of all the individual profiles. In accumulating these statistics, the same samples are considered twice, once at their nominal latitude and once at the latitude with opposite sign, so that the zonal mean profile is symmetric in latitude (the intention being to represent both winter and summer variability similarly at all latitudes).

In each case, Eigenvectors of the 101 level covariance matrix are determined using standard numerical methods such that:

$$\boldsymbol{S_a} = \boldsymbol{M \Lambda M^T}$$

Equation 13

Where $\boldsymbol{M}$ is the matrix of Eigenvectors forming an orthonormal basis for the profile in question. $\boldsymbol{\Lambda}$ is a diagonal matrix with values the correspond to the variances of each Eigenvector. In the retrieval, the coefficients of a subset of the Eigenvectors

with largest variability (largest Eigenvalue) are retrieved. 28 vectors are fitted for temperature, 18 for H_2O, 10 for O_3 and 10 for CO.

Using the Eigenvectors of this covariance, temperature profiles in (K) on the 101 RTTOV pressure levels are defined from the corresponding 28 elements of the state vector as follows:

$$\boldsymbol{T} = \boldsymbol{m_T}(\lambda) + \boldsymbol{M_T x_T}$$

Equation 14

Where $\boldsymbol{m_T}$ is the mean profile, interpolated to the latitude of a specific observation; $\boldsymbol{M_T}$ is the matrix of Eigenvectors of the covariance matrix and $\boldsymbol{x_T}$ contain the relevant sub-set of state vector.

H_2O, O_3 and CO profiles (in ppmv) are defined similarly (now with exponent):

$$\boldsymbol{W} = e^{\boldsymbol{m_W}(\lambda)+\boldsymbol{M_W x_W}}$$

Equation 15

In terms of the state vector representation used in the OEM algebra, the *a priori* state vector is all zero (the mean profile is added in the FM). The prior covariance is diagonal with variances given by the Eigenvalues of the covariance matrix.

The prior state and covariance for each species are illustrated, along with the fitted Eigenvectors, in Figure 2-18.

In order to speed up convergence the first guess state for temperature and H_2O is estimated using the NWP analysis profiles. This implemented by performing a linear optimal estimation fit of the state vector elements to the NWP profile, i.e using the NWP profile as “measurement” and Equation 14 as forward model. The prior state is as defined above (a zero vector and diagonal covariance). This ensures the first guess state is consistent with the way profiles are represented in the full retrieval. In this way the impact of using NWP analysis to define the first guess is only to reduce the number of iterations required to achieve convergence; the approach does not significantly affect the retrieval solution.

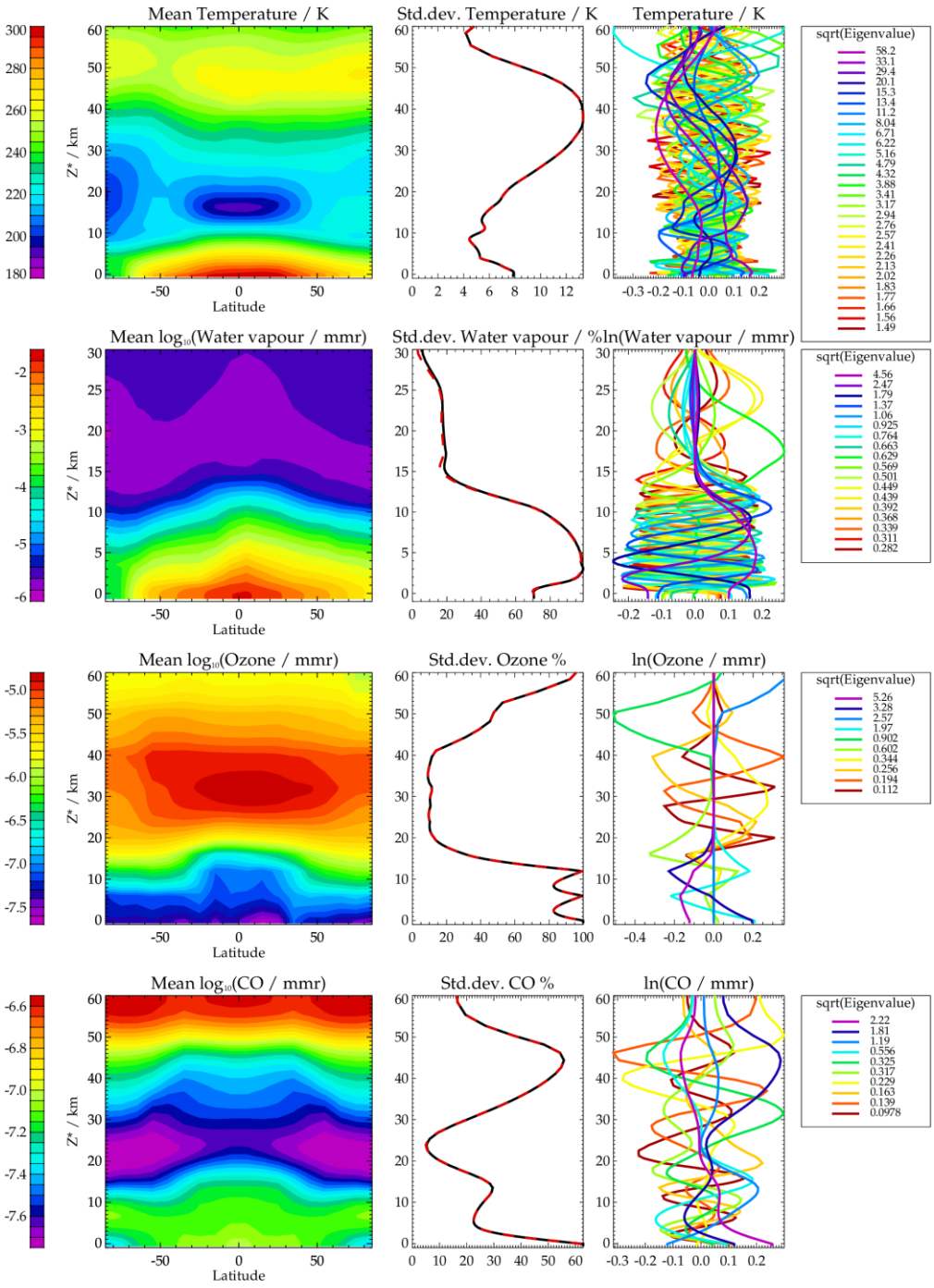

Figure 2-18 : Illustration of the climatology used to define the prior state and covariance for temperature, water vapour, ozone and carbon monoxide (respectively, from top to bottom). Left hand panels show the zonal mean profiles. Centre panels show the standard deviation of individual profile departures from the zonal mean. Right-hand panels show the Eigenvectors of the covariance matrix. The legend gives the square-root of the corresponding Eigenvalue.

2.8.2 Surface Temperature

The surface temperature prior state is defined similarly to the temperature profile: The zonal mean surface temperature derived from ECMWF analysis on the 3 days is used as the *a priori* value and the error is given by the standard deviation of departures from the zonal mean (accumulated globally). This gives an assumed prior standard deviation of 8.65K. The first guess value is taken from the NWP analysis.

2.8.3 Minor gases

As described in section 2.7.7, IMS-extended retrieves minor gas scale factors for assumed profiles of HNO_3, NH_3, CH_3OH, SO_2, HCOOH (IASI only) and isoprene (CrIS only). In each case, the assumed *a priori* and first guess value is 0, with *a priori* error 10.

Note that the scale factor is not defined in logarithmic terms so scale factors can be negative. In the case of HNO_3, NH_3 negative values are expected to arise as the scaled profile acts as an offset to the fixed profile assumed in the RTTOV coefficients. Negative values for all minor gases are also expected to arise when the true amount is smaller than the detection limit, simply as a consequence of measurement noise. In that situation it is important to include negative values when averaging results.

2.8.4 Surface Emissivity

Emissivity has been included in the state vector in terms of eigenvectors, analogous to the approach use to represent the atmospheric profiles. The basis of the approach is to construct the covariance of the global variation of spectral emissivity in the MW and IR channels using the RTTOV emissivity atlases. RTTOV has separate built-in atlases of emissivity for the MW and IR channels. These are combined to obtain a joint spectral covariance by running RTTOV to generate emissivity in all the channels used by IMS for all IASI scenes (land and sea) for the three test days used in the study (17 April, 17 July, 17 October 2013). The eigenvectors and values of this covariance are obtained and used as the basis of the set of spectral patterns used, and the associated *a priori* covariance. Because RTTOV provides co-located emissivity spectra for both MW and IR ranges, the principal, components include correlations between MW and IR, which enables IASI measurement to constrain the emissivity used in the MW and vice-versa. Also, because the values span global variation in a realistic manner, the eigenvalues provide suitable values to use as diagonal elements of the *a priori* covariance for emissivity (off diagonal elements being zero). However, this approach is not sufficient, because only a limited

amount of spectral information is represented in the RTTOV atlases. To accurately simulate spectra in all used IASI channels, it is necessary to introduce further spectral patterns (see below).

Note that in RTTOV MW land emissivity can come from two atlases, either TELSEM ([RD20]) or CNRM ([RD21]). Sea emissivity is calculated using the FASTEM model independent of the selection of land atlas. TELSEM is based on SSMI observations (and is the default setting for RTTOV v10.2). The CNRM atlas is based on AMSU A and B. IMS uses emissivity patterns based on the TELSEM Atlas.

Both MW databases are interpolated spectrally in RTTOV to define vales in the strong absorbing channels from (measurements of emissivity are only available in the window channels). The spectral interpolation is (probably) of little importance for the simulation of radiances, but is found to introduce some (presumably numerical) artefacts into the spectral emissivity eigenvectors. We therefore simplify the representation of spectral emissivity in the MW before computing the covariance and eigenvectors as follows:

- AMSU channels 1-3 and 15 and MHS channel 5 are taken as provided by RTTOV.
- AMSU channels 4-14 (all in range 52.8-57.3 GHz) are assumed to have the same emissivity as channel 3 (50.3 GHz)
- MHS channel 1 is assumed to have the same emissivity as AMSU channel 15 (both 89 GHz), in IMS v1 only (not IMS-extended).
- MHS channels 2-4 (in range 157-183 GHz) are assumed to have the same emissivity as channel 5 (190 GHz).

A similar approach is adapted to ATMS:

- Channels 1,2,3 and 16 and 22 are taken as provided by RTTOV.
- Channels 4-15 (all in range 52.8-57.3 GHz) are assumed to have the same emissivity as channel 3 (50.3 GHz)
- Channels 17-21 (in range 157-183 GHz) are all assumed to have the same emissivity as Channel 22 (183 GHz).

This means there are at most 5 independent values which define the emissivity in all the MW.

For IASI, RTTOV uses the Borbas/ University of Wisconsin emissivity database ([RD10]). This is based on a set of 416 eigenvectors of the measured emissivity of a set of natural materials, defined on a 416 element spectral grid spanning a spectral range of 699.3 to 2774.30 cm^{-1}. Emissivity values are extrapolated at fixed value for the channels in the CO2 band below 699.3 cm^{-1}. Spatial distributions of emissivity are determined by fitting these eigenvectors to MODIS observations. Only the first 6 spectral patterns are used

for this (due to the limited number of MODIS channels), so only these spectral patterns are represented in the emissivity atlas.

By deriving emissivity patterns from the RTTOV atlases, we can therefore only obtain up to 6 characteristic spectral patterns, together with realistic estimates of their variability to use in the *a priori* covariance. A few more patterns might be expected from the joint IASI+MW covariance (potentially adding 5 degrees of freedom), however in practise there is substantial correlation, and we therefore only take the first 6 spectral patterns from this matrix. IASI retrievals are affected by additional spectral patterns which are not represented in the atlases. In order to address this, further patterns from the set of 416 Wisconsin eigenvectors are added to the set of spectra to be fitted as follows:

1. The 416 Wisconsin patterns, in 416x416 matrix **M,** are interpolated onto the spectral sampling of IASI used in the retrievals (139 channels), defined in 139x416 matrix $\mathbf{M_I}$.
2. The first six Eigenvalues corresponding to the $\mathbf{M_I}$ can be obtained from the variability of the associated patterns in the RTTOV climatology. The Eigenvalues associated with the Wisconsin patterns are not known however it is assumed that they should decrease in magnitude in the order in which they are provided by Wisconsin. For what follows it is mainly important that the order of the additional patterns is maintained (so the most likely spectral variations remain occur first in the final set of patterns). We assume that each pattern from number 7 onwards has an eigenvalue which is 1.3 times smaller than the previous pattern.
3. Having defined the Eigenvectors $\mathbf{M_I}$ and associated Eigenvalues $\boldsymbol{\omega_I}$. A new set of patterns which are orthogonal to the original six are obtained as follows
4. Each pattern (column i=1,416 of $\mathbf{M_I}$) is scaled by the square root of its Eigenvalue to obtain $\mathbf{p_i}$
5. The six original patterns are fitted to $\mathbf{p_i}$ to obtaining the residual pattern

$$\mathbf{p_i}' = \mathbf{p_i} - f(\mathbf{p_i}, \mathbf{R_I})$$

Equation 16

where $f(\mathbf{p_i}, \mathbf{R_I})$ is a simple least squares fit of the six RTTOV based patterns (for the IASI channels), $\mathbf{R_I}$, to $\mathbf{p_i}$.

6. A new spectral covariance is constructed from all 416 residual patterns ($\mathbf{p_i}'$ for i=1,N).
7. A new set of Eigenvectors, with appropriately ordered Eigenvalues are obtained by decomposing this covariance matrix to obtain $\mathbf{M_I'}$.

8. The patterns in $\mathbf{M_I'}$ are added to the 6 RTTOV based patterns, to obtain the full set **M'** (for both MW+IASI). Elements corresponding to MW channels are assumed to be 0. The combined list of Eigenvalues is also obtained, **ω'**.
   In principle this results in a list of 422 patterns, however many of these have numerically negligible Eigenvalue. Only a limited number of these patterns are fitted in the retrieval. The retrieval fits the weights (defined in vector **v**) of each pattern such that the emissivity modelled in RTTOV, **e**, is given by

$$\mathbf{e} = \mathbf{v}\,\mathbf{M'}$$

Equation 17

The *a priori* errors for each element of **v** are assumed to be the minimum of the square root of the corresponding Eigenvalue in ω' or 0.01 (values smaller than this are not allowed to prevent too tight a prior constraint). The *a priori* covariance is assumed to be diagonal. A *priori* values for **v** are set by fitting the chosen set of patterns to the standard emissivity given by the RTTOV emissivity atlas for a given scene. Differences between this fit and the RTTOV predicted emissivity are small.

A number of options have been investigated as follows:

- Spectral correlations between IASI and MW emissivity can be included or not. In the latter case the first six patterns are determined independently from the IASI channels. Then the first 5 patterns are taken from the RTTOV covariance for the MW channels. Then additional patterns for IASI are added to the list.
- Similarly, spectral correlation between AMSU and MHS+IASI can be included or not, while maintaining correlations between MHS and IASI. For ATMS, a similar option to include/ignore correlations with channels 1-16 is implemented. The motivation for this is that AMSU (and ATMS channels 1-16) have much larger footprint (at least factor 2, see tables in section 2.4.1.2) than the other MW and IR channels. Assuming emissivity is correlated can lead to difficulty fitting the measurements, especially over coastlines when the footprint of low frequency channel includes sea while the higher frequency channels sense over land.
- In test retrievals over desert (which are particularly prone to high cost due to presumed issues with RTTOV emissivity), it was noted that fit residuals could be significantly reduced if a pattern representing the first spectral derivative of the Wisconsin mean IASI emissivity spectrum was included in the fit (this has quite sharp gradients in the 10 micron region). This effectively corresponds to fitting a wavelength shift of the mean emissivity. Residuals improve further if pattern representing a wavelength stretch of the mean emissivity is included. We therefore include both these patterns in the main simulations reported here.

These are inserted into **M'** in order after the RTTOV based patterns, before the additional IASI patterns discussed above.

- Tests have been run with 10, 20 or 30 patterns (columns of **M'**) fitted (including 6 RTTOV patterns and the 2 wavelength shift related patterns).

In the version 1 scheme, MW/IR correlations are assumed and 20 patterns are used (including the spectral shift pattern). Spectral patterns between MW and IASI are included. Emissivity from the RTTOV atlas is used to define the prior state itself, via fitting the retrieval Eigenvectors to the RTTOV estimate of emissivity for the given scene (analogous to the approach used to defined the first guess state for profiles described in the previous section).

In IMS-extended the same settings are used (with patterns extended to the additional spectral points), with the exception that no correlations are assumed between the emissivity in AMSU (ATMS channels 1-16) channels and the other MW+IR channels. Correlations between MHS (ATMS channels 17-22) and IASI (CrIS) are still included.

The spectral patterns used are illustrated in Figure 2-19.

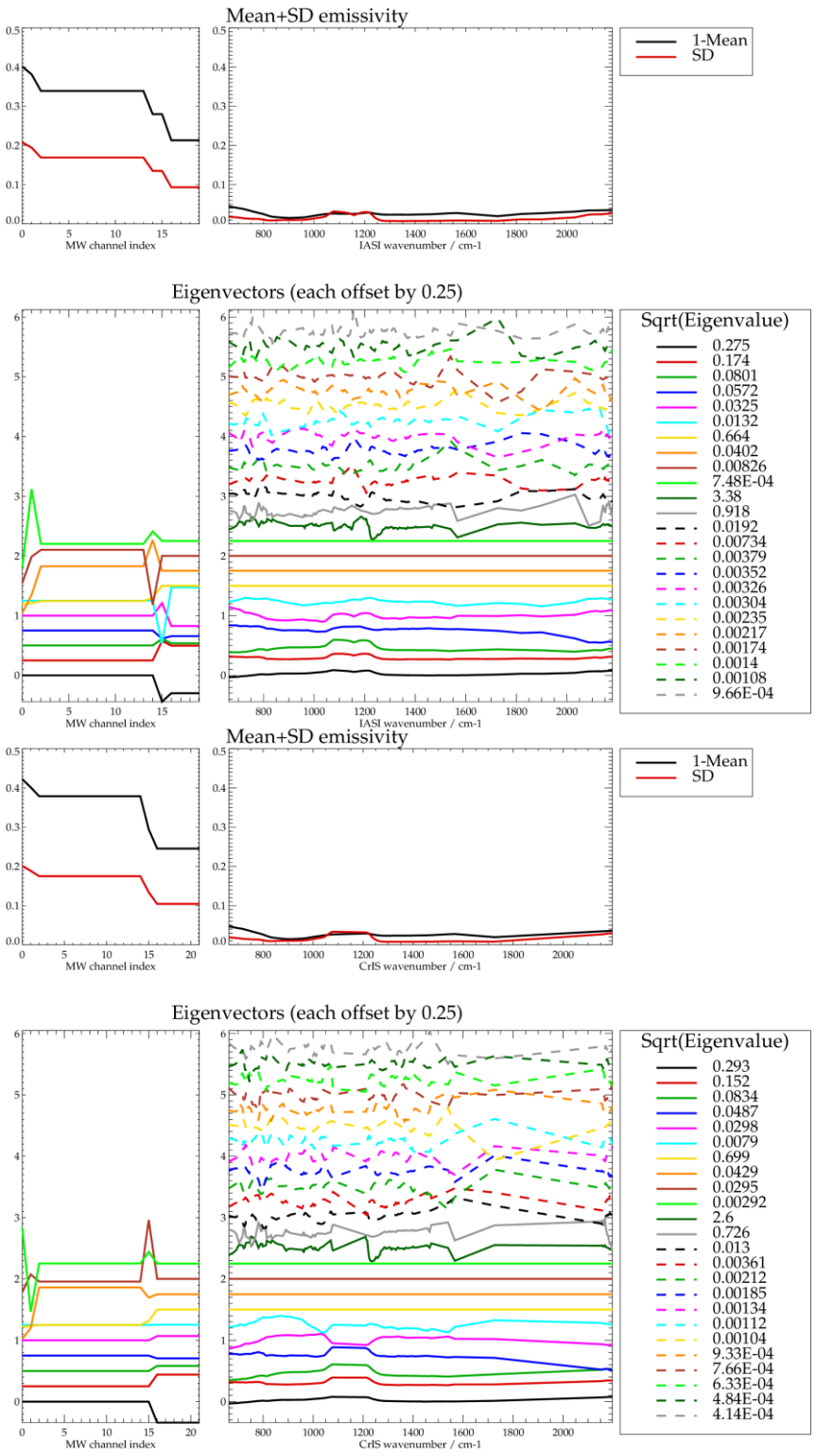

Figure 2-19 : Illustration of the spectral patterns used to fit IASI (upper set of panels) and CrIS (lower). Within each set, the lower panel shows the first 30 spectral patterns used to represent surface emissivity in the retrieval. Each eigenvector is shown offset by 0.25 with respect to the previous vector (for clarity). Only non-zero MW Eigenvectors are shown. The top panels show the mean and standard deviation of the emissivity (note 1 minus the mean emissivity is shown).

2.8.5 Cloud

In IMS v1, the area fraction and top pressure of a black-body cloud are both retrieved:

- For cloud fraction, the state vector is the natural logarithm of cloud fraction with prior and first guess value $\ln(0.01)$ and prior error 10. The log representation is adopted to prevent negative values of cloud fraction arising.
- For cloud top height, the state vector is z* pressure-altitude of the cloud (Equation 11). The prior and first guess value is assumed to be 5km with *a priori* error also 5km.

In IMS-extended, as described in section 2.7.6, cloud is simulated as scattering media using the RTTOV optical properties. In this case the retrieval assumes each scene is fully cloudy (fraction=1) and retrieves the optical depth, effective radius and height of that cloud. (A cloud free scene is expected to be retrieved with negligible optical depth.):

- To decide which cloud phase to assume, each scene is classified (before any retrieval) using observed brightness temperatures near 11, 12, 9.3 and 8.3 microns[8]. Referring to these brightness temperatures as B_{11}, B_{12}, B_{93} and B_{83}, respectively, the classification is performed as follows (in this order).
    a. Scene is assumed “liquid cloud” (class 1) unless the following tests change this classification.
    b. Scene is classified “possible boundary layer cloud” (class 0) if $(B_{11} - B_{12}) < -0.1$.
    c. Scene is classified “ice cloud” (class 2) if $B_{11} < 290K$ *and* $[(B_{93} - B_{12}) > 2]$ or $[\big((B_{11} - B_{12}) > -0.1\big)\ and\ (B_{11} < 270))]$.
    e. Scene is classified “desert dust/ash” if $((B_{11} - B_{12}) < -0.1)\ and\ ((B_{83} - B_{89}) > 0.5)$.
- If the scene is classified as “ice cloud” then RTTOV ice cloud properties are assumed for the retrieval, otherwise liquid cloud properties are assumed. Note that aerosol is always retrieved together with cloud so, in principle, a scene containing desert dust would be fit by the aerosol parameters (see below) and a low cloud optical depth would be retrieved.
- For optical depth, the state vector is the natural logarithm of cloud optical depth with *a priori* and first guess value $\ln(0.001)$ and *a priori* error 10.

[8] Channels at 903.25, 831.75, 1072.5, 1204.25 cm^{-1} are used for IASI. The closest matching channels are used for CrIS.

- For effective radius, first guess and a priori value is 10 microns for liquid cloud and 40 microns for ice cloud, *a prior*i error is 10.
- For cloud-top height, the same a priori assumptions as IMS-v1 are assumed (5km z* height and error). The cloud extinction profile is assumed to be a Gaussian function which peaks at the retrieved cloud-top height and has a full-width-half-maximum of 1km (in z* units). This is normalised to integrate to the retrieved cloud optical depth. In case the profile extends below the surface pressure, then only the part of the Gaussian which is above ground is modelled, and this part of the function is normalised to the retrieved optical depth. Extinction is set to zero where it is smaller than 0.01% of the peak value, to limit the number of layers with cloud scattering (which has an influence on the RTTOV run time).
- If a retrieval finishes with fit cost > 1000 and cloud transmittance < 0.1 (i.e retrieved cloud optical depth > 2.30259), then the retrieval will be re-run with first guess cloud top height set to 30km and the scene class set to “ice cloud”. This can yield better results in the case of cloud at or above the tropopause. If this occurs, then the retrieval which gave the lowest fit cost is taken as the final result for this scene.

2.8.6 Aerosol

As described in section 2.7.6, two aerosol types are modelled in IMS-extended. State vector elements are as follows:

- Natural logarithm of the dust and sulphate aerosol optical depth, each with *a prior* and first guess value $\ln(0.01)$ and *a priori* error 1.
- The z* altitude of the dust layer, with *a prior* and first guess value 2km and *a priori* error 4km, assuming a Gausian profile shape with full-width-half maximum 1km. A similar profile shape is assumed for the sulphate aerosol but this is assumed to have a fixed height of z*=20km.

2.8.7 Bias correction pattern weights

Weights for the systematic bias correction patterns (section 2.6.1.2) are retrieved. The prior value for each weight is assumed to be zero, with a prior error of 1.

2.8.8 Glint reflectance factor

The factor g_f which is used to scale the RTTOV modelled water reflectance (see section 2.7.4), is retrieved assuming an *a priori* and first guess value of 1, and *a prior* error of 3.

2.9 Characterisation of uncertainty and vertical sensitivity

The error covariance of the solution from an OEM retrieval is given by

$$\boldsymbol{S_x} = \left(\boldsymbol{S_a^{-1}} + \boldsymbol{K^T S_y^{-1} K}\right)^{-1}$$

Equation 18

Where $\boldsymbol{K}$ is the weighting function matrix which contains the derivatives of the FM with respect to each element of the (solution) state vector. The square-roots of the diagonal elements of this matrix are referred to as the *estimated standard deviation* (ESD) of each element of the state vector.

For IMS, the transformation from the state vector to derived profiles, is expressed as a matrix operation (Equation 14). Given the error covariance on the state (from the OEM equations), corresponding error covariance for the layer averages is obtained (e.g. for temperature) by

$$\boldsymbol{S_T} = \boldsymbol{M_T}\, \boldsymbol{S_{x:T}} \boldsymbol{M_T}^{\boldsymbol{T}}$$

Equation 19

Where $\boldsymbol{S_{x:T}}$ here is the (square) sub-matrix of the full $\boldsymbol{S_x}$ for the temperature state vector elements only.

For water vapour, ozone and carbon monoxide, the additional conversion from log units is required to obtain the covariance of the mixing ratio profile in ppmv:

$$\boldsymbol{S_W} = (\boldsymbol{w}\boldsymbol{w^T})\, \boldsymbol{M_W}\, \boldsymbol{S_{x:w}} \boldsymbol{M_W}^{\boldsymbol{T}}$$

Equation 20

Where $\boldsymbol{w}$ is the retrieved profile in ppmv (from Equation 15).

$\boldsymbol{S_x}$ can be considered in two terms:

$$\boldsymbol{S_x} = \boldsymbol{S_n} + \boldsymbol{S_s}$$

Equation 21

Where $\boldsymbol{S_n}$ describes the retrieval noise, the uncertainity directly related to the specified measurement errors (characterised by $\boldsymbol{S_y}$). $\boldsymbol{S_s}$ describes the smoothing error, i.e. departure from the true state related to variability in the state (expressed in $\boldsymbol{S_a}$) to which the measurements are not sensitive.

$\boldsymbol{S_n}$ is evaluated using retrieval gain matrix (which gives the sensivity of the retrieval to perturbations in the measurement):

$$\boldsymbol{G = S_x K^T S_y^{-1}}$$

Equation 22

$$\boldsymbol{S_n = G^t S_y G}$$

Equation 23

The corresponding error covariance for the layer averages is given by

$$\boldsymbol{S_{Tn} = M_T\, S_{n:T} M_T{}^T}$$

Equation 24

The standard deviations of the noise on a derived layer-averages, ΔT_n, are given by the square-root diagonals of this matrix.

Issues relating to the vertical sensitivity of the retrieval and influence of the prior can be addressed using the averaging kernel which characterises the sensitivity of the retrieved state to the actual state (e.g. for temperature):

$$\boldsymbol{A_{f:T} = G K_{f:T}}$$

Equation 25

Where weighting function $\boldsymbol{K_f}$ is distinguised from $\boldsymbol{K}$ in that derivatives are computed with respect to perturbations on fine atmospheric grid, $\boldsymbol{p_{atm}}$ (as opposed to the state vector). In IMS this fine grid is defined by the 101 RTTOV pressure levels. This matrix is not square and has dimensions number of Eigenvector weights in the state vector by 101 „true“ profile pressure levels.

The (square) averaging kernel derived using the state vector weighting function ($\boldsymbol{A = GK}$) would give the derivative of the retrieved Eigenvector weights with respect to true profile perturbations with shape given by the Eigenvectors. These are of relatively little practical use and averaging kernels in this form are only used in IMS to obtain the degrees of

freedom for signal (DOFS) for specic retrieval products. This is given by the trace (sum of the diagonal elements) of the sub-matrix of $\boldsymbol{A}$ corresponding to a specifc product.

The averaging kernel of retrieved temperautre profiles (defined on the RTTOV levels) with respect to perturbations on the fine atmospheric grid a layer-average is

$$\boldsymbol{A_{Tf} = M_T A_{xf:T}}.$$

Equation 26

For water vapour, the averaging kernel for the retrieved profile in ln (ppmv), with respect to perturbations in the true profile is given by

$$\boldsymbol{A_{Wf} = M_{Wf} A_{xf:W}}.$$

Equation 27

Where $\boldsymbol{A_{xf:W}}$ is the averaging kernel for the water vapour state vector elements with respect to perturbations in ln(ppmv) on the fine atmospheric levels.

Note that the RTTOV 101 level pressure grid spans the range 0.005 to 1100 hPa, i.e. from below surface to approximately 84km altitude. RTTOV will cut-off the defined profiles at the defined input surface pressure. Averaging kernels will be by definition zero for true perturbations below the profile-specific surface pressure.

2.10 Comparing retrievals to independent profiles

The consistency of an independent profile with a retrieved profilecan be tested using the averaging kernels. E.g for temperature:

$$\boldsymbol{T_{ind:AK} = m_T}(\lambda) + \boldsymbol{A_{Tf}}\left(\boldsymbol{T_{\mathrm{ind}}} - \ \boldsymbol{m_T}(\lambda)\right)$$

Equation 28

A similar equation holds for water vapour, ozone and carbon monoxide, though it should be noted that $\boldsymbol{m_T}(\lambda)$ is defined in ln(ppmv) and $\boldsymbol{A_{Tf}}$ similarly derivatives of retrieved log(ppmv) profiles with respect to perturbations in the true ln(ppmv). $\boldsymbol{W_{\mathrm{ind}}}$ should therefore also be given in units of ln (ppmv). The exponent of the resulting $\boldsymbol{W_{ind:AK}}$ will give the estimated profile in ppmv.

Considering a sufficiently large set of independent profiles, differences between $\hat{T}$ and $T_{ind:AK}$ is expected to be consistent with the estimated retrieval noise matrix, $\boldsymbol{S_{Tn}}$.

Differences between the retrieved profile and that of the independent data itself should be consistent with the total solution covariance, $\boldsymbol{S_{Tx}}$ (provided $\boldsymbol{S_a}$ is consistent with the true variability and this is also consistently represented in the set of independent profiles).

Note that Equation 28 applies to profiles defined on the RTTOV grid. The value of an averaging kernel at a given fine grid level applies to an atmospheric layer, of finite thickness, centred on the grid level in question. The application of averaging kernels requires that the model and a priori profiles are interpolated onto the fine grid levels on which the averaging kernels are defined. Comparisons can also be made using profiles defined on an alternative fine grid (e.g. a native model grid), provided that a) the differences in layer thickness between the original and new grids are taken into account and b) the new grid is sufficiently fine to ensure that the averaging kernel captures sufficient variation in both the vertical sensitivity of IASI and the methane profile. The procedure to convert an averaging kernel from its original fine grid to a new fine grid is as follows:

1. Normalise the averaging kernel by dividing its value at each grid level by the corresponding grid layer thickness. The boundaries of a layer corresponding to a given grid level are defined as half the pressure difference between the grid level pressure, p_{i}, and the pressures at the adjacent levels above and below it, $p_{\mathrm{i-1}}$ and $p_{\mathrm{i+1}}$ respectively, i.e.

$$\Delta p_i = \frac{1}{2}(p_{i+1} - p_{i-1})$$

Equation 29

   If the layer in question contains the surface pressure, then p_{i+1} should be set equal to the surface pressure. RTTOV levels which bound layers which are entirely below the surface will have zero averaging kernel value so normalisation of the kernel values for these levels is not needed.

2. The normalised averaging kernel, $\boldsymbol{A}'_{\mathrm{Tf}}$, for a given retrieval level, k, and fine grid level, *i*, can therefore be written as:

$$\mathrm{A'_{Tf:ki}} = \frac{A_{Tf:ki}}{\Delta p_i}$$

Equation 30

3. Interpolate the normalised averaging kernels (for each retrieval level) to the new fine grid levels, linearly in pressure.

4. Multiply the normalised averaging kernel by the layer thicknesses of the new fine grid (defined as in step 1 above, applied to the new fine grid pressures).

Once the averaging kernel has been converted to the new fine grid, on which the model data is provided, Equation 28 can then be applied.

Use of averaging kernels to compared the minor gas column amounts with independent data is similar and discussed in section 2.11.1, below.

2.11 Derived geophysical quantities

The following geophysical parameters are derived from the directly retrieved parameters.

2.11.1 Minor gas column average mixing ratio

As described above minor gases are retrieved in terms of a scale factor, C_j, for an assumed volume mixing ratio profile, $\boldsymbol{r_s}$, which may be modelled in addition to a background profile, $\boldsymbol{r_b}$, which is implicit in the RTTOV coefficients. For each gas, the profile shape which is assumed in the retrieval and that assumed in RTTOV are both provided in the IMS output file (see section 3.3.3). L2 files report the scale factors and also the implied column average mixing ratio derived as follows:

The estimated minor gas volume mixing ratio, $\boldsymbol{r}$, profile can be calculated from the variables in the L2 file via:

$$\boldsymbol{r} = \boldsymbol{r_b} + C_j \boldsymbol{r_s}$$

Equation 31

Where $\boldsymbol{r}$, $\boldsymbol{r_b}$and $\boldsymbol{r_s}$are vectors containing the profile on all the RTTOV presure levels. Considering $\boldsymbol{r}$ as a continuous function of pressure, $\boldsymbol{r(z)}$, $\boldsymbol{t}$he column average mixing ratio is calculated (assuming the hydrostatic equation) as follows:

$$\bar{\boldsymbol{r}} = \frac{1}{p_0} \int_{p_0}^{0} r(p)\, dp$$

Equation 32

Numerically the integration is performed as a summation over the subset of N RTTOV layers which are above the surface:

$$\bar{\boldsymbol{r}} = \frac{1}{2p_1}\sum_{i=1}^{N}(p_i - p_{i+1})(r_i + r_{i+1})$$

Equation 33

Where $p_1$is the surface pressure and r_i is the minor gas profile interpolated to that pressure. For all other indices, $i = 2, N,$ values are those on the RTTOV levels which are above the surface.

Although it is not reported in the L2 files, the total column amount of the gas (in molec/cm^2) can be simply calculated from the column averaged mixing ratio via:

$$\boldsymbol{c} = \frac{N_a}{100gM}\int_{p_0}^{0} r(p)\,dp = \frac{N_a p_s \bar{r}}{100gM}$$

Equation 34

Where g is the acceleration due to gravity (9.80665m/s^2), N_a is the Avogadro constant (6.0221367x10^{23} moles^{-1}) and M is molecular mass of air (28.964x10^{-3} kg/mole).

The retrieved column averaged mixing ratios can be compared to those derived from an independent profile, using the provided vertically resolved averaging kernels:

$$\overline{r_{ind:AK}} = \bar{r_0} + \boldsymbol{A_f}\,(\boldsymbol{r_{ind}} - \boldsymbol{r_0})$$

Equation 35

Quantities $\bar{r_0}, A_f$ and $\boldsymbol{r_0}$ are all provided in the L2 files for each minor gas. For minor gases other than HNO3 and NH3, $\bar{r_0}$ and $\boldsymbol{r_0}$ are zero.

2.11.2 Air-surface temperature contrast

The difference in temperature between the surface and the air above it is an important parameter in determining the sensitivity of the retrieval to gases, particularly close to the ground. It is therefore a useful diagnostic which can be used to select scenes where sensitivity is particularly good (positive air-surface temperature) or exclude scenes where sensitivity is ambiguous (when air-surface contrast is negative, weighting functions for trace gases can change sign through the troposphere). IMS reports two measures of air-surface contrast:

- dt2: The differences between the surface temperature and the temperature profile interpolated to the assumed surface pressure (analogous to the 2m air temperature from NWP).

- dt1000: The differences between the surface temperature and the temperature profile interpolated to z* = 1km above the surface z* (i.e. surface pressure converted to z*).

2.11.3 Total Precipitable Water (TPW)

Total Precipitable Water (TPW) is calculated from the retrieved water vapour profile, and has been defined (in units of mm) as:

$$\mathrm{TPW} = \frac{1\mathrm{x}10^{-5}}{\rho g}\int_{\mathrm{Psurf}}^{0} \mathrm{q(p)dp}$$

Equation 36

where q is the mixing ratio of water vapour in the atmosphere [kg/kg], ρ is the density of water vapour in kg/m3 and g is the acceleration due to gravity (m/s^2).

In IMS the integration is performed by setting up and integration matrix (**M**), with

$$\mathrm{TPW} = \mathbf{M}\,\hat{\boldsymbol{x}}_{\boldsymbol{h2o}}$$

Equation 37

and $\hat{\mathbf{x}}_{\boldsymbol{h2o}}$ is the retrieved water vapour profile on the RTTOV grid. The retrieved error (variance) on TPW is then calculated by

$$S_{TPW} = M\,Sx_{h2o}M^{T}$$

Equation 38

2.11.4 Stability indices

Two stability indices (the K-index and the lifted index) are calculated to provide information on the vertical stability of the atmosphere at the retrieval location, following the methodology used in the Global Instability Indices (GII) retrieval scheme developed for the MTG-FCI [RD36] and SEVIRI [RD37].

2.11.4.1 K-index

The K-index is defined by the equation:

$$\mathrm{Kindex} = (\mathrm{T}_{850-}\,\mathrm{T}_{500}) + \mathrm{D}_{850} - (\mathrm{T}_{700} - \mathrm{D}_{700})$$

Equation 39

Where T = temperature (in °C), and D = dew point temperature at the respective pressure levels indicated by the subscripts. Values greater than 20°C are a good indicator of unstable conditions [RD37].

The value of the K-index has been derived from the retrieved temperature and water vapour profiles, following the procedure set out in [RD36]. The retrieved temperature and water vapour profiles were first interpolated to the respective levels required in the above equation, and dew point temperatures were calculated as per section 3.5.7 of [RD36].

2.11.4.2 Lifted Index

The lifted index is defined by:

$$\text{Lifted Index} = T_L - T_{500}$$

Equation 40

Where T_L is the temperature of a parcel of air near the surface lifted to 500 hPa dry-adiabatically to saturation and then moist adiabatically after that. A negative lifted index indicates that the atmospheric layer is potentially unstable. Following the GII algorithm [RD36] this surface parcel is represented by the average temperature and humidity of the lowest 100 hPa of the atmosphere. The value of the lifted index has then been calculated from the retrieved temperature and humidity profiles following the equations given in [RD36], section 3.5.7.

3. L2 PRODUCT

3.1 Overview

L2 products are output in CF-compliant NetCDF format. IMS can potentially generate a huge amount of output data, particularly if all retrieval diagnostics (averaging kernels, covariances matrices etc) are to be included. The following choices are made as a trade-off between maximising the amount of information retained without generating excessively large products (or unnecessarily complicating their use):

- IASI orbits are divided into granules of 50 scan lines for processing. L2 files are reported on this basis.
  - Profiles are reported, with their estimated errors (total and noise), on the 101 RTTOV pressure levels (despite being retrieved in terms of fewer Eigenvector weights). These are stored as short integers with defined scale/offset values to convert to physical units. Where reported values are equal to defined valid_min/valid_max this should be taken to indicate that the true value (after applying the given scale factor and offset) has exceeded the range allowed by the data type used to store the values. Scale factors and offset values used are chosen such that this will rarely happen.
- Emissivity is reported as the spectrum sampled at the same spectral points used in the retrieval.
- The full state vector is also including in full floating point representation. If necessary profile values can be reconstructed using the state vector values in combination with the stored Eigenvectors.
- Full retrieval diagnostics (averaging kernels, and covariances) are only reported for a sub-set of scenes. The file format is defined such that the sampling can be different for each profile. Currently, for water vapour and temperature, diagnostics are reported for 1 pixel in 4 along and across-track (i.e. 1 in 16 pixels overall). This gives approximately uniform spatial sampling along/across-track (before considering the cloud mask). A quasi-regular sampling of the across-track scan is adopted so that each of the detector pixels are approximately evenly sampled (a strictly regular sampling would always take the same detector pixel). All diagnostics are reported for other gases.
- When reported, averaging kernels are in the form $\boldsymbol{A_{xf}}$ (see section 2.10), i.e. for state vector elements (Eigenvector weights) with respect to perturbation in the true profile on the 101 level RTTOV grid. To reduce their size, they are

only give for every other level in the 101 level grid, i.e. at 51 levels. Since averaging kernels are intrincically related to the grid on which true profiles are defined, a user must interpolate the kernels (in the „true“ dimension) from the 51 sub-set to the full 101 level grid before using them (or otherwise make allowance for the thickness of the layers associated with the kernels).

- When reported, the solution covariance and noise covariance are given only for the profiles separately (i.e. correlation between profiles are not retrained) and in a form which avoids storing the identical elements on both sides of the diagonal (these covarianes are by definition symetric). Each N x N covariance is stored as a vector of N*(N+1)/2 elements, comprising first the diagonal elements, then the 1st superdiagonal elements, then the 2nd superdiagonal elements etc.
- The „prior“ profiles for temperature, humidity, ozone and carbon monoxide are given tabulated as a function of latitude, not for every scene.
- The (fixed) Eigenvectors which relate the state to the full profile are also given so that the user can reconstruct averaging kernels and covariances for the profiles on the full pressure grid.
- NWP analysis profiles used are also reported for a sub-set of scenes. These are used to define the first guess state so are readily available when the processor is run. Outputting them to the L2 files enables straightforward monitoring of the L2 product performance against NWP.
- The measurement vector, brightness temperature difference spectra (at first guess) and fit residuals (at solution) are also given for only a sub-set of scenes. This corresponds to the same sub-set of scenes for which temperature and water vapour profile averaging kernels are reported. Note that in the retrieval the measurement vector is defined in radiance units. In the output files values are converted to brightness temperature (i.e. the tempature of a balck body which would emit the same spectral radiance at a given wavelength). This is done partly mainly to enable more efficient compression: Spectra are stored as short integers with wavelength independent scale and offset.

All variable names are composed of lower case characters. A number of variables are defined which contain similar information for different retrieved products. To avoid repetition, in the format description below, we use (capital) “X” in the names of such variables. In the file the variable will be present with “X” replaced by

- “w” for water vapour
- “t” for temperature
- “o” for ozone
- “c” for carbon monoxide

Minor gases are similarly defined with several variables using capital letter “Y” which in the file is replaced by

- “nh3”, for ammonia
- “so2”, for sulphur dioxide
- “hno3”, for nitric acid
- “ch3oh” for methanol
- “hcooh” for formic acid (Metop only)
- “isoprene” (NPP/JPSS only)

3.2 L2 File name

An example IMS-extended L2 file name is

```
ral-l2p-tqoex-iasi_mhs_amsu_metopa-tir_mw-
20070701203256z_20070701221456z_750_799-v0260.nc
```

Which contains the following tags, separated by “-“:

- [origin]: Indicator of where the data was processed, in this case “ral” for RAL.
- [processing level]: In this case “l2p”
- [retrieved species]: In this case “tqox” for temperature, humidity, ozone and emissivity; the “x” indicates extended set of co-retrieved parameters from IMS-extended..
- [instrument]: In this case “iasi_amsu_mhs”. Alternatively this can be “cris_atms”
- [platform]: In this case “metopa” for Metop A, alternatively “metopb”, “metopc”, “npp”, “jpss1”.
- [algorithm id]: In this case “tir_mw”, indicating combined use of TIR and MW measurements
- [start date/time] in format YYYYMMDDhhmmss (UT). This is identical to date/time used in the original L1 file (for a full orbit).
- [end date/time] (as above)
- [scanline sub-set start]: This contains the start scanline index within the L1 orbit of L2 processed data.
- [scanline sub-sent end]: (as above)
- [version ID]: Version ID for the product (v0260).

3.3 Format and content

3.3.1 Global attributes

- title: “RAL Infra-red/Microwave Souder (IMS) Extended Product containing temperature, water vapour, ozone, minor trace gases, surface emissivity, cloud and aerosol parameters”
- version: The product version.
- project: “NCEO, EOCIS, ESA CCI Water Vapour”
- licence: Text defining the license terms.
- sensor: Names of the sensors used.
- institution: “STFC Rutherford Appleton Laboratory”
- filename: The L2 filename
- input_filename: A list of input filenames used. This includes the L1 file name processed, and one of the input NWP filenames (sufficient to identify the type of NWP data used).
- processing_flags: List of processing flags set when the retrieval was run.
- conventions: “CF-1.6”
- Minor gas factor species: Defines the minor gases which are retrieved, in the order in which they are stored in “mgf” variables.

3.3.2 Dimensions

- npi: Number of input scenes (i.e. individual IASI measurements in the processed L1 granule)
- npres: Number of scenes for which retrieval results are reported. In the version 1 data, this is all scenes for which pas the brightness temperature difference test (see section 2.6.3). In IMS-extended this usually is the same as npi (i.e. all scenes), except where L1 has invalid geolocation (e.g. possibly due to non-standard measurement mode or corruption/processing error).
- nmgf: The number of minor gas profile scale factors which are fit.
- near: The number of aerosol types which are fit.
- npiak_X: Number of scenes for which averaging kernels are reported for profile product X
- npisx_X: As above for solution covariance matrices.
- nnwp: Number of scenes for which NWP profiles are reported.
- nbtds: Number of scenes for which measurements and brightness temperature difference spectra are reported (i.e. difference between measurement and simulation based on first guess state)
- nresid: Number of scenes for which solution fit residual spectral are reported.

- nbcf=2: Number of bias correction patterns fitted.
- nz=101: Number of RTTOV pressure levels (and pressure levels of the reported profiles)
- nXpc: Number of Eigenvectors used to represent profile product X.
- nlb: Number of latitude bands used to define the a priori data.
- nsp: Number of spectral points in measurement vector
- naks=51: Number of “true” profile levels for which averaging kernels are reported, corresponding to every other level of the RTTOV grid.
- navhrr=6: Number of Metop AVHRR channels. For CrIS this refers to the number of stored VIIRS channels
- nx: Total number of elements in the state vector.
- nvsxX: Number of stored covariance values for each profile product.

3.3.3 Variables

The following bullets give the variable type (upper case), variable name and dimensions (in brackets) of each variable in the L2 files. Sub-bullets define relevant attributes for each variable.

- NC_UBYTE do_retrieval (npi):
  - long_name: Flag indicating scenes for which retrievals results are reported. Usually all scenes with valid L1 geolocation for IMS extended.
- NC_UBYTE do_ak_X (npi)
  - long_name: Flag indicating scenes for profile product “X” for which full diagnostics are provided including averaging kernels
- NC_UBYTE do_sx_X (npi)
  - long_name: Flag indicating scenes for profile product “X” for which solution error covariance are provided
- NC_UBYTE do_resid (npi)
  - long_name: Flag indicating scenes for which fit residual spectra are provided
- NC_UBYTE do_sample (npi)
  - long_name: Flag indicating scenes forming regular sub-sampling of IASI observations
  - comment: All parameters will be output for these scenes if a retrieval is performed (i.e. when do_sample=1 and do_retrieval=1. Some parameters are provided for the sub-sampled scenes also when a retrieval is not performed
- NC_UBYTE do_station (npi)
  - long_name: Flag indicating scenes close to one of a list of predefined ground-stations (WOUDC ozone-sonde stations in version 1 product)

- NC_UBYTE do_btds (npi)
    - long_name: Flag indicating scenes for which measurements and clear sky brightness temperature difference spectra are provided
- NC_UBYTE do_nwp (npi)
    - long_name: Flag indicating scenes for which NWP profiles are provided
- NC_INT index_nwp (npi)
    - long_name: Index to nearest NWP record for each IASI scene (starts at 0).
- NC_SHORT iat (npi)
    - long_name: Along-track index – scanline within the current granule
- NC_SHORT ixt (npi)
    - long_name: Across-track index, counting individual detector pixels (0-119 for IASI; 0;269 for CrIS)
- NC_UBYTE idet (npi)
    - long_name: Detector pixel index (e.g. 0-3 for IASI; 0-8 for CrIS)
- NC_SHORT iclass (npi)
    - Long_name: Assumed cloud type: -1=black body; 0=possible boundary layer cloud; 1=liquid/clear; 2=ice; 3=dust.
- NC_FLOAT jx (npres)
    - long_name: State vector component of cost
- NC_FLOAT jy (npres)
    - long_name: Measurement component of cost
- NC_FLOAT p (nz)
    - long_name: Pressure grid for retrieved profiles (i.e. 101 RTTOV levels)
    - standard_name: air_pressure
    - units: hPa
- NC_SHORT t (nz,npres)
    - long_name: Retrieved atmospheric temperature profile
    - standard_name: air_temperature
    - units: K
- NC_SHORT w (nz,npres)
    - long_name: Retrieved natural logaritm of the atmospheric water vapour profile in parts per million by volume
    - units: ln(ppmv)
- NC_SHORT o (nz,npres)
    - Retrieved natural logaritm of the atmospheric ozone profile in parts per million by volume
    - units: ln(ppmv)
- NC_SHORT c (nz,npres)

    - Retrieved natural logaritm of the atmospheric carbon monoxide profile in parts per million by volume
    - units: ln(ppmv)
- NC_UBYTE X_err (nz,npres)
    - Contains the estimated error for profile variable X, derived from the square-root diagonals of the solution covariance.
- NC_SHORT X_nwp (nz,nnwp)
    - long_name: NWP profile for product X
    - units: depends on X
- NC_FLOAT xX (ntpc,npres)
    - long_name: State vector for profile product X in terms of Eigenvector weights
- NC_FLOAT X_ap (nz,nlb)
    - long_name: Climatological prior for profile product X
    - units: depends on X (K or ln (ppmv))
- NC_SHORT ak_X (nXpc,naks,npiak_X)
    - long_name: Averaging kernel for profile variable X
    - units: 1
- NC_FLOAT Y (npres)
    - long_name: Retrieved column averaged mixing ratio of minor gas Y.
    - units: ppbv
- NC_FLOAT xY (npres)
    - long_name: Retrieved profile scale factor of minor gas Y.
- NC_FLOAT Y_err (npres)
    - long_name: Estimated error on retrieved column averaged mixing ratio of minor gas Y.
    - units: ppbv
- NC_FLOAT Y_rttov (npres)
    - long_name: Column average mixing ratio of minor gas implicitly assumed in RTTOV
    - units: ppbv
- NC_SHORT ak_Y (nz, npres)
    - long_name: Averaging kernel for retrieved column average mixing ratio of minor gas with respect to perturbation in true mixing ratio profile.
    - units: 1
- NC_FLOAT tsk (npres)
    - long_name: State vector for surface temperature
    - standard_name: surface_temperature
    - units: K

- NC_FLOAT tsk_nwp (nnwp)
    - long_name: NWP surface temperature
    - standard_name: surface_temperature
    - units: K
- NC_FLOAT cfr (npres)
    - long_name: Effective cloud fraction. In IMS extended cloud fraction is not retrieved and the effective fraction is defined to be 1-exp(-cot).
- NC_FLOAT cth (npres)
    - long_name: Retrieved cloud top pressure in z-star scale-height.
    - units: km
- NC_FLOAT cot (npres)
    - long_name: Retrieved effective cloud optical thickness.
- NC_FLOAT grf(npres)
    - long_name: Retrieved sun-glint scale factor.
- NC_FLOAT aot(npres, near) ;
    - long_name: Retrieved aerosol optical depths. Two values are given for each scene, the first is for sulphate aerosol and the second is for desert dust.
- NC_FLOAT cre(npres) ;
    - long name: Retrieved cloud effective radius
    - units: microns;
- NC_FLOAT alh (npres)
    - long_name: Retrieved aerosol layer pressure in z-star scale-height.
- NC_FLOAT cot_err (npres)
    - long_name: Estimated error on retrieved effective cloud optical thickness.
- NC_FLOAT grf_err(npres)
    - long_name: Estimated error on retrieved sun-glint scale factor.
- NC_FLOAT aot_err(npres, near) ;
    - long_name: Estimated error on retrieved aerosol optical depths.
- NC_FLOAT cre_err(npres) ;
    - long name: Estimated error on retrieved cloud effective radius
    - units: microns;
- NC_FLOAT alh_err (npres)
    - long_name: Estimated error on retrieved aerosol layer pressure in z-star scale-height.
- NC_FLOAT bcf (nbcf,npres)
    - long_name: Retrieved bias correction factor
- NC_SHORT em (nsp,npres)
    - long_name: Retrieved emissivity
    - units: 1

- NC_UBYTE em_err (nsp,npres)
    - long_name: Estimated error on retrieved emissivity
    - units: 1
- NC_FLOAT cth_err (npres)
    - long_name: Estimated error on retrieved cloud top height
    - units: km
- NC_FLOAT cfr_err (npres)
    - long_name: Estimated error on retrieved cloud fraction.
- NC_FLOAT tsk_err (npres)
    - long_name: Estimated error on retrieved surface temperature
    - units: K
- NC_FLOAT bcf_err (nbcf,npres)
    - long_name: Estimated error on retrieved bias correction factors
    - units:
- NC_FLOAT tsk_ap (nlb)
    - long_name: Climatological prior for surface temperature
    - units: K
- NC_FLOAT avhrr_radiance (navhrr,npi)
    - long_name: Mean of co-located AVHRR radiances (or VIIRS in the case of CrIS)
- NC_FLOAT avhrr_stddev (navhrr,npi)
    - long_name: Standard deviation of of co-located AVHRR radiances (or VIIRS in the case of CrIS).
- NC_FLOAT evecs_X (nz,nXpc)
    - long_name: Eigenvectors to reconstruct profile variable X.
- NC_FLOAT profiles_mgf(nmgf, nz) ;
    - long_name: Minor gas profiles scaled by the retrieved minor gas factors
    - units: ppmv
- NC_FLOAT: profiles_mgf_rttov(nmgf, nz) ;
    - long_name: Minor gas profiles assumed always present in RTTOV (should be added to estimated scaled profile)
    - units: ppmv
- NC_SHORT conv (npres)
    - long_name: Flag indicating retrieval convergence (1=fully converged). Results with other values should be used with more caution
- NC_INT n_step (npres)
    - long_name: The average number of retrieval steps (number of calls to the forward model)

- NC_SHORT pixel_number (npi)
    - long_name: IASI detector pixel (0-3)
- NC_FLOAT longitude (npi)
    - long_name: Longitude
    - standard_name: longitude
    - units: degree_east
- NC_FLOAT latitude (npi)
    - long_name: Latitude
    - standard_name: latitude
    - units: degree_north
- NC_FLOAT satzen (npi)
    - long_name: Sensor view zenith angle
    - standard_name: sensor_zenith_angle
    - units: degree
- NC_FLOAT solzen (npi)
    - standard_name: solar_zenith_angle
    - long_name: Solar zenith angle
    - units: degree
- NC_FLOAT satazi(npi) ;
    - long_name: Sensor view azimuth angle
    - standard_name: sensor_azimuth_angle
    - units: degree
- NC_FLOAT solazi(npi) ;
    - standard_name: "solar_azimuth_angle" ;
    - long_name: "Solar azimuth angle" ;
    - units: degree
- NC_FLOAT land_fraction(npi)
    - long_name: Land fraction
- NC_UINT sensingtime_msec (npi)
    - long_name: Time of day in msec since midnight (UTC)
    - units: s
- NC_UINT sensingtime_day (npi)
    - long_name: Day of measurement since 00:00h 01-01-2000
    - units: day
- NC_FLOAT u(npi)
    - long_name: Eastward 10m wind component
    - units:m/s;
- NC_FLOAT v(npi) ;
    - long_name: Nortward 10m wind component

    - units: m/s
- NC_FLOAT sp (npi)
    - long_name: Assumed surface pressure in retrieval
    - units: hPa
- NC_FLOAT nwp_altitude (npi)
    - long_name: Estimated surface altitude from interpolated NWP data
    - units: m
- NC_FLOAT iasi_altitude (npi)
    - long_name: Estimated surface altitude from interpolated GTOPO30 atlas
    - units: m
- NC_SHORT resid (nsp,nresid)
    - long_name: Residual spectra
    - units: K
- NC_FLOAT cwn (nsp)
    - long_name: Wavenumbers associated with measurement vector
    - units: cm^{-1}
- NC_SHORT bt (nsp,nbtds)
    - long_name: Measurement vector in terms of brightness temperature
    - units: K
- NC_SHORT btds (nsp,nbtds)
    - long_name: Brightness temperature difference spectra between observed and simulated measurements for first guess state
    - units: K
- NC_FLOAT btd (npi)
    - long_name: Brightness temperature difference between observed and simulated measurements for first guess state, in a window channel at 955.25 cm-1
    - units: K
- NC_UBYTE btd_flag (npi)
    - long_name: Flag used as indicator of cloud derived from reported variable btd (at $950cm^{-1}$). 0 indicates no cloud; 1 indicates cloud detected.
- NC_FLOAT sa_X (ntpc)
    - long_name: Globally averaged a priori covariance for profile product X in terms of Eigenvector weights
- NC_FLOAT sa_ts (n1)
    - long_name: Global surface temperature a priori variance
    - units: K^2
- NC_FLOAT dsx_X (nvsxX,npisx_X)

    - long_name: Square-root-diagonals of product X solution covariance matrix in terms of Eigenvector weights
- NC_UBYTE csx_X (nvsxX,npisx_X)
    - long_name: Flattened half of profile product X solution correlation matrix in terms of Eigenvector weights
- NC_FLOAT dsxn_X (nvsxX,npiak_X)
    - long_name: Square-root-diagonals of product X noise covariance matrix in terms of Eigenvector weights
- NC_UBYTE csxn_X (nvsxX,npiak_X)
    - long_name: Flattened half of profile product X noise correlation matrix in terms of Eigenvector weights
- NC_FLOAT X_dofs (npres)
    - long_name: Degrees of Freedom for Signal of profile product X.
- NC_FLOAT em_dofs (npres)
    - long_name: Degrees of Freedom for Signal of surface emissivity
- NC_FLOAT cfr_dofs (npres)
    - long_name: Degrees of Freedom for Signal of Cloud Fraction
- NC_FLOAT cth_dofs (npres)
    - long_name: Degrees of Freedom for Signal of Cloud Top Height
- NC_FLOAT tsk_dofs (npres)
    - long_name: Degrees of Freedom for Surface Temperature
- NC_FLOAT bcf_dofs (npres)
    - long_name: Degrees of Freedom for Bias Correction Factors
- NC_FLOAT dt2 (npres)
    - long_name: Difference between the surface temperature and the temperature profile interpolated to the surface pressure.
    - Units: K
- NC_FLOAT dt1000 (npres)
    - long_name: Difference between the surface temperature and the temperature profile interpolated to 1km z* altitude above the surface.
    - Units: K
- NC_FLOAT tpw (npres)
    - long_name: Total precipitable water vapour
    - units: kg/m2
- NC_FLOAT tpw_err (npres)
    - long_name: Estimated error on retrieved total precipitable water vapour
    - units: kg/m2
- NC_FLOAT k_index (npres)
    - long_name: k-index

    - units: K
- NC_FLOAT lifted_index (npres)
    - long_name: lifted index
    - units: K
- NC_UBYTE imode (npi)
    - long_name: Flag indicating instrument observing mode; 0 indicates standard mode; 1=nadir static view for IASI.
- NC_UBYTE iasc (npi)
    - long_name: Flag indicating if satellite is in on ascending (1) or descending node (0).

3.4 Quality control

The main parameter which can be used for quality control are:

- Cost function at solution. It is recommended that retrievals with total cost function (the sum of variables jx and jy) greater than 1000 are not used.
- Variable “btd_flag”, which enables grossly cloud free scenes to be identified and potentially removed from further analysis.
- Variable “cfr”, can also be used to provide a more stringent test on cloud occurrence.
- Variables “dt2” and “dt1000” can be used to identify scenes with strong negative surface/air thermal contrast. It may be advisable to remove such scenes (e.g. dt1000<-1K), because in these conditions the sensitivity to trace gases (averaging kernels) can be weak and even change sign through the troposphere introducing uncertainties which are not well characterised by retrieval diagnostics. It is also found that removing such scenes also tends to remove scenes with low altitude cloud not captured by “btd_flag” or “cfr”.
- For most purposes it is advisable to only use cloud-free observations. If cloudy scenes are used the cloud height (“cth”) can be useful to screen retrievals e.g. to select profile values only above the cloud top. More relaxed cloud screening can be performed using the product of cloud fraction and height “cfr*cth”. Threshold on this can be set such that only scenes with a high fraction of high altitude cloud are removed from analysis, while results which have significant sensitivity in the troposphere are retained (because either fraction is low or altitude is low).

4. PRODUCT QUALITY

4.1 Sensitivity and vertical resolution

Some basic retrieval diagnostics from the IMS-extended data are presented for four example cloud-free scenes, over land and sea, in tropics and mid-latitudes, in Figure 4-1 to Figure 4-4. Each of these figures show similar (close in space and time) scenes from Metop-B in the top panels and Suomi-NPP in the lower panels.

These figures summarise the key output from IMS-extended as follows:

- Top-right text legend: Gives some basic information about the scene including date, geolocation, scan geometry, together with some cloud/aerosol/surface related output variables (using the names as in the L2 file (see section 3.3.3). Retrieval output variables are generally given "±" their estimated standard deviation (ESD, the corresponding L2 variable ending "_err"). Note that "aot0" and "aot1" are the optical depths of sulphate and dust aerosol, respectively. These scenes do not contain significant levels of aerosol, but the sensitivity to aerosol can still be gauged by the estimated errors on the aerosol optical depths (the estimated error on the optical depths is not strongly dependent on the optical depth itself, until it becomes optically thick).
- Bottom-right panel shows the averaging kernels (or vertical sensitivity functions) for the retrieved minor gas profile scale factors. The legend below gives the retrieved column averaged mixing ratio and its estimated error. These kernels are displayed normalised such that they show the derivative of the retrieved total column with respect to perturbation of unit column amount in an infinitesimal layer as a function of height. Normalised like this, ideal kernels would be 1 at all altitudes. In practise the kernels vary in the range 0-3 as a function of altitude, the shape of the curves reflecting the vertical sensitivity being controlled by temperature contrast with the surface. The absolute values in the kernels depends largely on the assumed profile which is scaled - they will tend to cross a value of 1 on the x-axis around the altitude of the centre of mass of the assumed profile. This version of IMS-extended assumes a fixed mixing ratio so the kernels cross AK=1 around 500hPa or ~4.8km. These functions can be negative near the ground when surface-air temperature contrast is negative. Kernels for the gases in window regions are very similar to each other. Kernels for SO_2 (in a strong water vapour absorption region) show less sensitivity lower down, and more amplified sensitivity to perturbations at high altitude. E.g. in the case of a volcanic plume of SO_2 injected at 20km in the atmosphere, IMS would report an estimated column amount ~3 times larger than the true column. Knowing the height of the layer from independent information, the kernels can be used to correct for this bias related to the simple profile shape assumption.

- Other panels illustrate retrievals of the main profile variables, temperature, water-vapour, ozone and carbon monoxide. For each of these profiles a pair of panels is shown:
    - Left-hand panels: Comparison of the retrieved (Ret, black), a priori (AP, red), “NWP” analysis (NWP, green) and NWP analysis after applying averaging kernels via Equation 27 (NWPxAK, blue). For water vapour and temperature “NWP” is from ECMWF ERA-5 [RD32]. For carbon monoxide and ozone, “NWP” is from CAMS reanalysis[RD31]. Dashed lines about the retrieved profile indicate the range of the ESD from the solution covariance. In these cases results are generally close to NWP despite large differences from the climatological prior in some cases/altitude ranges.
    - Right-hand panels: Averaging kernels. For water vapour and temperature, kernels for a sub-set of retrieval levels is shown (see legend on the extreme right). These are shown in the retrieval units i.e. K/K for temperature and log mixing ratio for water vapour (so the kernels can be interpreted as showing the relative change in the retrieval with respect to a relative change in the true profile as a function of height). The degrees of freedom for signal (DOFS) are given in the panel title. These examples illustrate the capability of IMS to resolve temperature throughout the troposphere and stratosphere and water vapour throughout the troposphere. The altitude up to which the water vapour profile is well resolved follows the tropopause: Sensitivity to stratospheric water vapour is generally low (due mainly to the relatively low stratospheric mixing ratio). For ozone and carbon monoxide (which have relatively limited information content) the kernels are shown for derived integrated (sub-) column amounts (see legend under each panel), normalised like the minor gas kernels, with respect to delta function column perturbations in the true profile. In this case, ideal kernels would be box-car functions with value 1 within the relevant layer and 0 outside. Ozone has 3-4 degrees of freedom, including some discrimination of upper and lower tropospheric ozone. Carbon monoxide has very limited vertically resolution (results are effectively limited to a column amount).

Figure 4-5 shows Suomi-NPP scenes for mid-latitude *cloudy* scenes over land and sea, close to the corresponding cloud-free mid-latitude scenes in Figure 4-1 and Figure 4-3. As should be expected, the impact of cloud is to strongly reduce sensitivity below the cloud height, especially for the ozone, carbon monoxide and the minor gases. Some sensitivity remains for water vapour and temperature, due to the assumed sensitivity of the microwave observations even in the presence of cloud. Averaging kernels for temperature actually peak very sharply at the cloud top (the signal for the cloud-top temperature is particularly strong). In general the profiles agree

well with NWP down to the cloud top. Below cloud the quality of the retrievals is questionable. Care should be taken in using results in cloudy scenes, particularly profile values below the cloud top. Further analysis of the sensitivity to cloud is given in the E3UB [RD38].

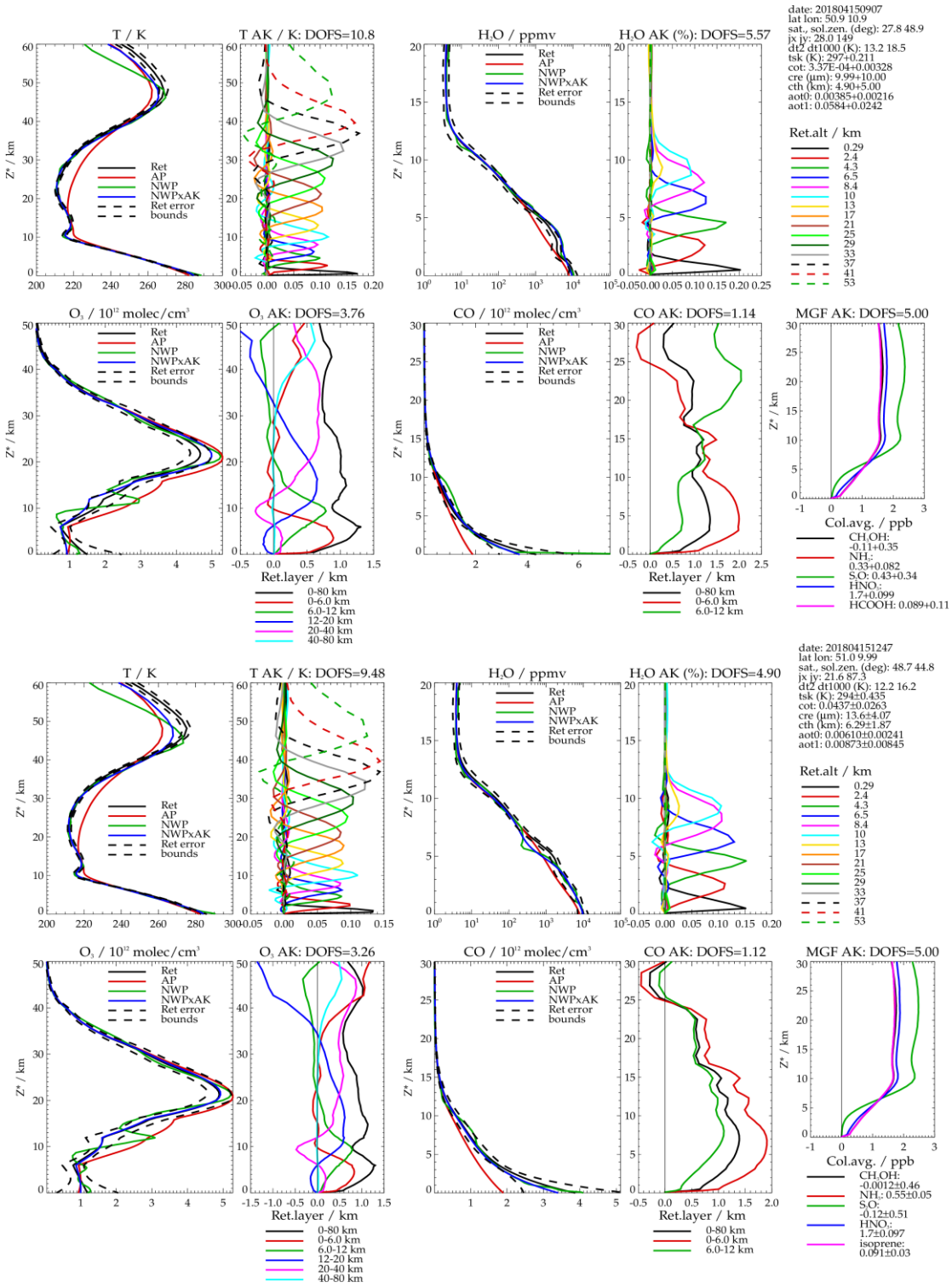

Figure 4-1 : Example retrieval output for mid-latitude cloud-free land conditions. Upper set of panels show IASI results. Lower set of panels results for a nearby comparable CrIS scene.

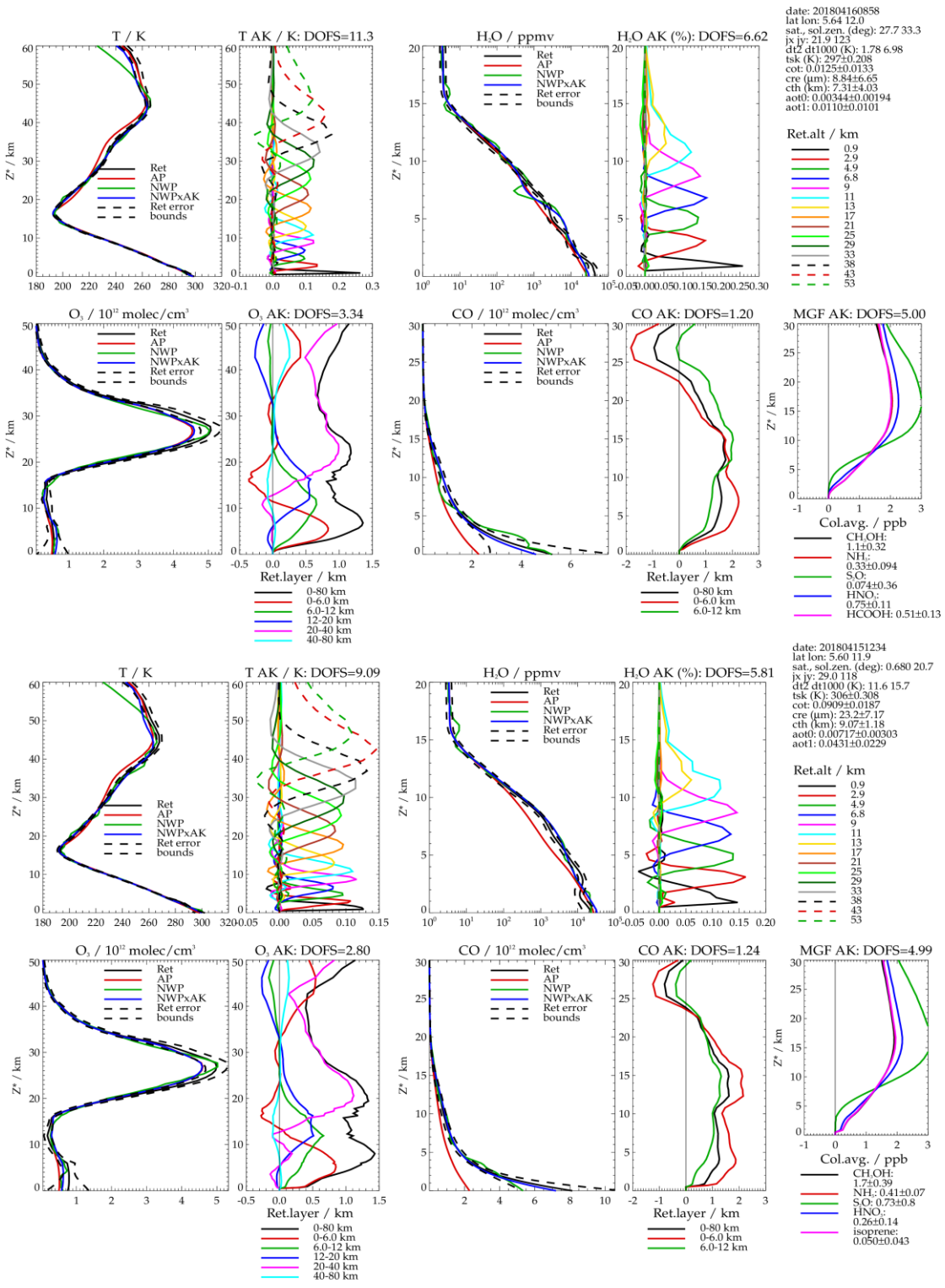

Figure 4-2 : Example retrieval output for tropical cloud-free land conditions. Upper set of panels show IASI results. Lower set of panels results for a nearby comparable CrIS scene.

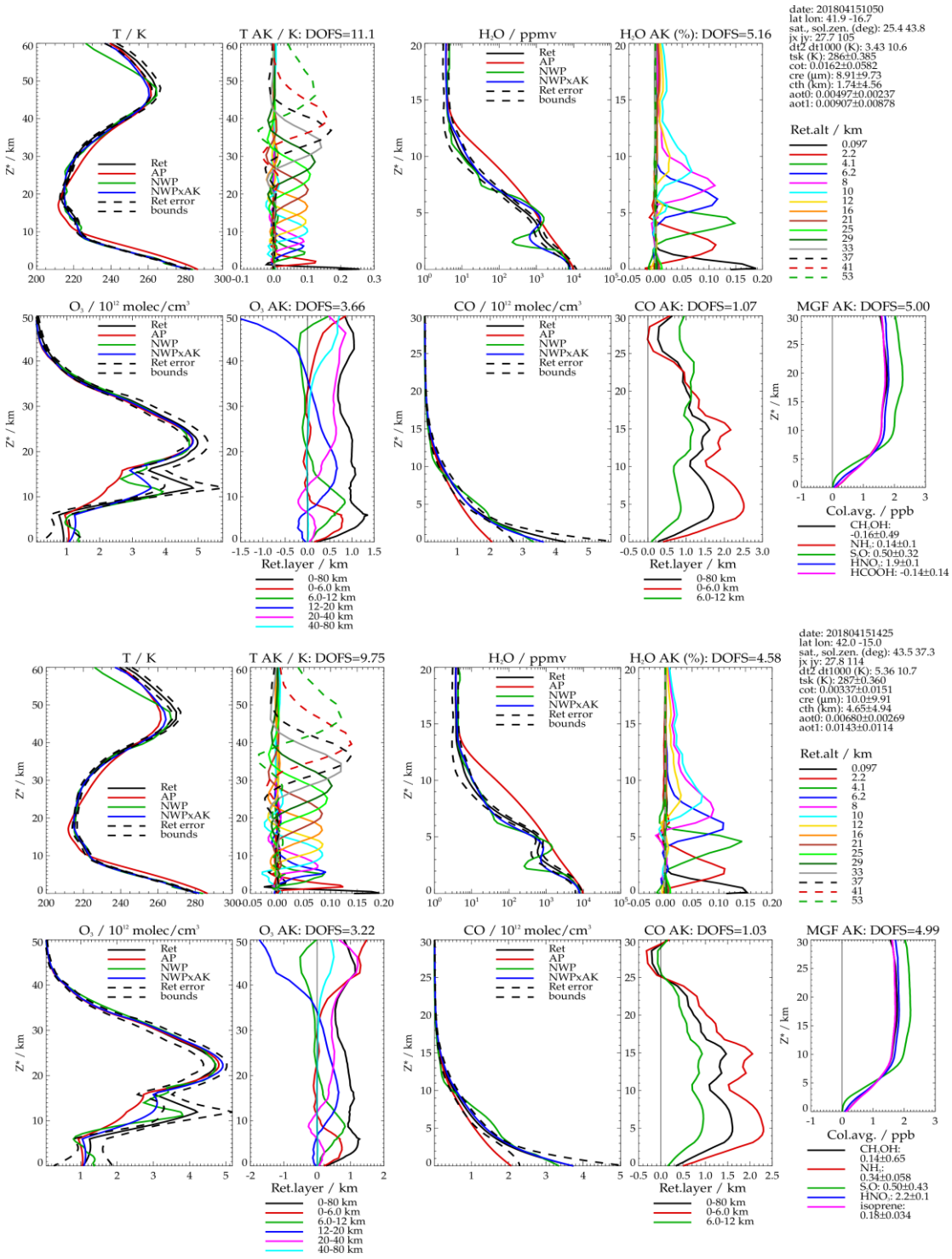

Figure 4-3 : Example retrieval output for mid-latitude cloud-free sea conditions. Upper set of panels show IASI results. Lower set of panels results for a nearby comparable CrIS scene.

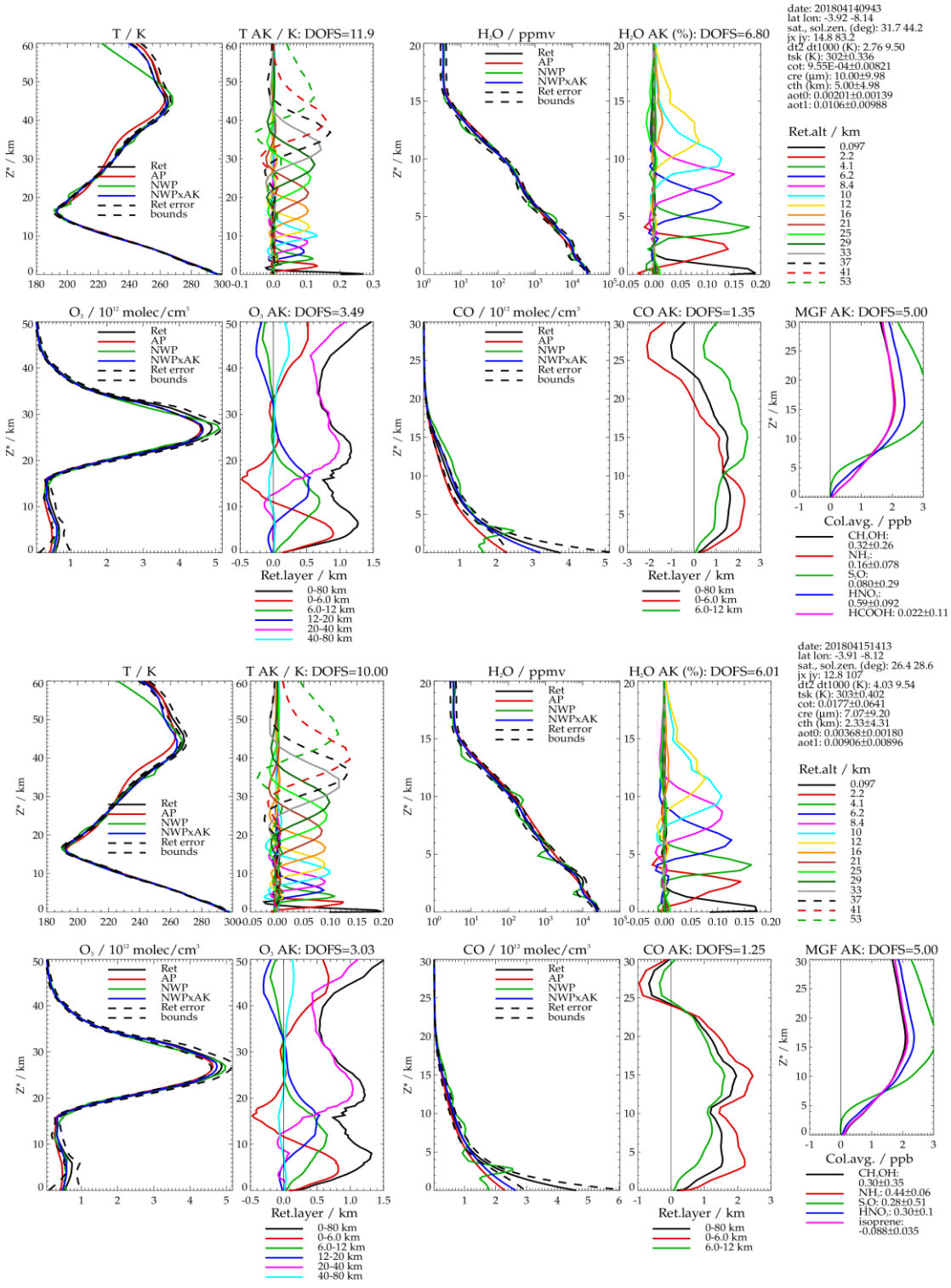

Figure 4-4 : Example retrieval output for tropical cloud-free sea conditions. Upper set of panels show IASI results. Lower set of panels results for a nearby comparable CrIS scene.

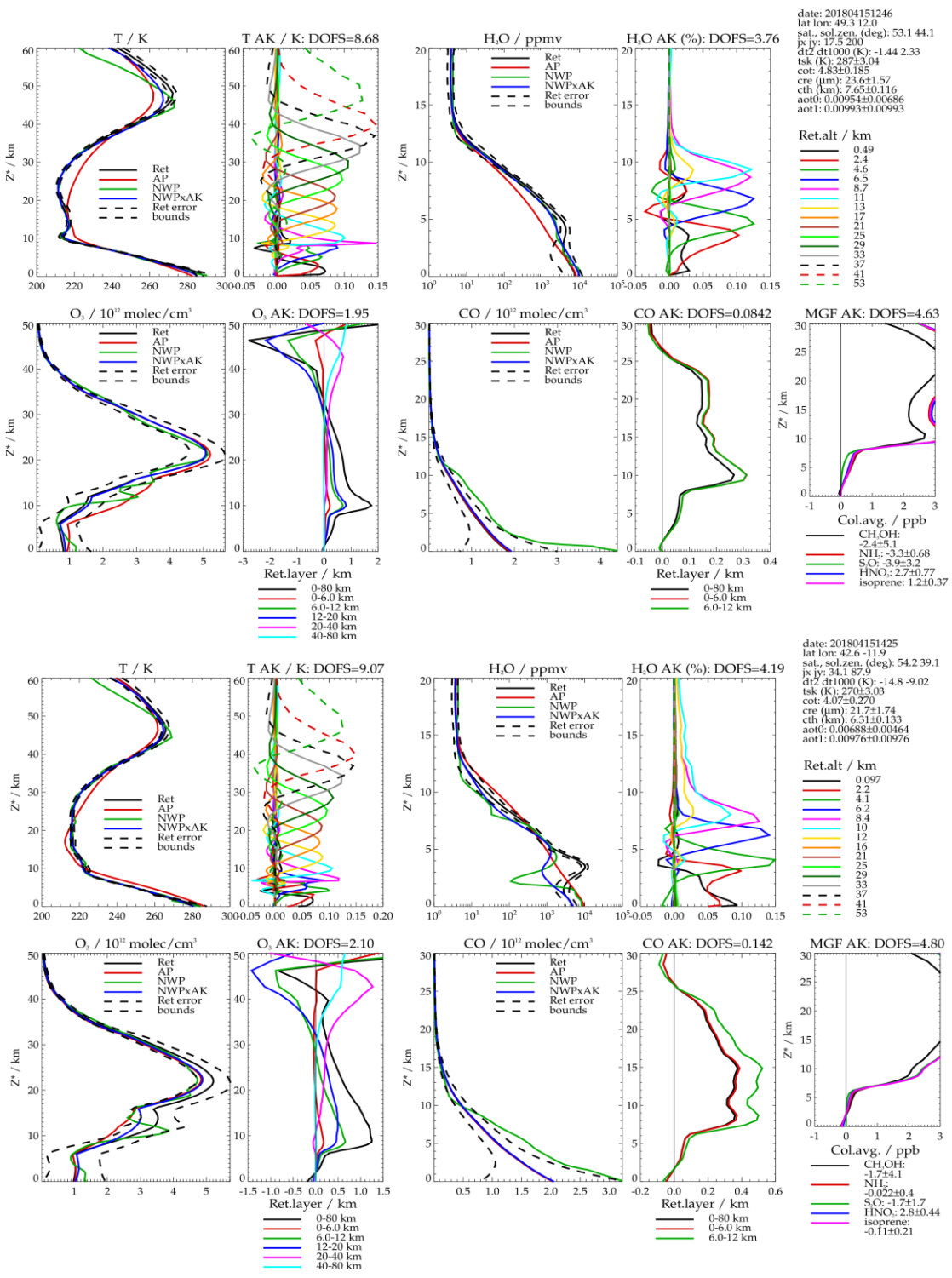

Figure 4-5 : Example retrievals from CrIS for mid-latitude cloudy scenes over land (top) and sea (bottom).

4.2 Time-series comparisons to ERA-5

Results from the full time-series of IMS-extended data, applied to Metop, are illustrated via Hovmoller diagrams in Figure 4-6 to Figure 4-15. Each figure has six panels showing results at different pressure levels throughout the troposphere up to the UT/LS. Data from Metop-A run from mid 2007 (beginning of the Metop-A operational phase) to the end of 2017. The plots then show data from Metop-B from the beginning of 2018 to the end of 2022. Data up to the end of 2021 are compared to NWP re-analysis from ERA-5. Data in 2022 were produced using IMS-extended in near-real time mode and are compared to ECMWF operational forecast data available at the time of processing.

Figure 4-6 shows (mainly for context) the zonal mean time-series of retrieved water vapour. Note that the prior distribution has no time variation, so all the seasonal cycle is derived from the measurements. Throughout results are shown in units of ln(ppmv).

Figure 4-7 shows the estimated standard deviation (ESD) of solution covariance (averaging into the latitude/time bins). This is an estimate of the total error (noise + smoothing) on the individual retrieved profiles. Given the log unit, these can be approximately interpreted as relative errors. Within the troposphere errors are at best ~10-20%, with larger uncertainty where the water mixing ratios are smaller (towards higher altitude or polar winter). Errors are particularly large near the surface over Antarctica, due to dry conditions are very low surface temperature.

Figure 4-8 shows mean differences between IMS and ERA-5. These errors follow the distribution of the ESD to some extent (this would be expected for the smoothing error contribution which may give rise to systematic error).

Figure 4-9 shows differences after taking into account retrieval sensitivity by applying the averaging kernels via Equation 28. Differences are generally much reduced compared to the previous figure, indicating that averaging kernels can explain much of the deviation between ERA-5 and the retrievals. There remains some systematic bias particularly in the upper troposphere, which IMS is 10-20% dryer than ERA-5 in the tropics and 30% wetter in polar winter.

Figure 4-10 and Figure 4-11 show the standard deviation of the difference between individual retrieved profiles and ERA-5, before and after accounting for averaging kernels, respectively. These also show the importance of the averaging kernels in explaining much of the differences.

Figure 4-12, Figure 4-13 and Figure 4-14 show the ability of IMS to capture the interannual variability of water vapour. They show the de-seasonalised anomaly i.e. the difference between individual monthly zonal means and the multi-annual zonal mean (considering all years 2007-

22) for the same month. Figure 4-12 shows the retrieved time-series while Figure 4-13 and Figure 4-14 show ERA-5 before and after applying averaging kernels. The retrieval tends to smooth the “true” variability towards the higher altitudes but captures very well both the quasi-random structure and the high anomalies associated with the El Nino in 2015-16 and (to a lesser extent) 2009-10 and 2019-20.

Figure 4-15 shows the de-seasonalised anomaly of the difference between IMS and ERA-5 with averaging kernels. This could reveal any time dependent instrumental bias (drift, discontinuities) in the retrieval (assuming ERA-5 to be drift free). The following discontinuities are small compared to inter-annual variability but are highlighted in this plot:

- Around April 2014, caused by an extended break in the availability of data from MHS (IMS retrieval is performed using AMSU and IASI only).
- At the beginning of 2018, associated with the change from Metop-A to Metop-B data (particular at higher latitudes).
- At the beginning of 2022, when IMS was processed in near-real time, and the comparison is performed with respect to operational forecast data instead of ERA-5.

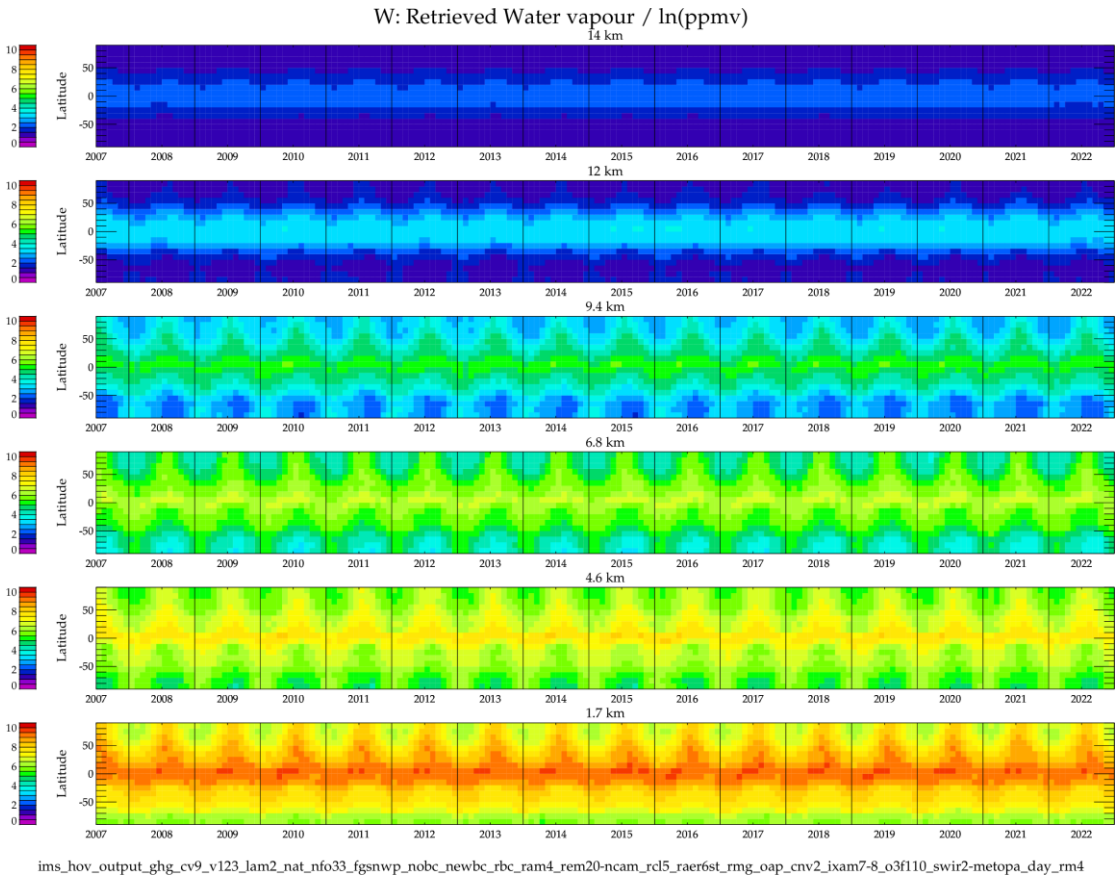

Figure 4-6 : Time series of Metop-A (2007-2017) and Metop-B data (2018-2022) water vapour data on 6 levels: Mean retrieved water vapour.

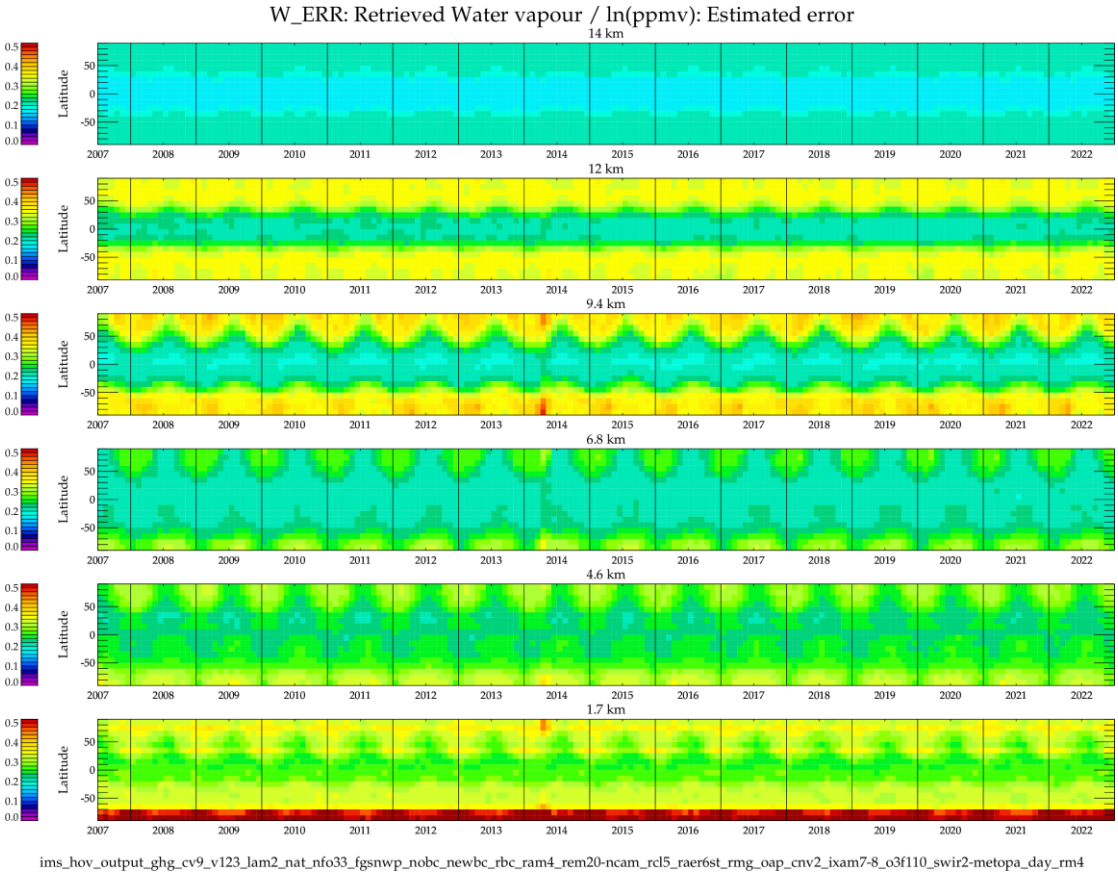

Figure 4-7 : Time series of Metop-A (2007-2017) and Metop-B data (2018-2022) water vapour data on 6 levels: Mean ESD of retrieved water vapour.

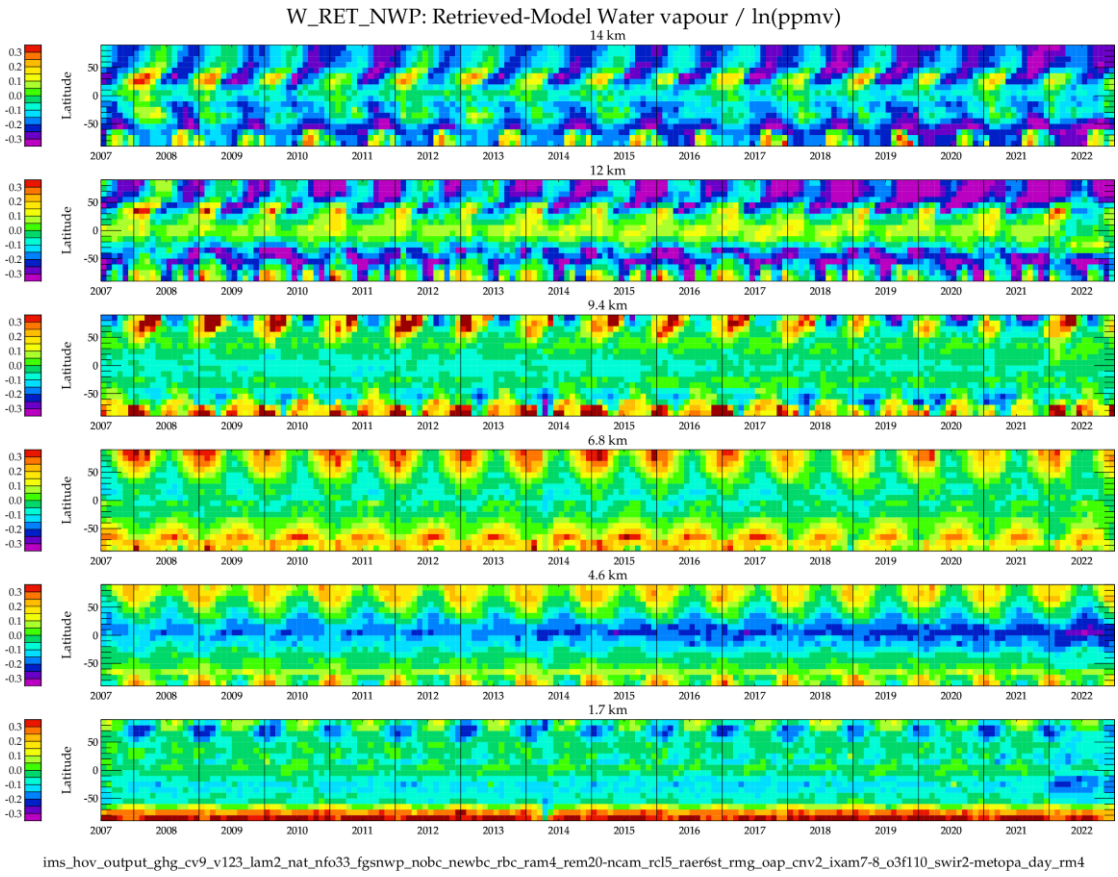

Figure 4-8 : Time series of Metop-A (2007-2017) and Metop-B data (2018-2022) water vapour data on 6 levels: Mean difference beyween retrieved and NWP water vapour.

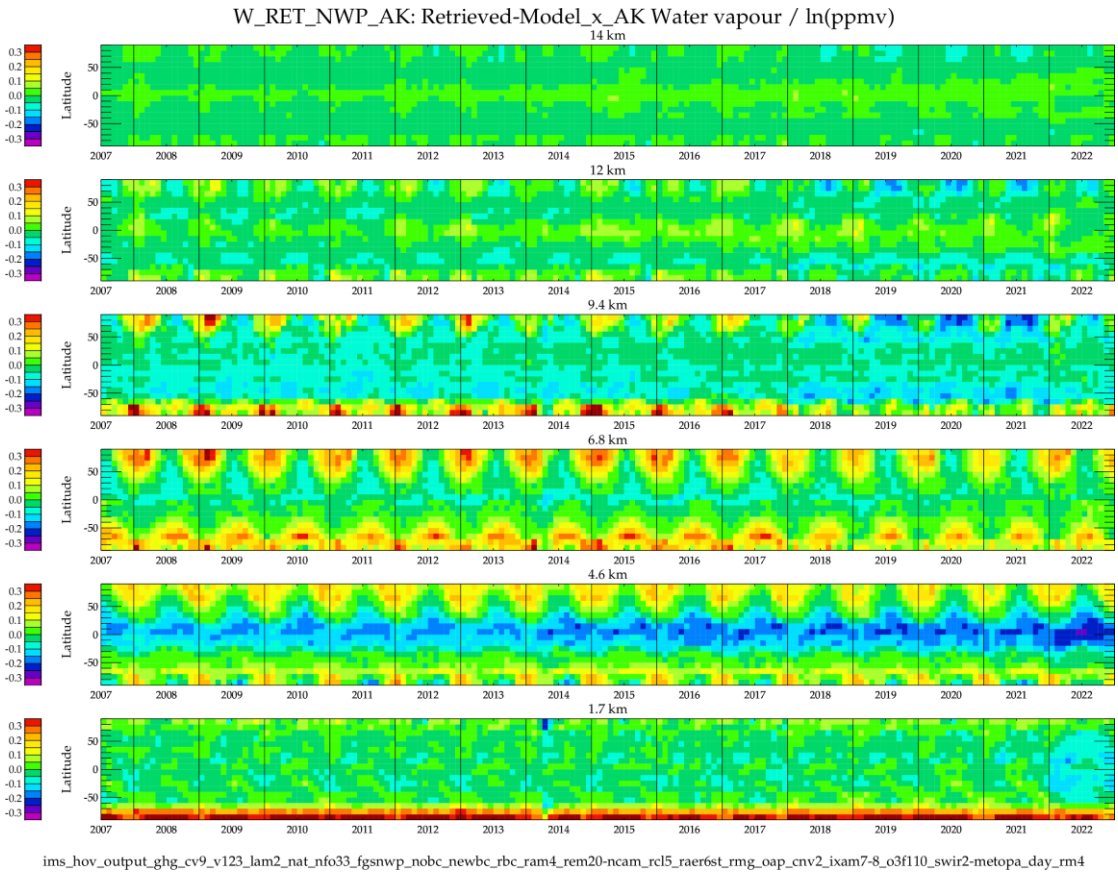

Figure 4-9 : Time series of Metop-A (2007-2017) and Metop-B data (2018-2022) water vapour data on 6 levels: Mean difference between retrieved and NWP water vapour, accounting for averaging kernels.

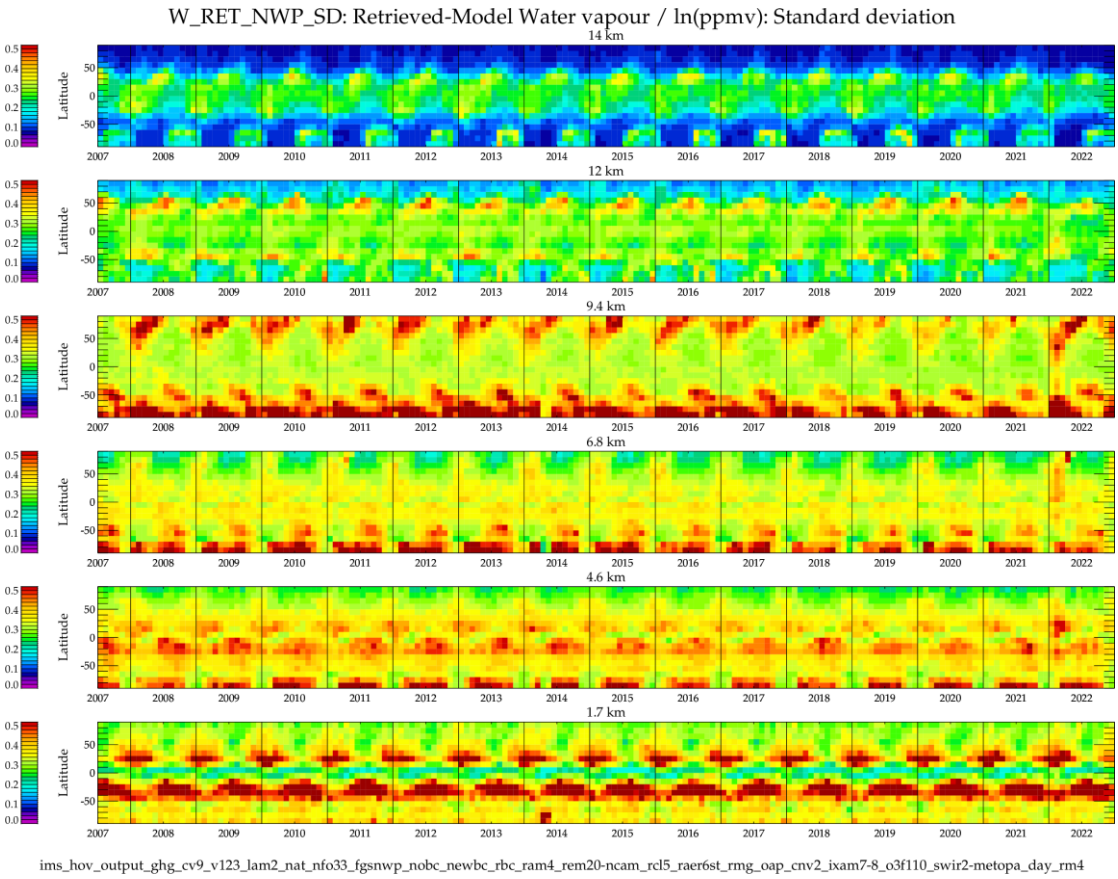

Figure 4-10 : Time series of Metop-A (2007-2017) and Metop-B data (2018-2022) water vapour data on 6 levels: Standard deviation in the mean difference between retrieved and NWP water vapour.

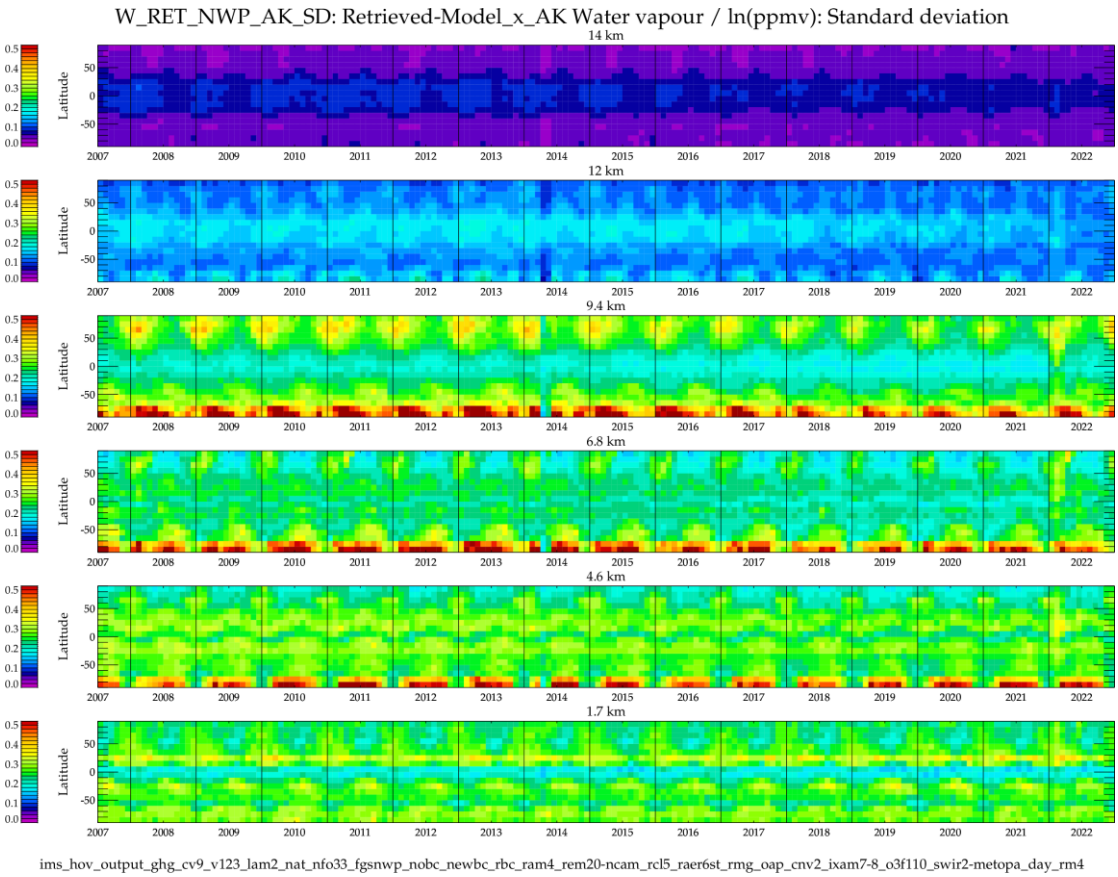

Figure 4-11 : Time series of Metop-A (2007-2017) and Metop-B data (2018-2022) water vapour data on 6 levels: Standard deviation in the mean difference between retrieved and NWP water vapour, accounting for averaging kernels.

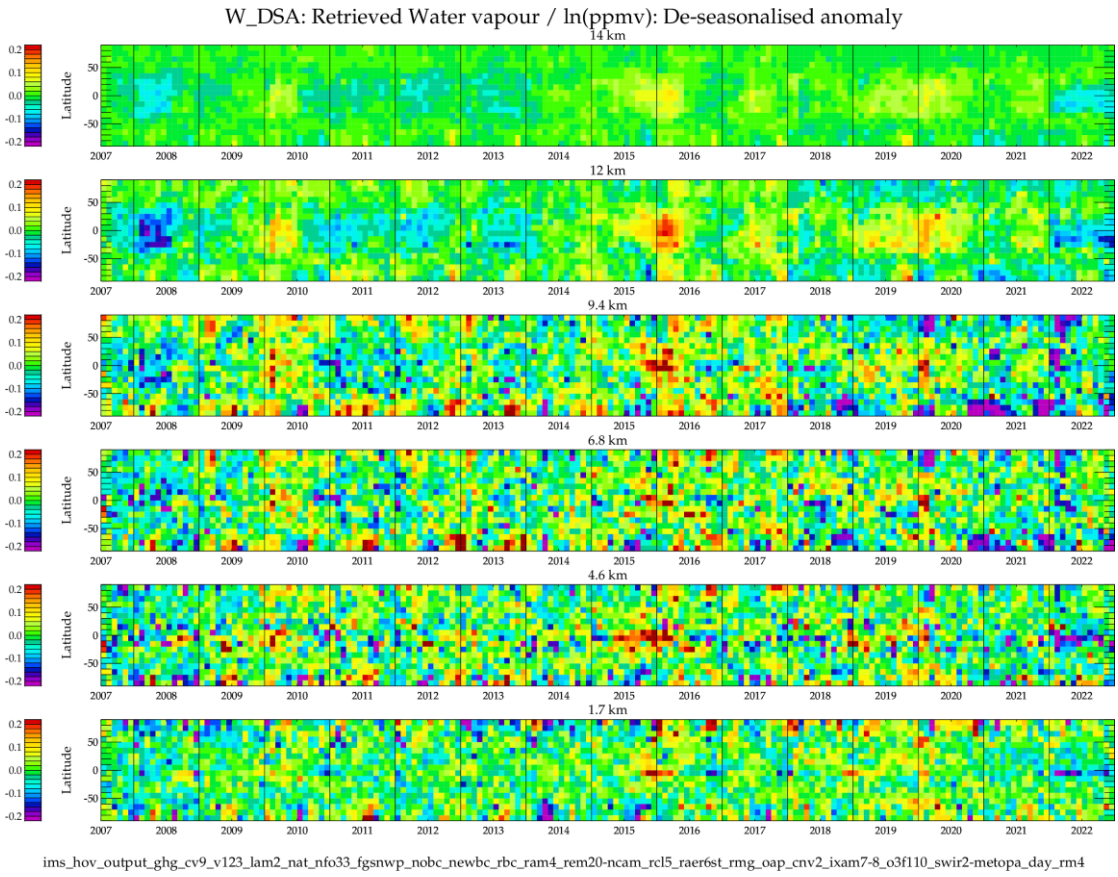

Figure 4-12 : Time series of Metop-A (2007-2017) and Metop-B data (2018-2022) water vapour data on 6 levels: De-seasonalised anomaly of the mean retrieved water vapour.

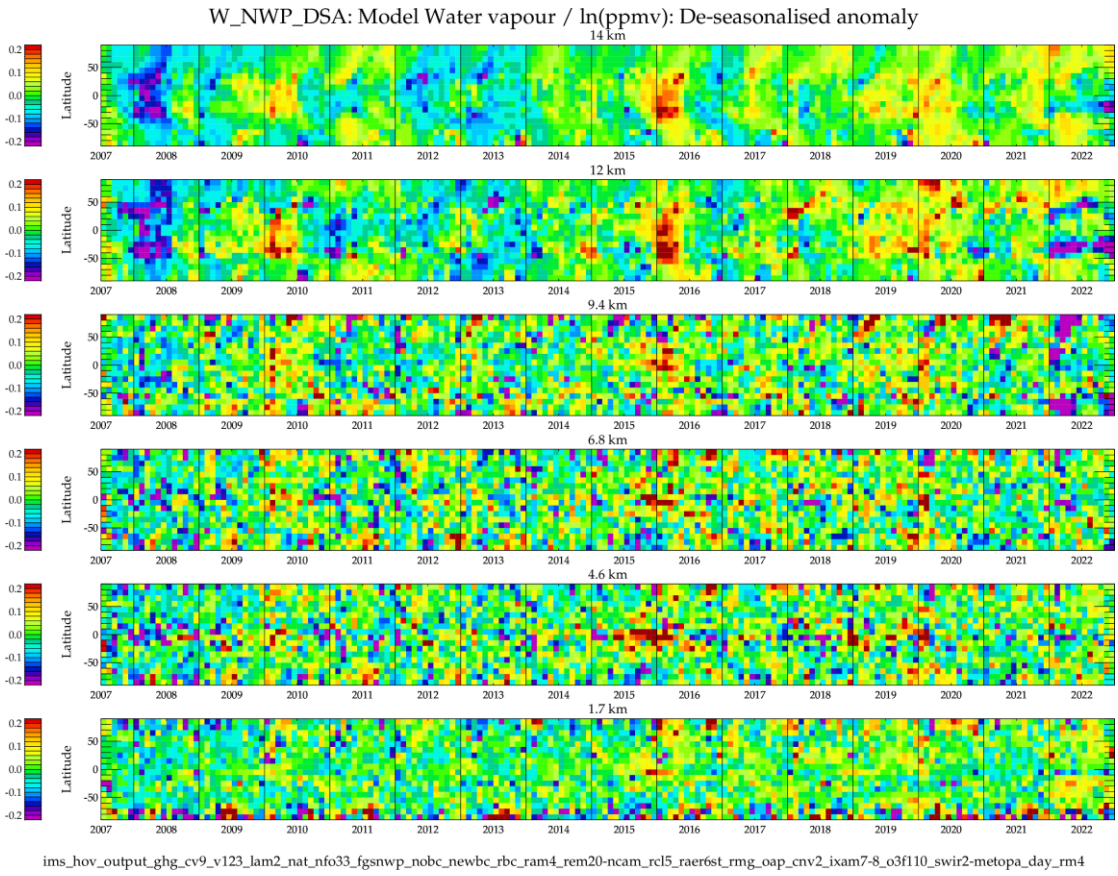

Figure 4-13 : Time series of Metop-A (2007-2017) and Metop-B data (2018-2022) water vapour data on 6 levels: De-seasonalised anomaly of the mean NWP water vapour.

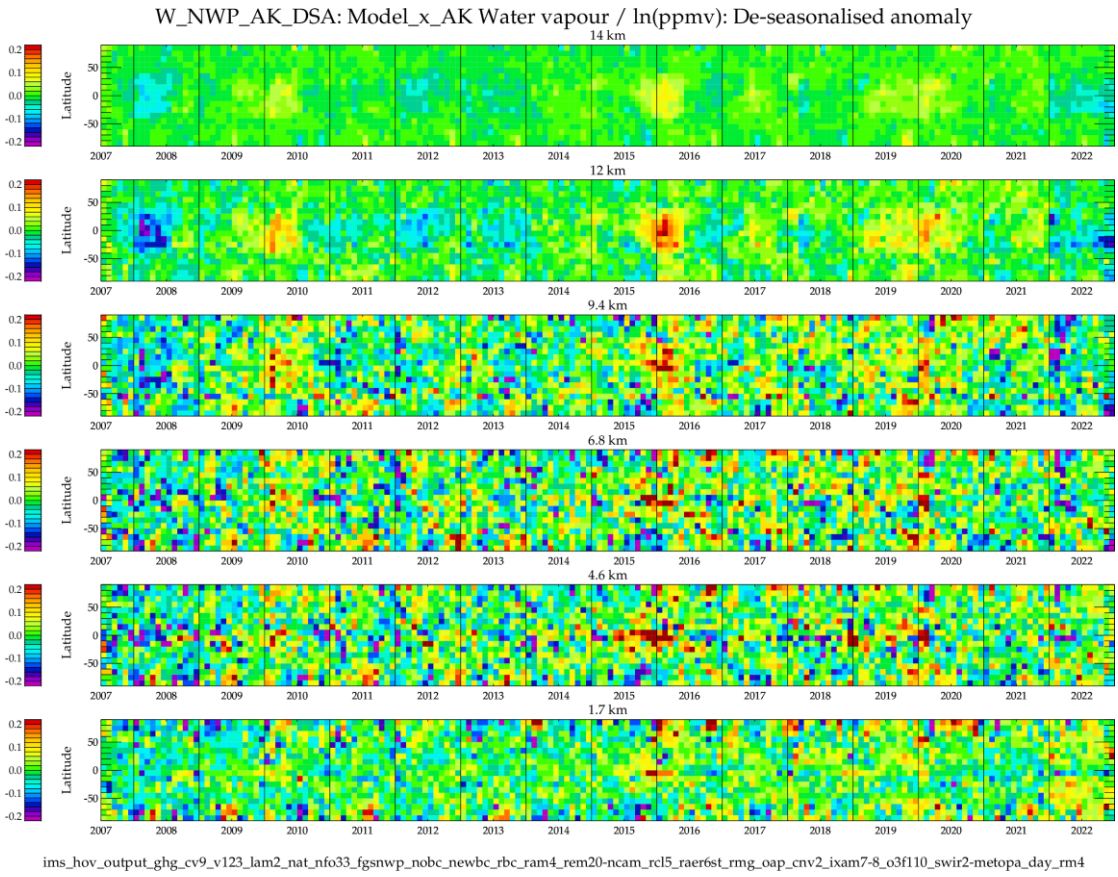

Figure 4-14 : Time series of Metop-A (2007-2017) and Metop-B data (2018-2022) water vapour data on 6 levels: De-seasonalised anomaly of the mean NWP water vapour, accounting for averaging kernels.

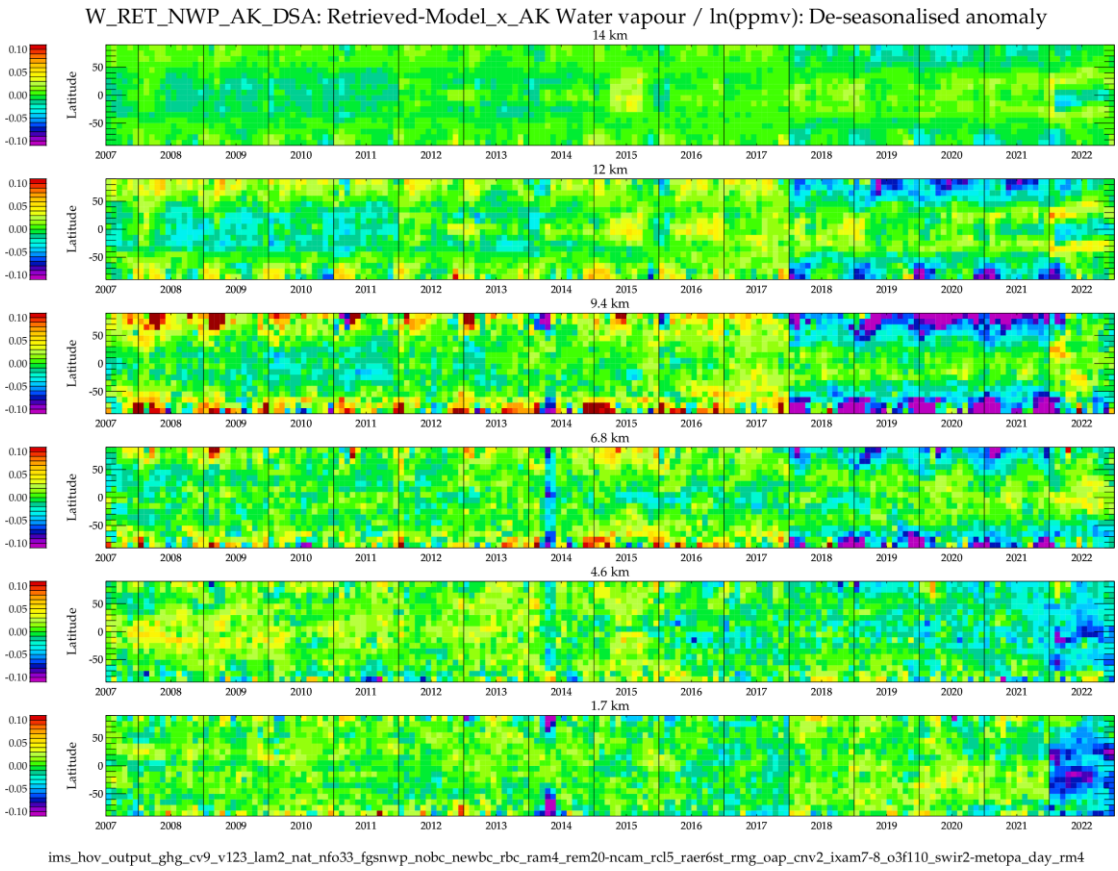

Figure 4-15 : Time series of Metop-A (2007-2017) and Metop-B data (2018-2022) water vapour data on 6 levels: De-seasonalised anomaly of mean difference between retrieved and NWP water vapour, accounting for averaging kernel.

APPENDIX 1: REFERENCES

[RD01] R. Siddans, D. Gerber, B. Bell, Optimal Estimation Method retrievals with IASI, AMSU and MHS measurements. Final Report, EUM/CO/13/46000001252/THH, 2015

[RD02] Siddans, R., Knappett, D., Waterfall, A., Hurley, J., Latter, B., Kerridge, B., Boesch, H., and Parker, R.: Global height-resolved methane retrievals from the Infrared Atmospheric Sounding Interferometer (IASI) on MetOp, *Atmos. Meas. Tech. Discuss.*, https://doi.org/10.5194/amt-2016-290, accepted for publication Sept'2017.

[RD03] Eumetsat; IASI Level 2: Product Guide; EUM/OPS-EPS/MAN/04/0033; v3E e-signed, 11 July 2017

[RD04] Blumstein, D.; Chalon, G.; Carlier, T.; Buil, C.; Hébert, Ph.; Maciaszek, T.; Ponce, G.; Phulpin, T.; Tournier, B.; Siméoni, D.; Astruc, P.; Clauss, A.; Kayal, G.; Jegou, R. (2004). "IASI instrument: technical overview and measured performances". Proceedings of the SPIE. Infrared Spaceborne Remote Sensing XII 5543: 196–207. doi:10.1117/12.560907.

[RD05] ATOVS Level 1b Product Guide; EUMETSAT; Doc.No. : EUM/OPS-EPS/MAN/04/0030; Issue : v3; Date : 11 January 2010.

[RD06] ATOVS Level 2 Product Guide; Eumetsat; Doc.No: EUM/OPS-EPS/MAN/04/0031; v2, 22 July 2009

[RD07] Rodgers, C. D.: Inverse Methods for Atmospheric Sounding: Theory and Practice, World Sci., Hackensack, N.J., 2000.

[RD08] Press, W.H., Teukolksy, S., Vetterling, W.T. and Flannery, B., Numerical Recipes: the art of scientific computing, Second edition, Cambridge University Press, 1995.

[RD09] Siddans, R.; Walker, J.; Latter, B.; Kerridge, B.; Gerber, D.; Knappett, D. (2018): RAL Infrared Microwave Sounder (IMS) temperature, water vapour, ozone and surface spectral emissivity. Centre for Environmental Data Analysis, *date of citation*. doi:10.5285/489e9b2a0abd43a491d5afdd0d97c1a4. http://dx.doi.org/10.5285/489e9b2a0abd43a491d5afdd0d97c1a4

[RD10] Borbas, E. E. and B. C. Ruston, 2010. The RTTOV UWiremis IR land surface emissivity module. NWP SAF report. http://research.metoffice.gov.uk/research/interproj/nwpsaf/vs_reports/nwpsaf-mo-vs-042.pdf

[RD11] Hultberg and August, CANONICAL ANGLES BETWEEN THE IASI OBSERVATION AND FORWARD MODEL SUBSPACES

[RD12] Hultberg and August, THE PIECEWISE LINEAR REGRESSION RETRIEVAL OF TEMPERATURE, HUMIDITY AND OZONE WITHIN THE EUMETSAT IASI L2 PPF VERSION 6

[RD13] Roger Saunders, James Hocking, Peter Rayer, Marco Matricardi, Alan Geer, Niels Bormann, Pascal Brunel, Fatima Karbou and Filipe Aires, RTTOV-10 SCIENCE AND VALIDATION REPORT; NWPSAF-MO-TV-023; Version : 1.11; Date : 23/1/2012

[RD14] Roger Saunders, James Hocking, David Rundle, Peter Rayer, Stephan Havemann, Marco Matricardi, Alan Geer, Cristina Lupu, Pascal Brunel, Jérôme Vidot, RTTOV-12 Science and Validation Report, Doc ID : NWPSAF-MO-TV-41,Version 1.0, Date : 16/02/2017

[RD15] James Hocking, Peter Rayer, David Rundle and Roger Saunders, Marco Matricardi and Alan Geer, Pascal Brunel and Jérôme Vidot, RTTOV v12 Users Guide Doc ID : NWPSAF-MO-UD-037, Version 1.3, Date : 05/03/2019.

[RD16] Atkinson, N.C, F. I. Hilton, S. M. Illingworth, J. R. Eyre and T. Hultberg; Potential for the use of reconstructed IASI radiances in the detection of atmospheric trace gases; Atmos. Meas. Tech., 3, 991-1003, 2010; https://doi.org/10.5194/amt-3-991-2010

[RD17] Dudhia, A; Zenith Sky Optical Thickness Infrared Spectrum; http://eodg.atm.ox.ac.uk/ATLAS/zenith-absorption

[RD18] Bergamaschi, P., Segers, A., Scheepmaker, R., Frankenberg, C., Hasekamp, O., Dlugokencky, E., Sweeney, C., Ramonet, M., Tarniewicz, J., Kort, E., and Wofsy, S.(2013b): Report on the quality of the inverted CH4 fluxes, MACC-II Deliverable D_43.3, Tech. rep., available at: https://atmosphere.copernicus.eu/documents/maccii/deliverables/ghg/, Joint Research Center, European Commission.

[RD19] D. P. Dee, S. M. Uppala, A. J. Simmons et al, The ERA-Interim reanalysis: configuration and performance of the data assimilation system, QJRMS; 28 April 2011; https://doi.org/10.1002/qj.828

[RD20] Liu, Q, F. Weng, S.J. English, An Improved Fast Microwave Water Emissivity Model, IEEE Transactions on Geoscience and Remote Sensing (Impact Factor: 3.47). 05/2011; DOI: 10.1109/TGRS.2010.2064779

[RD21] Karbou, F., E.Gérard, and F. Rabier, 2006, Microwave land emissivity and skin temperature for AMSU-A and –B assimilation over land, Q. J. R. Meteorol.Soc., vol. 132, No. 620, Part A, pp. 2333-2355(23), doi :10.1256/qj.05.216

[RD22] Paul I. Palmer, Margaret R. Marvin, Richard Siddans, Brian J. Kerridge, and David P. Moore, Nocturnal survival of isoprene linked to formation of upper tropospheric organic aerosol , Science, 3 Feb 2022, Vol 375, Issue 6580, pp. 562-566., DOI: 10.1126/science.abg4506

[RD23] Edward Kim, Cheng-Hsuan J. Lyu, Kent Anderson, R. Vincent Leslie, William J. Blackwell, S-NPP ATMS instrument prelaunch and on-orbit performance evaluation, JGR Atmospheres, First published: 27 March 2014, https://doi.org/10.1002/2013JD020483

[RD24] Jet Propulsion Laboratory: Bjorn Lambrigtsen ; JPSS-1 ATMS Level 1B Brightness Temperature V3Version: 3; Goddard Earth Sciences Data and Information Services Center (GES DISC); Release Date: 2020-12-01T00:00:00.000Z;DOI: 10.5067/MUNII2DHSSY3

[RD25] Y. Han, H. Revercomb, M. Cromp, D. Gu, D. Johnson, D. Mooney, D. Scott, L. Strow, G. Bingham, L. Borg, Y. Chen, Suomi NPP CrIS measurements, sensor data record algorithm, calibration and validation activities, and record data quality, J. Geophys. Res. Atmos., 118 (22) (2013), pp. 12-734

[RD26] W-Madison Space Science and Engineering Center: Hank Revercomb; UMBC Atmospheric Spectroscopy Laboratory: Larrabee Strow (2020), JPSS-1 CrIS Level 1B Full Spectral Resolution V3, Greenbelt, MD, Goddard Earth Sciences Data and Information Services Center (GES DISC), 10.5067/LVEKYTNSRNKP

[RD27] Carolyn Root, Joint Polar Satellite System (JPSS) Cross Track Infrared Sounder (CrIS) Sensor Data Records (SDR) Algorithm Theoretical Basis Document (ATBD); 474-00032; Effective Date: November 19, 2014; Revision C

[RD28] NASA Cross-track Infrared Sounder (CrIS) ; Level 1B Delta Algorithm Theoretical Basis Document (ATBD); University of Maryland Baltimore County Atmospheric Spectroscopy Laboratory, University of Wisconsin Madison Space Science and Engineering Center, Version 3, Product Version: 3, Software Version: 3.0

[RD29] EUMETSAT (2018): IASI Level 1C Climate Data Record Release 1 - Metop-A, European Organisation for the Exploitation of Meteorological Satellites, DOI: 10.15770/EUM_SEC_CLM_0014. http://doi.org/10.15770/EUM_SEC_CLM_0014

[RD30] K. C. Wells, D. B. Millet, V. H. Payne, C. Vigouroux, C. A. B. Aquino, M. De Mazière, J. A. de Gouw, M. Graus, T. Kurosu, C. Warneke, A. Wisthaler, Next-Generation Isoprene Measurements From Space: Detecting Daily Variability at High Resolution, 20 February 2022, https://doi.org/10.1029/2021JD036181

[RD31] Inness, A., Ades, M., Agustí-Panareda, A., Barré, J., Benedictow, A., Blechschmidt, A.-M., Dominguez, J. J., Engelen, R., Eskes, H., Flemming, J., Huijnen, V., Jones, L., Kipling, Z., Massart, S., Parrington, M., Peuch, V.-H., Razinger, M., Remy, S., Schulz, M., and Suttie, M.: The CAMS reanalysis of atmospheric composition, Atmos. Chem. Phys., 19, 3515–3556, https://doi.org/10.5194/acp-19-3515-2019, 2019. CAMS rean

[RD32] Hersbach, H, Bell, B, Berrisford, P, et al. The ERA5 global reanalysis. Q J R Meteorol Soc. 2020; 146: 1999–2049. https://doi.org/10.1002/qj.3803

[RD33] Dudhia, A , The Reference Forward Model (RFM), Journal of Quantitative Spectroscopy and Radiative Transfer 186 (2017) 243–253, doi:10.1016/j.jqsrt.2016.06.018

[RD34] Miles, G.M. R. Siddans, B. J. Kerridge, B. G. Latter, and N. A. D. Richards, Tropospheric ozone and ozone profiles retrieved from GOME-2 andtheir validation, Atmos. Meas. Tech., 8, 385–398, 2015, www.atmos-meas-tech.net/8/385/2015/, doi:10.5194/amt-8-385-2015

[RD35] McPeters, R. D., Lebow, G. J., and Logan, J. A.: Ozone climatological profiles for satellite retrieval algorithms, J. Geophys. Res.,112, D05308, doi:10.1029/2005JD006823, 2007

[RD36] MTG-FCI: ATBD for Global Instability Indices Product, EUMETSAT 2013, EUM/MTG/DOC/10/0381

[RD37] M. Koenig and E. de Coning, “The MSG Global Instability Indices Product and Its Use as a Nowcasting Tool”, Weather and Forecasting, Vol 24, pp.272-285, 2009

[RD38] Water Vapour Climate Change Initiative (WV_cci) - CCI+ Phase 1, End to End ECV Uncertainty Budget (E3UB) - Part 2: CDR-3 & CDR-4, D2.3, 14 June 2022, Issue :3.0

[RD39] Inness, A., Baier, F., Benedetti, A., Bouarar, I., Chabrillat, S., Clark, H., Clerbaux, C., Coheur, P., Engelen, R. J., Errera, Q., Flemming, J., George, M., Granier, C., Hadji-Lazaro, J., Huijnen, V., Hurtmans, D., Jones, L., Kaiser, J. W., Kapsomenakis, J., Lefever, K., Leitão, J., Razinger, M., Richter, A., Schultz, M. G., Simmons, A. J., Suttie, M., Stein, O., Thépaut, J.-N., Thouret, V., Vrekoussis, M., Zerefos, C., and the MACC team: The MACC reanalysis: an 8 yr data set of atmospheric composition, Atmos. Chem. Phys., 13, 4073–4109, https://doi.org/10.5194/acp-13-4073-2013, 2013.

APPENDIX 2: ACRONYMS

Term	Definition
AMSU	Advance Microwave Sounding Unit (on Metop)
ATBD	Algorithm Theoretical Basis Document
ATMS	Advanced Technology Microwave Sounder
CAMS	Copernicus Atmosphere Monitoring Service
CCI	ESA Climate Change Initiative
CEDA	Centre for Environmental Data Analysis
CrIS	Cross-track Infrared Sounder
DOFS	Degress of freedom for signal
E3UB	End to End ECV Uncertainty Budget
ECMWF	European Centre for Medium Range Weather Forecasting
EOCIS	UK Earth Observation Climate Information Service
EPS	European Polar System
ERA	ECMWF re-analysis
ESA	European Space Agency
FM	Forward Model
FOR	Field-of-regard
GII	Global instability indices
IASI	Infrared atmospheric sounding interferometer
IMS	Infra-red Microwave Sounder scheme
IR	Infra-red
JPSS	Joint Polar Satellite System
L1C	Level-1C data (top of atmosphere geolocated radiances)
L2	Level-2 data (geophysical product)
MACC	Monitoring Atmospheric Composition and Climate
MHS	Microwave Humidity Sounder
MTG	Meteosat Third Generation
MW	Microwave
NASA	(US) National Aeronautics and Space Administration
NCEO	UK National Centre for Earth Observation
NEBT	Noise equivalent brightness temperature

Term	Definition
NESR	Noise-equivalent spectral radiance
NOAA	(US) National Oceanic and Atmospheric Administration
NPOESS	National Polar-orbiting Operational Environmental Satellite System
NPP	NPOESS Preparatory Project
NWP	Numerical Weather Prediction
OEM	Optimal estimation method
PVIR	Product Validation and Intercomparison Report
PWLR	Piece-wise Linear Retrieval (Eumetsat)
RAL	Rutherford Appleton Laboratory
RD	Reference Document
RFM	University of Oxford Reference Forward Model
RTTOV	Radiative transfer for TOVS (radiative transfer model)
SA	Sulphate aerosol
SAF	Satellite Application Facility
SEVIRI	Spinning Enhanced Visible Infra-Red Imager
TOVS	TIROS operational vertical sounder (package of MW+IR sounders on operational polar platforms)
UV	Ultra-violet
VIIRS	Visible Infrared Imaging Radiometer Suite
WOUDC	World Ozone and UV Data centre

End of Document